

Reproduced in part with permission from

Jain, D., Zhang, C., Cool, L.R., Blackledge, T.A., Wesdemiotis, C., Miyoshi, T. & Dhinojwala, A. Composition and Function of Spider Glues Maintained During the Evolution of Cobwebs. *Biomacromolecules* **16**, 3373-3380 (2015).

Copyright [2015] American Chemical Society

Jain, D., Blackledge, T. A., Miyoshi, T., & Dhinojwala, A. Unraveling the Design Principles of Black Widow's Gumfoot Glue. in *Biological Adhesives* (ed. Smith, A.M.) 303–319 (2016).

Copyright [2016] Springer International Publishing Switzerland

Stark, A. Y., Subarajan, S., Jain, D., Niewiarowski, P. H., & Dhinojwala, A. Superhydrophobicity of the gecko toe pad: biological optimization versus laboratory maximization. *Phil. Trans. R. Soc. A* **374**, 20160184 (2016).

Copyright [2016] The Royal Society Publishing

© 2018

DHARAMDEEP JAIN

ALL RIGHTS RESERVED

HUMIDITY DRIVEN PERFORMANCE OF BIOLOGICAL ADHESIVES

A Dissertation

Presented to

The Graduate Faculty of The University of Akron

In Partial Fulfillment

of the Requirements for the Degree

Doctor of Philosophy

Dharamdeep Jain

May, 2018

HUMIDITY DRIVEN PERFORMANCE OF BIOLOGICAL ADHESIVES

Dharamdeep Jain

Dissertation

Approved:

Advisor
Dr. Ali Dhinojwala

Committee Chair
Dr. Mesfin Tsige

Committee Member
Dr. Todd. A. Blackledge

Committee Member
Dr. Toshikazu Miyoshi

Committee Member
Dr. Abraham Joy

Accepted:

Department Chair
Dr. Coleen Pugh

Dean of the College
Dr. Eric Amis

Dean of the Graduate School
Dr. Chand Midha

Date

ABSTRACT

Biological adhesives are sticky secretions or structures produced by several organisms in nature to serve roles such as locomotion, prey capture and defense. These adhesives stick in a variety of environmental conditions and can maintain their adhesion exceptionally well. The present work focuses on understanding one such environmental factor, ‘humidity’ and presents its correlation with the material composition in influencing the adhesion mechanism in two diverse biological attachment systems: Capture silk and Gecko setae. Understanding adhesion in these natural systems is essential with respect to humidity since many synthetic materials including glues fail in presence of water.

The first and second studies focus on the glue laden capture silk produced by web building spiders. In the first study, we explored the capture silk of cobweb weaver ‘black widow spider’ known as ‘gumfoot glue’. We first investigated the chemical composition of the glue and for the first time reported that it is majorly a combination of hygroscopic organic salts (low molecular mass compounds, LMMCs) and novel glycoproteins, apart from previously known peptides. Next, we correlated the glue composition with humidity based macro and molecular level studies and showed the synergistic role of LMMCs and glycoproteins in adhesion across the range of humidity conditions.

Based on the first study which showed the presence and importance of diverse LMMCs in capture silk adhesion, we designed our second study in understanding the role of LMMCs in the capture silk. Based on hypothesis that LMMC’s compositions control

the maximum adhesion and viscosity trends across species, we designed the study in which by using Solution-State NMR, we first analyzed the water-soluble extract of glues for four different spider species from diverse habitats and found extract belonging to each species is a distinct combination of organic LMMCs present in varied proportions. Next, we studied the water uptake of glues and their isolated LMMCs compositions. The results showed that hygroscopic strength of LMMCs alone can't explain the adhesion response of glues. We believe it is the chemical interactions of diverse LMMCs with glycoproteins that controls the adhesion mechanism of capture silks in presence of humidity.

In the third, fourth and fifth studies, we switch to a different adhesive system and present investigations based on the hairs present on gecko feet, known as 'setae'. In the third study, we first time established the chemical composition of hairs by characterizing molts from gecko feet and showed the presence of β -keratin and unbound lipids. Also, we showed lipids in hairs were more mobile as compared to lipids in epidermal skin based on which we proposed structural arrangement of lipids and keratin in the setal hairs. The fourth study focused on understanding the role of surface lipids detected in the third study. By means of shear adhesion and contact angle experiments, we found those lipids do not affect adhesive and anti-adhesive properties respectively. The existing hypothesis of β -keratin softening and leading to higher adhesion in presence of humidity was tested in our fifth study. By series of water uptake and NMR measurements, we found β -keratin absorbs water and gets soft at a macro and molecular level. Friction cell based shear adhesion measurements on setae supported the hypothesis and showed an increase in adhesion with increase in humidity.

The research studies presented provides a detailed account of correlation of environmentally relevant parameter, 'humidity' with the building blocks of capture silk and gecko setae and their adhesion performance. The results provide design insights in developing synthetic materials such as adhesives that can work in different humidity environments.

DEDICATION

I dedicate this dissertation to Guruji Acharya Sushil Kumarji for his everlasting blessings, my loving parents, Rajiv Jain and Meenu Jain, who have been a strong source of support and motivation throughout my educational career.

ACKNOWLEDGEMENTS

I am extremely thankful to my advisor Dr. Ali Dhinojwala for always being there. He has been an important guiding support and source of encouragement throughout my PhD journey. This is strange but today when I am writing this thank you note to him, I must admit it has been one of the toughest things to do in my PhD. I can't thank him enough for everything he has done be it having immense faith in my abilities, providing me liberty in choosing research problems, encouraging me towards interdisciplinary research, giving opportunities to mentor students and to attend conferences. Working under his guidance never felt intimidating or pressurizing but a fun way of understanding science. I have learnt a lot from him whether it being tackling complex problems from the basics or presenting research in a simply effective manner. I strongly feel working with him has shaped my technical and non-technical skills and made me a better learner. I am privileged to graduate under his valuable mentorship and turn my PhD dream a reality.

I want to thank my committee members, Dr. Todd. A. Blackledge, Dr. Mesfin Tsige, Dr. Toshikazu Miyoshi and Dr. Abraham Joy for agreeing to be part of my dissertation committee, reviewing my dissertation and providing useful feedback, especially during my research presentation. The projects in my dissertation are a result of collaboration with different labs at University of Akron. I would like to thank all my collaborators and co-authors for helping me in driving different projects from start to finish.

First and foremost, I would like to extend gratitude to Dr. Todd. A. Blackledge and Dr. Peter Niewiarowski for their mentorship and for introducing me to the fascinating world of spiders and geckos. Working with both has been a breeze and an enjoyable experience (I must mention the fun spider walks and gecko demos). I had never imagined foraying into the field of biology, an area that was totally new to me before I joined Akron and I sincerely thank them for instilling in me the knowledge to appreciate materials from a biological point of view. I would take the opportunity to thank Dr. Toshikazu Miyoshi and his student Wei for the experience with Solid State NMR, for instrument training sessions, for always being flexible in providing NMR machine time and for helping in interpretation of results; Dr. Chrys Wedemiotis, Dr. Abraham Joy and their students, Lydia and Ying respectively for their collaboration on different projects; Dr. Brent Opell (Virginia Tech) for his support on spider silk projects and for sending out the capture silk samples and Dr. Mark. A. Townley (University of New Hampshire) for help with black widow literature and synthetic hygroscopic compounds. I am thankful for the support from Magnetic Resonance Center (MRC) at Akron (Dr. Venkat Duddipala and his team of students: Liladhar, Stephanie, Jessie and Dan) in Solution State NMR experiments. Many experiments in my research required the use of special equipments, for which I would like to thank Edward Laughlin (Machine Shop) and Jack Gillespie (Glass Blowing Shop) for their timely assistance in fabrication of devices.

The PhD research experience gave me the opportunity to mentor high school, undergraduate and master level students. I want to thank Kelly Chen, Nicolette Khan, Ci Zhang, Shairani Subarajan and Jordan Fitch for their enthusiasm and important contributions to the different projects during my doctoral studies. A lot of effort in shaping

the research projects has come from the discussions and suggestions from group members. I would like to thank Vasav and Alyssa for guiding me in the initial years and for being awesome mentors for the spider silk and gecko projects respectively. I would like to mention Gaurav and Saranshu, my colleagues in spider silk and gecko research for their support in different projects. A big thank you to the Dhinojwala, Spider and Gecko group members, who over the years in one way or the another have helped me in my doctoral studies whether being by providing useful feedback during group meetings, by reviewing my technical papers and presentations or helping with experiments. I am grateful to Department of Polymer Science, University of Akron and National Science Foundation (NSF) for providing the funding for my doctoral studies.

I would like to thank my parents and family for their efforts, blessings, unconditional love and support throughout my PhD journey. I am happy and proud that I have made their dream possible and broken the tradition to come out as a first PhD in my family. The support of friends from school and undergraduate days: Pallavi, Sushant, Neeraj and Piyush during my initial graduation school application days till present has been important. The weekend getaways, coffee breaks and frequent get-togethers with Akron friends helped in breaking the graduate life monotony and bringing in a fresh change. I would like to thank Sarfaraz, Ila, Saurabh (Batra), Kushal, Poonam and my beloved 'Bollywood Night' group: Sarang, Saumil, Vrushali, Brinda, Ankit, Nishad, Ajay, Hari, Stuti, Mayank, Prasad, Kaushik and Sayali for being like a close-knit family and creating zillions of everlasting memories which made Akron life totally memorable! I can't help but specially mention 'Saumil', my Akron housemate, brother and best friend for all his support and love.

TABLE OF CONTENTS

	Page
LIST OF FIGURES	xiv
LIST OF TABLES	xx
CHAPTER	
I INTRODUCTION	1
II BACKGROUND REVIEW	9
2.1 Humidity driven biological materials	9
2.2 Biological adhesives	13
2.3 Capture silk	16
2.3.1 Viscid glue	18
2.3.1.1 Secretion mechanism	18
2.3.1.2 Chemical composition	19
2.3.1.3 Structural arrangement	22
2.3.1.4 Viscoelasticity	24
2.3.1.5 Humidity mediated adhesion	25
2.3.2 Gumfoot glue	26
2.3.2.1 Secretion mechanism	28
2.3.2.2 Chemical composition	28
2.3.2.3 Viscoelasticity	30

2.3.2.4 Humidity mediated adhesion	30
2.4 Gecko setae	32
2.4.1 Characteristics of gecko adhesive system	32
2.4.2 Chemical composition of setae.....	37
2.4.2.1 β -keratin.....	37
2.4.2.2 Lipids.....	41
2.4.3 Gecko adhesion in presence of water	47
III. STICKY BUSINESS IN COBWEBS OF BLACK WIDOWS: DESIGN, HUMIDITY DRIVEN ADHESION AND MOLECULAR MECHANISM OF GUMFOOT GLUE.....	53
3.1 Introduction.....	53
3.2 Experimental Section	57
3.3 Results.....	62
3.4 Discussion.....	73
3.5 Conclusion	78
IV. ROLE OF HYGROSCOPIC LOW MOLECULAR MASS COMPOUNDS IN HUMIDITY RESPONSIVE ADHESION OF CAPTURE SILK	79
4.1 Introduction.....	79
4.2 Experimental Section	83
4.3 Results.....	88
4.4 Discussion.....	98
4.5 Conclusion	103

V. LIPIDS IN GECKO SETAE: TRACING THEIR PRESENCE AND ASSOCIATION WITH β -KERATIN	104
5.1 Introduction.....	104
5.2 Experimental Section	108
5.3 Results.....	111
5.4 Discussion.....	117
5.5 Conclusion	124
VI. ROLE OF SURFACE LIPIDS IN ADHESIVE AND ANTI-ADHESIVE PROPERTIES OF GECKO SETAE.....	125
6.1 Introduction.....	125
6.2 Experimental Section.....	130
6.3 Results	133
6.4 Discussion.....	136
6.5 Conclusion.....	137
VII. MACRO AND MOLECULAR RESPONSE OF GECKO SETAE TO HUMIDITY: IMPLICATIONS FOR ADHESION	139
7.1 Introduction.....	139
7.2 Experimental Section.....	143
7.3 Results.....	146
7.4 Discussion	150
7.4 Conclusion	154

VIII. SUMMARY AND RECOMMENDATIONS FOR FUTURE WORK.....	155
REFERENCES	161
APPENDICES	179
APPENDIX A: STATISTICAL ANALYSIS.....	179
APPENDIX B: CALCULATIONS	182
APPENDIX C: LIST OF PUBLICATIONS.....	188

LIST OF FIGURES

Figure	Page
2.1 Various categories of bioadhesives.....	13
2.2 Diversity of biological adhesives.....	14
2.3 Characteristics of biological adhesives.....	14
2.4 Schematic of function-specific seven types of silks produced by spider glands	16
2.5 Diversity of spider web architectures	17
2.6 Picture of an orb web	18
2.7 Bead on a string (BOAS) geometry for viscid glue from <i>Larinioides cornutus</i>	19
2.8 (A) Glycoprotein core in viscid glue of <i>Larinioides cornutus</i> . Scale bar: 20 μm . (B) Fibrous glycoproteins in glue of <i>Araneus diadematus</i> . Scale bar: 10 μm . (C) Schematic illustrating types of aggregate spider glue proteins (ASG) constituting glycoproteins	21
2.9 Hygroscopic LMMCs found across viscid glues of different species of orbweb weaving spiders	21
2.10 Heterogenous structure of viscid glue with different regions.....	23
2.11 (A) Rate dependent pull-off forces for viscid glue droplets. (B) Load-relaxation analysis for viscid glue droplets stretched at 100 μms^{-1} (black), 10 μms^{-1} (blue) and 1 μms^{-1} (red). Inset is an enlargement of the plateau regions for the three conditions.....	24
2.12 (A) Picture of a western black widow spider (<i>Latrodectus hesperus</i>). (B) Model structure of the three-dimensional cobweb prepared by <i>Latrodectus</i> spiders depicting the two regions: dry scaffolding silk (upper part) and gumfoot silk (lower part) consisting of glue droplets.....	26
2.13 The real-time image depicts the structural arrangement of gumfoot silk in a cobweb. The strands are attached to the base and comprise of axial major ampullate silk thread coated with glue droplets. The inset is a SEM micrograph of a strand of gumfoot silk.....	27

2.14 Types of spider coating peptides in gumfoot glue of <i>Latrodectus hesperus</i>	29
2.15 (a)-(c) are the load relaxation plots of single gumfoot glue droplet stretched by a constant length at 15% RH, 40% RH and 90% RH respectively. The different symbols represent pull off rates: 1 $\mu\text{m/s}$ (inverted triangles), 10 $\mu\text{m/s}$ (upright triangles), 50 $\mu\text{m/s}$ (squares) and 100 $\mu\text{m/s}$ (circles)	31
2.16 (a) shows comparison between gumfoot glue (circles) and viscid glue (squares) droplets for change in volume with time under high humidity conditions. (b) is the single droplet load vs extension at 50 $\mu\text{m/s}$ at 15% RH (circles), 40% RH (squares) and 90% RH (triangles)	31
2.17 Diversity of foot pad architecture in different kinds of geckos	32
2.18 (a) A tokay gecko (<i>Gekko gecko</i>). (b) Foot of a tokay gecko highlighting scansors or adhesive lamellae (mesoscale) that are covered with rows of setae. (c) A cross sectional view of an isolated setal array. (d) Tetrads of setae present in the scansors (microscale). (e) Numerous branched spatular ends arising from single setae. (f) and (g) Flat and triangular spatular tips (nanoscale) responsible for adhesion to a surface	33
2.19 (a) The non-wetting Cassie Baxter state highlighting superhydrophobicity of gecko toe pad. (b) Schematic illustrating the non-wetting state. (c) Thermodynamically stable wenzel wetting state. (d) Schematic illustrating wetting of toe pad in wenzel state	36
2.20 (A) and (B) are the images of toe with contaminants, before and after steps (~8) respectively taken on a clean surface highlighting self-cleaning property	36
2.21 Structural arrangement of polypeptides chains in (A) α -keratin and (B) β -keratin ...	38
2.22 Different layers in the keratin based epidermis of a gecko	39
2.23 Structural features present on the epidermis of a gecko	40
2.24 Different classes of lipids found in biological systems	42
2.25 Schematic outlining various hypothesis for role of lipids in gecko setae	43
2.26 (A) and (B) are moisture condensation images of a gecko (Tokay) footprint on clean glass substrate. The footprints in (A) were subjected to 98% humidity while those in (B) were first cooled with dry ice and then exposed to humid air. Hydrophobic regions were outlined with the droplets of water. (C) Gecko footprint stained with Oil Red O dye	44
2.27 Light microscopy image of scansor belonging to <i>P. dubia</i> showing the presence of lipids (indicated by orange staining) in outer setae (os), inner setae (is), oberhautchen layer (o), dermis (d). Scale bar: 200 μm	44

2.28 (A) General structure of phosphocholine based lipids. (B) Mapping image collected for peak m/z 184. (C) Tandem mass spectrum for the detection of m/z 184.....	46
2.29 (A) Experimental set up for SFG of a gecko toe in contact with sapphire. (B)-(D) are the SFG spectra collected for dry toe contact, water wetted sapphire in contact with toe and dry footprint contact after peeling the toe from the sapphire surface respectively.....	46
2.30 Models of arrangement of lipids (yellow) in setal hairs. (A) shows the homogeneous model where lipids cover keratin spatulae (red). (B) and (C) are the heterogeneous models where lipids are hypothesized to present between two spatular ends (B) or intimately mixed with keratin in the hairs (C)	47
3.1 (a) Schematic of a cobweb built by the western black widow. The gumfoot silk thread is composed of beads of adhesive glue (black arrow) on a major ampullate silk thread (green arrow). (b) Collection of gumfoot threads (yellow arrow) from the base of web by using a glass fork. (c) SEM micrograph of a gumfoot silk thread (glue; black arrow and major ampullate silk; green arrow).....	56
3.2 Schematic of gumfoot thread pull-off experiments	61
3.3 (a) ¹ H NMR spectrum for the water- soluble extract from gumfoot threads. Inset in (a) shows the extended chemical shift range (5-12 ppm) depicting the absence of peptide peaks (SCPs) in the amide region. (B) Different material components in the gumfoot silk relative to the total mass of collected gumfoot	62
3.4 (a) Bundle of washed gumfoot threads. (b) Single washed gumfoot silk thread. (c) and (d) SEM micrographs of number of washed threads scraped from the collection rod single washed gumfoot silk thread respectively	63
3.5 (a) Trypsin digested water-soluble extract from gumfoot silk of <i>Latrodectus hesperus</i> highlighting the presence of peaks related to spider coating peptides (SCPs) particularly at m/z 812.2, 826.3, 979.4, 1116.4, 1206.4, 1222.6 and 1555.5. (b) CAD MS/MS of the 1206.4 peak showing the different fragments of AVHHYEVPR.....	64
3.6 Periodic acid Schiff (PAS) staining. (a) and (b) Washed gumfoot silk from <i>Latrodectus hesperus</i> . (c) Washed viscid silk from the orb weaver <i>Larinioides cornutus</i> . (d) Major ampullate silk from <i>Latrodectus hesperus</i>	66
3.7 CP/MAS spectra for pristine reeled major ampullate (MA) silk, pristine gumfoot silk and washed gumfoot silk. Inset schematic shows the arrangement of gumfoot silk (glue and MA silk). Ideally after washing, gumfoot silk and MA silk spectrum should match if they are chemically identical, but the presence of heightened shoulder around 25-35 ppm (C _β for amino acids), 55-60 ppm (C _α for amino acids) (inset spectrum) and peaks related to glycoproteins (75 ppm and 105 ppm, labeled as G) indicates the presence of additional proteinaceous residue in gumfoot silk that is absent in the control major ampullate silk sample. The starred peak refers to a spinning sideband. All spectra are measured at 30% RH, 25 ^o C and MAS frequency ~ 6 kHz.....	67

3.8 (a) Pristine gumfoot silk. (b) Washed gumfoot silk. (c) and (d) Variation of work of adhesion (W_a) with relative humidity (% RH) ranging from 10%-90% for pristine and washed threads respectively.....	68
3.9 Comparative CP/MAS spectra of pristine gumfoot silk and major ampullate silk. Inset depicts the gumfoot silk arrangement. All spectras were recorded at MAS frequency of 6 kHz, 60% RH and 25 ⁰ C. Starred peak is unidentifiable component and ssb refers to the spinning sideband.....	70
3.10 (a) and (b) CP/MAS spectra of pristine and washed gumfoot silk spectra respectively at 10% RH (red), 60% RH (green) and 90% RH (blue). Insets in each spectrum shows the peaks affected in aliphatic region with humidity exposure. All spectras were recorded at MAS frequency of ~ 6 kHz and 25 ⁰ C. ssb refers to the spinning sideband.....	72
3.11 (a) and (b) DP/MAS spectra of pristine and washed gumfoot silk at 10% RH, 60% RH and 90% RH. (A: Isethionic acid, B: Choline and C: GABamide) Starred peaks in (a) are unidentified peaks. Spectras were recorded at MAS frequency of ~6 kHz and 25 ⁰ C	73
4.1 (a)-(e) Different types of samples for water uptake measurements. (a) Synthetic organic LMMC (l-proline shown here). (b) Extracted LMMCs in a centrifuge tube after lyophilization. (c) Synthetic LMMCs mixture mimcking recipe from glue of <i>Tetragnatha laboriosa</i> . (d) Washed capture silk. (e) Pristine immobilized glue threads on an aluminum foil. All natural samples shown are related to the capture silk from the webs of <i>Larinioides cornutus</i> . (f) Set up for water uptake experiments showing different parts including the custom built humidity controller and Cahn Microbalance	88
4.2 (a)-(d) Water solubles LMMCs (black arrow) extracted from the webs of <i>Latrodectus hesperus</i> , <i>Argiope trifasciata</i> , <i>Larinioides cornutus</i> and <i>Tetragnatha laboriosa</i> respectively	89
4.3 (a)-(d) ¹ H Solution-State NMR spectra of the extracted LMMCs mixtures from the webs of <i>Latrodectus hesperus</i> , <i>Argiope trifasciata</i> , <i>Larinioides cornutus</i> and <i>Tetragnatha laboriosa</i> , respectively. Each spectrum is accompanied with a color coded pie chart (each color representing a distinct LMMC) showing the details of relative composition of each LMMC component in different capture silks.....	90
4.4 (a)-(d) Optical images of the single capture glue droplet of <i>Latrodectus</i> exposed to 10%, 30%, 60% and 90% RH respectively. Scale bar is 50 μ m. (e) Normalized increase in volume (%) of pristine capture silk glue belonging to <i>Latrodectus</i> , <i>Argiope</i> , <i>Larinioides</i> and <i>Tetragnatha</i> , as a function of relative humidity. The error bars show \pm 95% confidence interval, and sample size is \geq 15	92
4.5 Normalized percent increase in mass of different synthetic organic LMMCs over the range of humidity conditions (30%, 60% and 90% RH). Insets are the zoomed in regions for 30% and 60% RH. The data is represented as mean \pm standard deviation from a set of three measurements.....	94

4.6 Schematic illustrating the major organic LMMCs in the glue droplets across various species. The LMMCs are divided into less active, moderately active and highly active based on the total water uptake of synthetic LMMCs at 90% RH.....	94
4.7 (a) shows normalized increase in mass (%) of natural LMMCs extracts obtained from webs of <i>Latrodectus</i> , <i>Argiope</i> , <i>Larinioides</i> and <i>Tetragnatha</i> as a function of humidity. (b) shows the comparison of normalized increase in mass (%) for synthetic LMMCs mixtures species from extreme habitat: <i>Argiope</i> and <i>Tetragnatha</i>	96
4.8 Theoretical water uptake of LMMCs mixtures.....	97
4.9 Normalized increase in mass (%) of washed glue (residual proteins) vs pristine glue for <i>Argiope</i> and <i>Larinioides</i> as a function of relative humidity	98
5.1 Scanning electron micrographs (SEM) for pristine (a) delipidized (b) toe sheds, showing the adhesive hairy features known as ‘setae’ and pristine (c) delipidized (d) skin sheds, showing the ‘spinulae’ structures respectively	106
5.2 The phospholipid structure shows the positions of various methylene (CH ₂) _n , (ω-1)CH ₂ , (ω-2)CH ₂ , αCH ₂ and βCH ₂ and methyl ωCH ₃ groups. These signatures are detected in the NMR experiments. The structure is shown as a model example to understand the different peaks in the NMR results	107
5.3 (a) Removal of freshly molted gecko toe shed from <i>Gekko gekko</i> . (b) Removed shed from the toe region.....	108
5.4 (a) ³¹ P NMR for standard phospholipids (PC and SM). (b) ³¹ P NMR for extracted phospholipids. (c) ³¹ P Solution NMR of lipid extracts from skin shed. (d) ¹ H NMR for lipid extract from toe sheds. Inset in (d) is the enlarged spectrum from 2-6 ppm	113
5.5 CP/MAS spectra shows the pristine (green) and delipidized (purple) for toe (a) and skin (b) sheds. The spectra are measured at MAS frequency ~6 kHz. Star labelled peak refers to spinning sideband.....	115
5.6 DP/MAS spectrum for the pristine (green) and delipidized (purple) toe (a) and skin (b) sheds respectively. The inset is enlarged aliphatic region (0-50 ppm) showing lipid signatures (CH ₂) _n , (ω-1)CH ₂ , (ω-2)CH ₂ , αCH ₂ and βCH ₂ and (ωCH ₃). All spectra are measured at MAS frequency ~6 kHz.....	116
5.7 (a) and (b) are the ¹ H MAS NMR spectra for toe and skin sheds respectively. The sheds have been analyzed in both pristine (green) and delipidized (purple) forms. All spectra are measured at MAS frequency ~6 kHz.....	117
5.8 (a) and (b) are the direct polarization and proton magic angle spinning spectra respectively for pristine toe (blue) and pristine skin (orange) sheds. The nature of the lipid	

region differs in the toe and skin shed samples highlighting the difference in the lipid mobility between the two types of sheds from the gecko epidermis. All spectra are measured at MAS frequency ~6 kHz.....	119
5.9 (a) Layers of skin shed including the brick and mortar-based mesos and alpha layer rich in lipids. (b) Layers in the toe pad shed, where setae (lipid rich) are added to the skin layers described in (a). The setae likely contains lipids in the form of a thin coating, in the adhesive spatulae (not shown) and matrix. The matrix is a combination of lipids (yellow) and unknown material (purple). The figures have not been drawn to scale and the spatula have not been included in the rendering of (b)	122
6.1 Adhesion of gecko toe pad sheds in air on hydrophilic glass, hydrophobic OTS-SAM coated glass and fine sandpaper (root mean square roughness ~500nm for a 50x50µm sample area) after treatment to remove the setal surface lipids. Letters above the bars indicate statistical significance, where bars with different letters are significantly different from one another. Error bars are mean ± 1 s.e.m.....	134
6.2. Adhesion of gecko toe pad sheds in air and water on hydrophobic OTS-SAM coated glass after treatment to remove the setal surface lipids. There was no significant difference between treatment in air or in water, but adhesion was overall higher in water than air. Error bars are mean ± 1 s.e.m	135
6.3. Maximum shear adhesion of toe pad sheds tested on a glass substrate either treated in acetone or untreated. There was no significant difference in adhesion between the treated (acetone) and untreated toe pad sheds (p > 0.05). Error bars are mean ± 1 s.e.m	137
7.1 Schematic showing humidity set up with the biaxial friction cell for shear adhesion measurements.....	146
7.2 (a) shows the water uptake (as a function of % RH) of pristine setae. (b) is the comparison of hygroscopicity at 90% RH between different keratin systems: setae, feather and wool. (c) is the comparison of water uptake of pristine setae with two types of treated setae, delipidized setae and oxygen plasma treated setae at 90% RH. The reported values are ± standard deviation	147
7.3 CP/MAS spectras of pristine toe sheds exposed at 50% RH (pink) and 100% RH (blue). There is an overall decrease in the intensity of various regions related to β-keratin (majorly) and lipids in presence of 100% RH indicating an increase in the softness of setae at molecular level. Starred peak refers to the spinning sideband. The spectra were recorded at MAS frequency at ~6 kHz	148
7.4 Shear force values normalized by the area of lamellae, measured for pristine and delipidized samples as a function of relative humidity. Levels connected by different letters are statistically different.....	150

TABLE OF CONTENTS

Table	Page
2.1 Summary of chemical compositions for major biological adhesive systems	15
2.2 Properties of two types of keratin	38
5.1 Retention factors for extracted lipids from toe and skin sheds measured using Thin Layer Chromatography	112

CHAPTER I

INTRODUCTION

An adhesive is a material that binds two or more surfaces together. Some general characteristics of adhesive include (1) ability to act as a liquid to flow and wet the substrate for bond formation, (2) formation of strong surface bonds during adhesion, (3) hardening from liquid to semisolid/solid to facilitate load bearing during the lifetime of the system. Depending on their end use, adhesives can be either structural or nonstructural. Structural adhesives such as epoxies have high mechanical strength and are used for applications requiring strong holding power and environmental resistance. Comparatively, non-structural adhesives like pressure sensitive films and elastomeric glues have lower strength, less permanence and are used for holding weak substrates or for temporary fastening.

Adhesives are of high importance in our day-to-day lives since they are used in various types of applications such as construction (roofing, flooring, concrete), transportation (auto assembly, marine, railroad), packaging (cartons, labels, envelopes, tapes), medical (dental, implants, sutures) and apparel (shoes, woven textiles, laminates). Chemically, adhesives are polymeric viscoelastic materials that can be applied at low viscosities and harden over time to demonstrate resistance to stress and environmental factors. Examples include natural glues (animal, vegetable and mineral based), elastomers

(natural rubber, synthetic rubber), thermoplastics (vinyls, polyesters, polyacrylates, polyether, polysulfones) and thermosets (amino plastics, epoxies, phenolics, polyesters, polyaromatics).

Over its lifetime, an adhesive joint experiences internal or external stresses that can lead to the failure of the system. Internal stress includes localized stress due to imperfections in adhesive or at the interface, stress due to differences in thermal expansion coefficients of adhesive and substrate, stress due to shrinkage of adhesive or substrate. External stress can be mechanical, thermal or chemical such as exposure to gases, fluids, temperature, humidity, radiations, salt spray, vacuum. These factors can cause premature failure by inducing additional internal stresses near the adhesive bond region, by degrading adhesive, substrate or interphase regions to reduce cohesivity and by creation of new interphase regions in the joint.¹

Among the environmental stresses mentioned previously, humidity poses serious problems to the stability of adhesive joints.¹⁻⁵ Most of the adhesives fail when a critical relative humidity (RH) is exceeded.^{1,3} There are different hypotheses in literature that account for the adhesion loss in high humidity including physical and chemical changes in adhesive due to water absorption as well as degradation of adhesive-substrate interface. Polymeric adhesives absorb moisture leading to change in the chemical nature and bulk properties such as glass transition temperature, tensile strength, modulus and elongation. Apart from degrading the adhesive, moisture can alter substrate properties like change in surface properties or geometrical dimensions. Moisture can permeate the adhesive layer, migrate to the interface and generate a weak boundary layer by replacing adhesive at the bond interface. Preventive measures such as (1) incorporation of additives (carbodiimides,

oxazolidines) to improve the hydrolytic stability of base polymer, (2) use of primers (organosilanes, phenolics) to prevent corrosion of substrate and (3) treating surfaces with chemical etching, inhibitors and anodization have been used to improve adhesion in presence of high humidity.¹

A potential solution for the humidity-adhesion problem lies in exploring natural systems known as biological adhesives.⁶⁻⁹ Several living systems secrete or produce structures that stick in harsh conditions including water or high humidity in an efficient manner. Prominent examples include cement like secretions from mussels,¹⁰ barnacles,¹¹ sea urchins,¹² caddisflies,¹³ sandcastle worms¹⁴ and oysters¹⁵; fibrillar hairs on gecko feet¹⁶; glues on spider webs¹⁷ and pollen grains.¹⁸ The remarkable attachment ability of these adhesives helps the living organism to locomote, capture prey or even defend themselves against predators.⁷ Biological adhesives have been in functioning since millions of years and it is critical to understand the fundamental adhesion mechanism behind their exceptional performance to solve the outstanding challenges we encounter with adhesion of polymeric adhesives in presence of high humidity.

With respect to that, the research work presented in the thesis aims at understanding the adhesive mechanism of two diverse biological attachment systems that function in presence of humidity, capture silk present on spider webs¹⁷ and hairy setae on gecko feet.¹⁹ The five studies presented in the thesis are based on the common hypothesis, ‘chemical composition is the driving factor for the humidity driven performance of the adhesive’. In the light of gaining holistic view of the adhesion mechanisms, the work involves two major aspects (1) characterization of the adhesives for their chemical composition (2) correlation

of their chemical compositions with macro level adhesion results and molecular level interactions in different relative humidity conditions.

Prey capture adhesives produced by web-building spiders have intrigued humans for many years and provide important insights to develop adhesives that work in humid environments. These humidity responsive glues are laid down by spiders in various types of webs, primarily orb webs and cobwebs. The formation and function of viscid glue in the capture spirals of orb webs is well-studied compared to the vertically aligned gumfoot glue strands in cobwebs. While the glue droplets in cobwebs contain some peptides, it acts as viscoelastic liquid, rather than viscoelastic solid, and the cause of glue stickiness are poorly understood. In the first study, gumfoot glue present in cobwebs of *Latrodectus hesperus* (Black widow) spider is investigated for its chemical composition and findings are correlated with adhesion and molecular interactions in presence of humidity. Spectroscopic and staining methods show glue is composed of hygroscopic organic low molecular mass compounds (LMMCs) and water insoluble glycoproteins, like viscid silk, in addition to a low concentration of spider coating peptides reported before. Adhesion studies reveal that the organic LMMCs play an important role in adhesion, like that seen in orb web spiders, but modulating function at much lower humidity. Molecular evidence based on NMR agrees with adhesion data and show that both LMMCs and glycoproteins are important for strong adhesion in a humid environment. The work shows more similarities in the viscid silk produced by orb web and cobweb spiders than previously anticipated and provide guidelines for developing synthetic adhesives that can work in dry to humid environments.^{20,21}

The first study showed that LMMC's absorb atmospheric water and participate with glycoproteins, to help in adhesion. The second study of dissertation focusses on the LMMCs and their role in the humidity mediated adhesion of capture silks. The viscosity of the glue changes over five orders of magnitude as a function of humidity, species of spiders from diverse habitats show maximum adhesion in a narrow range of viscosity between 10^5 to 10^6 Pa-s. The humidity where there is a maximum adhesion corresponds to the humidity closest to its foraging humidity.²² This suggests the possibility of adaptation of spiders to live in different habitats by tuning the quantity and chemical composition of LMMCs to control the absorption of water with humidity. To test this, firstly organic LMMCs present in the glues of four spiders from different habitats (*Latrodectus hesperus*, *Argiope trifasciata*, *Larinioides cornutus* and *Tetragnatha laboriosa*) with each having a different maximum adhesion trend were characterized. Next, their glues and isolated LMMC mixtures obtained from their respective glues were tested for amount of water uptake as a function of humidity. It was found that (1) there is a diversity of organic LMMCs among species, (2) a difference in water uptake properties of pristine capture silk threads with specifically *Tetragnatha* glue absorbing less at 90% RH, (3) an increase in hygroscopicity of LMMCs extracts with increase in humidity but no direct relationship with maximum adhesion and (4) reduced hygroscopicity of glycoproteins in absence of LMMCs. The differences in water uptake of the capture silk and extracted LMMCs suggest that LMMCs not only play an important role in water uptake but also help in solubilizing the glycoproteins to mediate adhesion. As many synthetic glues fail under humid conditions, studying the role of hygroscopic LMMCs in capture silk can provide insight in designing synthetic glues that work in wet environments.

Geckos are spread worldwide and can locomote efficiently over natural surfaces in environments that have different humidity patterns. Their movement is facilitated by the adhesive foot pad, lined with microscopic hairs called setae that function due to van der Waals forces and are made of β -keratin and more recently discovered component, lipids. Humidity studies are important since geckos are known to inhabit various geographical zones and understanding adhesion in relevant environmental conditions will convey a fresh perspective to the synthetic gecko adhesives community to fabricate mimics that match natural setae structure and functioning. The role of two material components of setae in the humidity dependent adhesion was investigated through a novel strategy involving use of toe and skin ‘molts’ or ‘sheds’ obtained from gecko epidermis. The third, fourth and fifth studies in the dissertation involve (1) first time characterization of β -keratin and lipids using NMR and establishing their organization in setal structure, (2) studying the role of surface lipids in adhesive and anti-adhesive (superhydrophobicity) properties of setae, (3) studying molts for molecular response of β -keratin and lipids on exposure to humidity and its correlation with macro level (water uptake and adhesion) findings.

Lipid and protein aggregates are one of the fundamental materials of biological systems. Examples include cell membranes, insect cuticle, vertebrate epidermis, feathers, hair and adhesive structures known as ‘setae’ on gecko toes. Until recently gecko setae were assumed to be composed entirely of β -keratin, but analysis of footprints left behind by geckos walking on surfaces revealed that setae include various kinds of lipids. However, the arrangement of lipids with keratin, their molecular-level behavior and role in the setae is still not known. In third study, we demonstrated, for the first time, the use of Nuclear Magnetic Resonance (NMR) spectroscopy techniques to confirm the presence of unbound

(non-covalent) lipids and investigate their association with β -keratin in 'pristine' sheds, or natural molts of the adhesive toe pad and non-adhesive regions of the skin. Analysis was also carried on the sheds after they were 'delipidized' to remove unbound (non-covalently attached) lipids. The results show a distribution of similar lipids in both the skin and toe shed but with different dynamics at a molecular level. Based on these results, a model of the structural organization of β -keratin and lipids in setae was developed showcasing lipids to be present as a surface coating and as disordered domains within β -keratin fibrils. This study represents the first direct investigation of setal constituents, keratin and lipids at a molecular level.²³

After establishing the chemical identity of the sheds, next step involved understanding the role of lipids and β -keratin in humidity driven gecko adhesion by analyzing sheds with different experimental methods. Since many geckos are found in tropical regions and frequently encounter wet surfaces, surface lipids may be helpful in protecting keratin fibrils from excessive softening. Additionally, their presence on setal surface may be responsible for generation of air-plastron needed for attachment of toe on wet surfaces. In the fourth study²⁴, we experimentally investigated the functional role of non-covalently attached surface lipids (detected in the third study) in gecko adhesion. We specifically focused on their potential contribution to adhesive and anti-adhesive (superhydrophobicity) nature of the setae. Shear adhesion results for sheds showed that surface lipids have a negative impact on adhesion on hydrophilic surfaces while their removal shows no effect on both rough as well as hydrophobic surfaces. Static contact angle measurements showed that superhydrophobic (anti-adhesive) state of setae is also not affected by the removal of surface lipids.

In the fifth part of the dissertation, we tested current hypothesis in literature that is, gecko setae (β -keratin) softens in presence of high humidity leading to enhanced adhesion. We investigated softening of sheds at molecular level and observed that water penetrates majorly protein backbone as compared to lipids and plasticizes the amino acids constituting β -keratin based setae leading to softening in high humidity. Also, to confirm this molecular observation, we tested the water absorption of sheds at macro level and saw an increase in setal water uptake with increase in humidity. Complementing these molecular and macro level findings and supporting published evidence were shear adhesion results for setal arrays carried out at different humidity conditions that demonstrated increase in adhesion with increase in humidity (upto 70% RH). The gecko studies presented can help us understand the system both biologically and for design of synthetic adhesives with the findings may be relevant to their performance in humidity, role of lipids and characteristics of lipid-protein interactions in other biological system.

CHAPTER II

BACKGROUND REVIEW

The chapter focusses on introducing to the concept of biological materials that function in presence of humidity followed by details on one of the examples, ‘Biological adhesives’. Next, a thorough review on the two biological adhesives relevant to presented work: spider’s capture silk and gecko setae systems is discussed. The two systems have been described extensively in terms of their properties including the two most important characteristics with respect to the current work, chemical composition and adhesion mechanism in presence of humidity.

2.1 Humidity driven biological materials

Systems in nature experience a host of environmental stimuli such as humidity, pressure, temperature, pH and mechanical stresses that dictates their performance.^{25,26} Out of these, humidity has been widely studied for various biological systems^{16,25,27–33} and these studies have inspired fabrication of a number bio-inspired responsive materials such as adhesives³⁴, hydrogels^{35–37}, actuators³⁸ and polymer films.³⁹ The driving mechanism behind humidity responsiveness is the interaction of the absorbed water with the building blocks or chemical constituents leading to various functions like movement, attachment, color change and mechanical deformation. Following is the description of some of the biological systems whose properties and performance are driven by changes in their chemical constituents on exposure to humidity:

(a) **Spores**

Spores are reproductive structures that help in multiplication in systems like microorganisms (bacteria, fungi, algae), plants and protozoans. Bacterial spores such as in the *Bacillus* family are dormant yet dynamic structures comprising of various multiple concentric layers in their structure including an anhydrous genetic core. These spores respond to fluctuations in relative humidity reflected by shrinkage and changes in their geometrical dimensions. This humidity response is triggered by the water absorption and swelling in the cortex shell formed of peptidoglycans. The interaction with water and resulting dynamics helps in the energy conversion process in bacteria.^{27,40}

(b) **Plants**

Cell walls in plants are made up of rigid cellulose fibrils present in a swellable matrix of hemicellulose, lignin and pectin. The cell wall structure responds to humidity by undergoing swelling and shrinking. Swelling is anisotropic, occurs in the direction perpendicular to the cellulose fibrils and depends highly upon cell wall architecture. This actuation response is seen in mosses as well as in pine cones and wheat awns, where it primarily helps in the seed dispersion process. In pine cones, the difference in the structural arrangement and orientation of cellulose microfibrils in the upper and lower scales leads to a combined effect on the shrinking and swelling processes, thus controlling the opening and closing of pine cones and release of ripe seeds. In wheat awns, humidity response of a well-defined cellulose cell wall architecture (outer ridged active part and inner capped resistive part) helps the awns to disperse their seeds to the ground and facilitates their unidirectional movement along or into the ground.^{28,31}

(c) **Biological adhesives**

Biological adhesives are attachment systems used by living organisms to serve different functions such as movement, attachment and protection.⁶⁻⁹ Humidity affects performance of (i) hair based attachment systems in spiders³², beetles³³ and geckos^{16,41}, (ii) capture silk present on spider webs^{22,25} and (iii) outer oily coating on pollen grains called as pollenkitt.¹⁸ Chitin and resilin based microscopic feet hairs in spiders and beetles respectively potentially show a reduction in the elastic modulus and increase in flexibility upon humidity exposure. This softening of hairs helps in better contact of hairs on surface and enhances adhesion.^{30,32,33} Pollenkit is an oily, sticky and yellow-colored complex mixture of majorly saturated and unsaturated lipids and in minor amounts carotenoids, flavonoids, proteins and carbohydrates. Exposure to humidity leads to an increase in the water uptake property of pollens, affecting the pollenkit wetting and viscosity properties and ultimately adhesion.^{18,42} The influence of humidity on gecko adhesive hairs and capture silk systems will be described in detail later.

(d) **Bird feathers**

Feathers are complex colored structures made up of keratin and melanin. Humidity affects the color production mechanism in feathers leading to rapid and reversible colors with changes in humidity. Color production occurs due to either absorption of selective wavelengths by pigments or by coherent scattering of light due to nanostructured keratinized features present on feathers. Keratin being hydrophilic structural protein comprising of polar amino acids, absorbs water leading to changes in color of feathers. In birds, such as tree swallows and dove, variation in ambient humidity leads to water uptake and swelling in the outer keratin layer of the feather structure. This response affects the

scattering mechanism thus producing a range of colors depending on the relative humidity of the environment.^{29,43,44}

(e) **Beetle's cuticle**

The protective waxy layer called as cuticle, present on the outer surface of beetles responds to changes in environmental humidity by showing reversible changes in color. Color in desert beetles changes from light bluish-white (low humidity) to jet black (high humidity) due to the water absorption and spreading of wax filaments present on the cuticle. Wing cuticles of longhorn beetles (*Tmesisternus isabellae*) change color from golden to red as environment surrounding them changes from dry to wet.⁴⁵ In wet conditions, water infiltrates the hydrophilic multilayer structure of cuticles and swells the melanoproteins producing red color.⁴⁵

(f) **Dragline silk**

Dragline silk is the structural silk used in web construction by spiders. It consists of amorphous α -helix glycine and crystalline β -sheet alanine domains. Upon exposure to water, the silk undergoes mechanical deformation called as supercontraction. Supercontraction is the phenomenon in which silk contracts to 50% of its initial length leading to generation of high stresses. Molecularly, it has been shown that supercontraction occurs due to water plasticization of glycine domains. Water penetrates the protein domains and disrupts the structure leading to mechanical stresses that makes the silk behave as an artificial muscle in presence of humidity.^{46,47}

2.2 Biological adhesives

Nature provides us with several examples where adhesion is of prime importance. Biological adhesives are one such system that have been broadly classified under the term, ‘Bioadhesives’, which includes other systems such as natural adhesives (adhesives based on bio-based feedstock), biocompatible adhesives (natural or synthetic biomedical adhesives that interfaces with biological tissues and fluids), biomimetic (synthetic adhesives mimicking natural molecular structure and mechanisms) and bio-inspired adhesives (adhesives based designs inspired by biological concepts) (Figure 2.1).⁴⁸

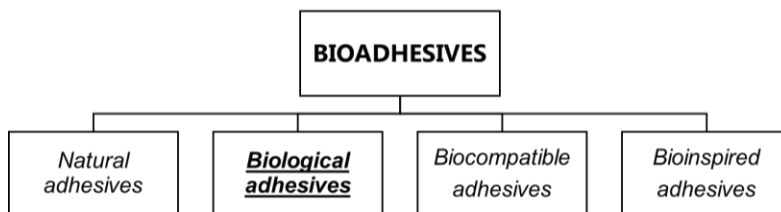


Figure 2.1 Various categories of bioadhesives

Biological adhesives are naturally occurring adhesives that are utilized by a wide range of systems (Figure 2.2) of diverse length scales including cells, bacteria, algae, aquatic organisms, insects, reptiles and plants.⁷⁻⁹ These adhesive systems either operate in air or water, adhere various natural hybrid organic-inorganic structures materials and are responsible for creating an interface between hard and soft materials for structural performance and functionality. The adhesives serve different functions such as locomotion, structure building and colonization, fixation and support, prey capture and predator defense. The different forms in which they are found include cements, fibrous holdfasts, threads, gels, fibrillar nanostructures and viscoelastic secretions.⁷ Figure 2.3 summarizes the form, functions and environment of biological adhesives.

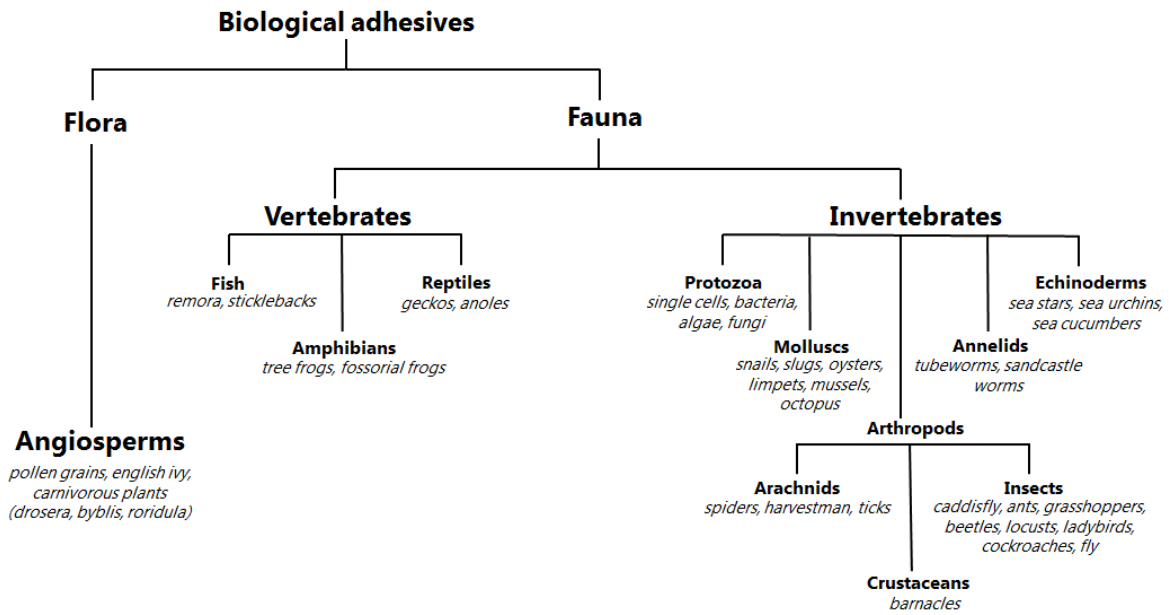


Figure 2.2 Diversity of biological adhesives

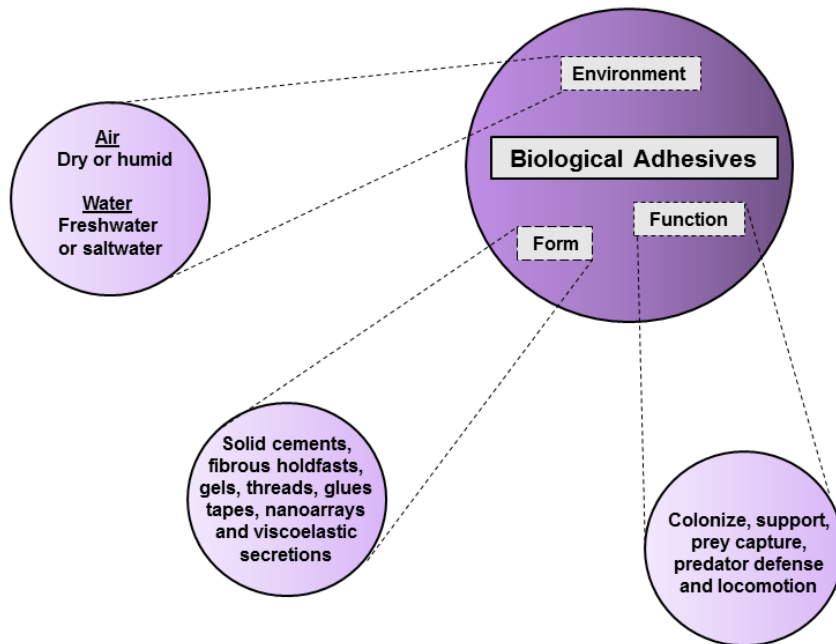


Figure 2.3 Characteristics of biological adhesives

The biochemical composition of biological adhesives is complex with majorly proteins present in combination with other components like carbohydrates, lipids and small molecules with organic or inorganic residues (Table 2.1).⁷⁻⁹ Some examples include proteins in the form of glycoproteins, mannoproteins or in some cases backbone in combination with a functional group such as catechol in mussels, that promotes adhesion; carbohydrates like polysaccharides based on glycosaminoglycans, N-acetylgalactos/glucosamines; lipids in forms of triglycerides, fatty acids, phospholipids, methoxy esters; inorganics residues based on Ca^{2+} , Mg^{2+} , Zn^{2+} and organic compounds like salts, enzymes, carotenoids, acids, peptides, alcohols.

Table 2.1 Summary of chemical compositions for major biological adhesive systems.

System	Types of chemical constituents				
	Proteins	Carbohydrates	Lipids	Inorganics	Organics
Algae	•	•			
Bacteria	•	•			
Barnacles	•	•	•	•	
Caddisworms	•			•	•
Echinoderms	•	•		•	
Frogs	•	•	•		
Fungi	•				
Gecko Feet	•		•		
Harvestmen (Setae)			•		
Harvestmen (Egg Coating)	•	•			
Insects	•		•		•
Ivy	•		•		•
Mussels	•				
Oysters	•		•	•	•
Pollen (Pollenkit)	•	•	•		•
Slugs	•	•			
Spiders (Capture Glue)	•		•	•	•
Spiders (Pyriform Glue)	•		•		
Sticklebacks	•				
Ticks	•	•	•		
Tubeworms	•			•	
Velvet Worms	•	•	•		

These adhesives hold many advantages such as versatility in adhering to surfaces of varying chemical and physical properties, withstanding stress distribution, binding dissimilar surfaces, biocompatibility and resistance to water. Thus, these stand out as potential candidates for studying and translating their basic biochemical and mechanical properties into successful synthetic mimics to solve day-to-day challenges in field of adhesion.⁷

2.3 Capture silk

The spinnerets present in a spider's body are known produce about seven kinds of diverse silk types with each having a dedicated role. The different silks produced include: major ampullate, minor ampullate, pyriform, aciniform, flagelliform, aggregate and tubuliform or cylindrical.⁴⁹ Figure 2.4 illustrates the silk producing glands and respective functions of types of silk they produce.

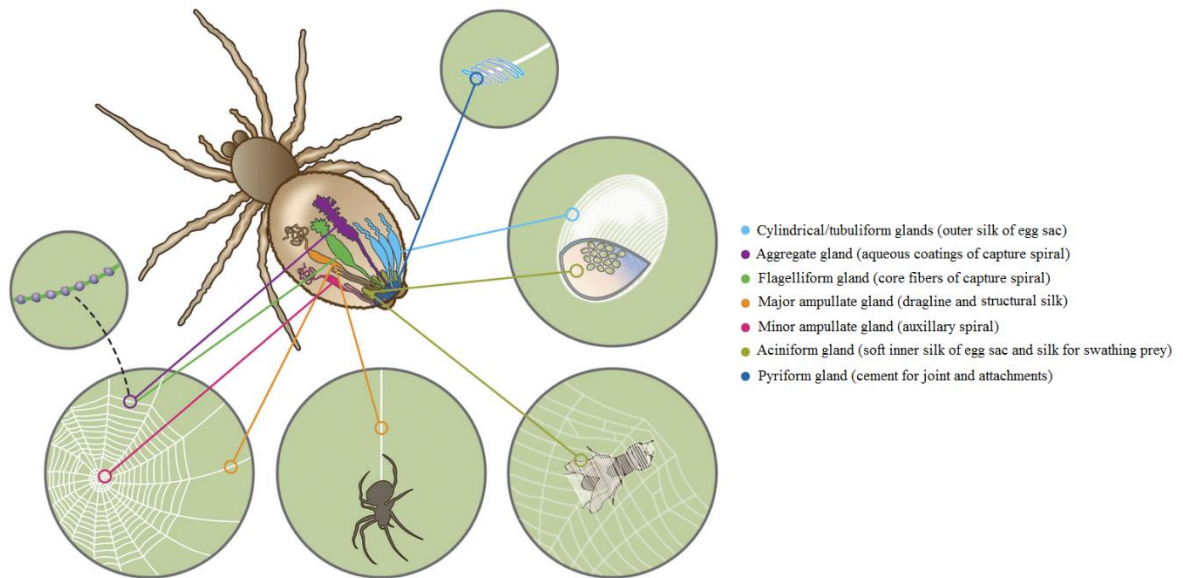


Figure 2.4 Schematic of function-specific seven types of silks produced by spider glands [Reprinted with permission from Ref. 49].

The silks including aggregate glue secretion are associated with web structures that form an integral part of most spiders' life cycles and serves multiple functions such as shelter, prey capture, reproduction, and predator defense⁵⁰⁻⁵². These silk-laden constructs evolved from ancestral sheet structures on the ground consisting of dry silks that might physically entangle prey into highly complex orb web and cobweb structures coated with sticky capture glue from the aggregate gland^{51,53} (Figure 2.5).

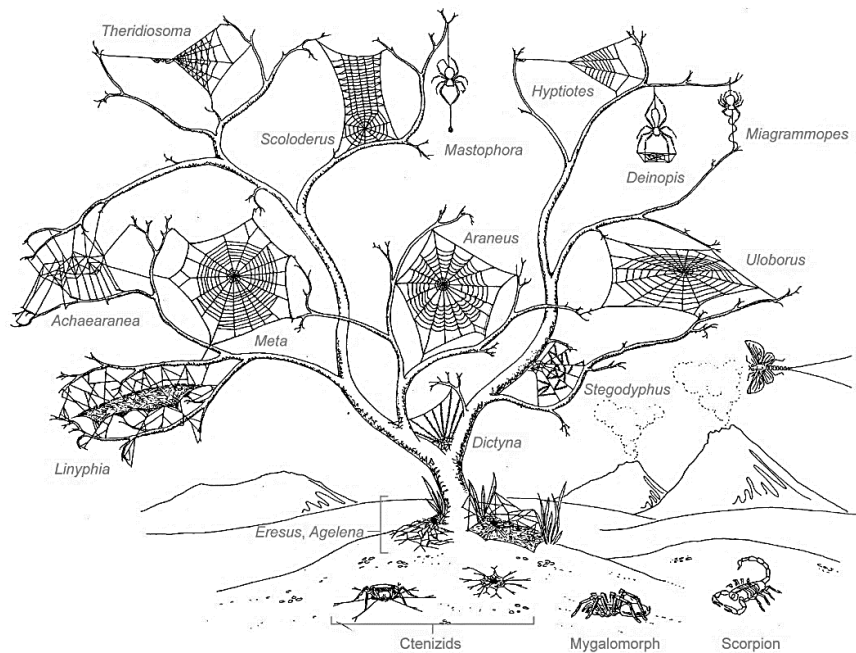


Figure 2.5 Diversity of spider web architectures [Reprinted with permission from Ref. 53].

The current section in the background chapter will focus on capture silks of orb weaving spiders (viscid glue) and cobweb weaving spiders (gumfoot glue) with emphasis on secretion mechanism, chemical nature, structural organization, viscoelasticity and humidity driven adhesion.

2.3.1 Viscid glue

About 4,600 species of spiders fabricate orb webs (Figure 2.6) that involve organization of the capture glue on the spiral part of the web.¹⁷ The glue threads in orb webs are of two types: cribellar and viscid. Cribellar glue is ancient, nanofiber based dry adhesive used by various web building spiders. On the other hand, viscid glue is more recently evolved aqueous and chemically adhesive glue employed by modern orb weaving spiders in entrapping prey on web structures.^{17,50,54} The focus here is on viscid glue whose important characteristics are enumerated as follows:

2.3.1.1 Secretion mechanism

The glue is a combination of axial flagelliform fibers and aqueous aggregate secretions. As a whole, the adhesive is produced by a triad assembly of spinning glands. Axial silk is produced by flagelliform gland, which after being drawn out, gets coated with the glue secretions from the pair of aggregate glands. The glue is coated over the axial fiber as a cylindrical film which ultimately breaks due to surface tension, into series of continuous beads leading to a bead on a string morphology (Figure 2.7) for capture threads.^{17,50}

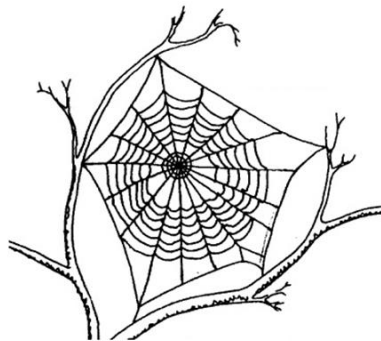


Figure 2.6 Picture of an orb web [Reprinted with permission from Ref. 53].

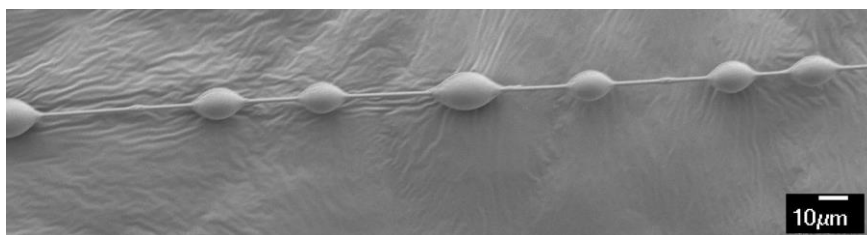


Figure 2.7 Bead on a string (BOAS) geometry for viscid glue from *Larinioides cornutus*.

2.3.1.2 Chemical composition

Viscid glues are known to be majorly composed of three components: glycoproteins, low molecular mass compounds (LMMCs) based on hygroscopic organic/inorganic salts and water. Other hypothesized components include enzymes such as proteinases and lipid like molecules.⁵⁵

Glycoproteins: Glycoproteins form the essential binding medium for adhesion for viscid glues. With the passage of time, many studies have shown the presence of glycoproteins in the glue. In one of the first attempts, trypsin digestion was carried on glue to analyze the smaller fragments by Masamune-Sakamoto method and amino acid analyzer to establish the presence of galactosamine, mannose, galactose, glucosamine, fructose and glucose in the glue.⁵⁶ Optical imaging based evidence showed fibrous core like region (Fig.2.8a,b) at the center of the droplet suggesting glycoproteins.^{57,58} The use of staining methods based on fluorescent lectin molecules confirmed the presence of glycoproteins based on sugar N-acetyl galactosamine in the core of glue.⁵⁸ Gene analysis for spider *Nephila clavipes*, indicated the presence of two genes called as aggregate spider glue 1 and 2 (asg1 and asg2) have been identified in the aggregate secretions. Based on this finding, glue proteins with potential sites for glycosylation have been classified as ASG1 and ASG2 (Fig 2.8c) ASG1

is a 406 amino acid based protein with molecular mass of 45.2 kDa. It possesses charged, hydrophilic amino acids (suggested to be helping in water retention) and characteristics resembling adhesive mucin. On the other hand, ASG2 is 714 amino acid based protein with molecular mass equivalent to 71.5 kDa, known to have similar features as chitin binding proteins and high proline content (like elastin) responsible for elasticity in the glue droplet. The combination of these proteins suggests for adhesion, extensibility and water uptake properties of glycoprotein in the glue.^{55,59} However, in a recent report by Collin et al., ASG1 has been shown to be absent in glue and is found to be a kind of a generic matrix protein common in arthropods, while ASG2 has been confirmed to have spider silk fibroin characteristics that finds itself in the glue apart from being part of other types of fiber base spider silks.⁶⁰

Hygroscopic LMMCs: Apart from the water insoluble proteinaceous material, about 30%-60% of a dessicated orb web mass accounts for water soluble components called as Low Molecular Mass (LMMCs) compounds.⁵⁵ This water-soluble LMMCs part comprises of organic and inorganic compounds that are hygroscopic in nature. Organic LMMCs are small polar aliphatic compounds (amine and sulphate based) accounting for 60% of water solubles.^{55,61-66} Commonly found organic LMMCs have been depicted in Figure 2.9. By far organic LMMCs compounds have been detected in the viscid glues of *Araneus diadematus*, *Araneus cavaticus*, *Argiope aurantia*, *Argiope trifasciata*, *Nephila clavipes*, *Lariniodes cornutus* and *Zygiella atrica*.

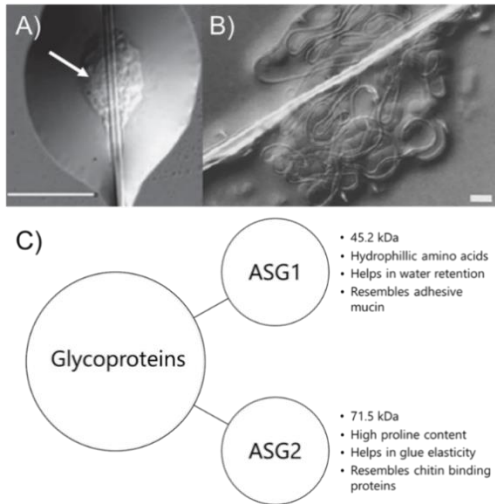


Figure 2.8 A) Glycoprotein core in viscous glue of *Lariniodes cornutus*. Scale bar: 20 μm . (B) Fibrous glycoproteins in glue of *Araneus diadematus*. Scale bar: 10 μm . (C) Schematic illustrating types of aggregate spider glue proteins (ASG) constituting glycoproteins [Figures 2.8a and 2.8b are reprinted with permission from Ref. 70 and 58 respectively].

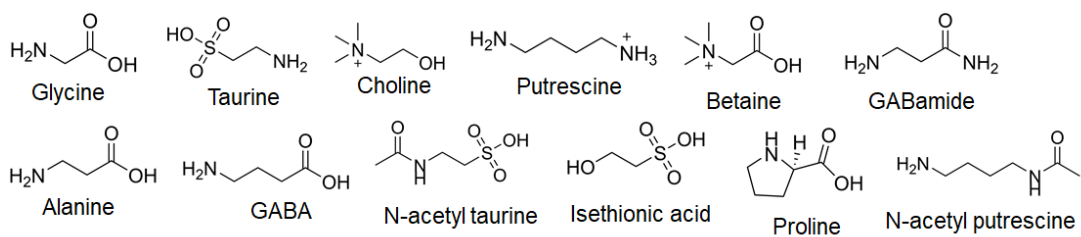


Figure 2.9 Hygroscopic LMMCs found across viscous glues of different species of orbweb weaving spiders.

Inorganic LMMCs comprise of 10-20% of water solubles that majorly include salts based on H_2PO_4^- , K^+ , NO_3^- , Na^+ , Cl^- and Ca^{2+} .^{55,63,65,66} Inorganic LMMs have been traced in adhesives of *Araneus diadematus*, *Araneus cavaticus*, *Argiope aurantia*, *Argiope trifasciata* and *Nephila clavipes* using techniques such as flame photometry, colorimetry, infrared spectroscopy and ascorbic acid method. Some of important characteristics of LMMCs present in viscid glues include:

1) LMMCs differ in their types and compositions across species of spiders. Spiders live in habitats with different humidity levels which has been suggested as a possible reason for salt diversity in their glues to aid in humidity responsive adhesion.²² Also, composition seems to vary depending upon the nutrition/starvation of the spiders.⁶³

2) The high concentration of LMMCs in the glue droplets (about 1-2 M in *Araneus diadematus*) provides vapor pressure to like ambient humidity matching that in habitats of different species. These LMMCs do not crystallize in glue droplets as that in the case of salts such as sodium chloride.⁶⁶

3) The primary role of LMMCs is to take up water from the environment, interact with glycoproteins and render the glue tacky and functional in different humidity conditions.⁶⁷ Apart from helping in water uptake, they are hypothesized to aid in flagelliform protein mobility, prevent water loss and drying of glue droplets, act as neurotransmitters and anti-microbial agents.⁵⁵

2.3.1.3 Structural arrangement

Over the years, different models for the structure (heterogeneous and homogenous) of viscid glue and their connection with adhesion of glue have surfaced:

1. **Heterogeneous:** Two major models describe the heterogenous arrangement of glue. In one case, when glue droplets are laid on glass substrates, optical microscopy evidence showed the formation of a glycoprotein core like region surrounded by a transparent sheet like shell containing salts and water.⁶⁸ Glycoprotein core was thought to be responsible for adhesion but in a study by Opell et al., no positive relationship was seen between size of core and glue adhesion.⁵⁷ Thus, a new type of heterogenous model (Figure 2.10) was proposed which modelled the glue structure to have three distinct regions: a central glycoprotein granule responsible for anchoring the axial thread, a layer of transparent glycoprotein glue surround granule and an outer aqueous cover containing salts. The presence of an additional glue layer was suggested to generate adhesion and contribute to the extensibility of glue droplets.⁵⁷

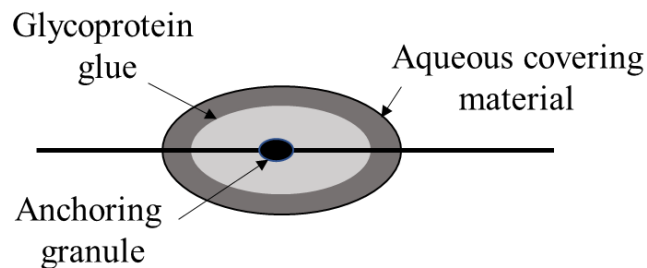


Figure 2.10 Heterogenous structure of viscous glue with different regions

2. **Homogenous:** A study based on Solid-State NMR analysis of viscous glue under different humidity conditions showed the importance of both salts and glycoproteins in adhesion of the glue. These results triggered a new hypothesis of uniform distribution of salt and glycoproteins in the glue droplet.⁶⁷ Amarpuri et al. constructed a three-dimensional map of the glue droplet using Raman spectroscopy and showed that salts and proteins do not segregate into different layers but are ubiquitously present through glue droplet.⁶⁹

2.3.1.4 Viscoelasticity

The adhesion of viscid glues is controlled by viscoelastic forces generated by the glycoprotein present in the glue. Glycoproteins in viscid glue are viscoelastic solids that exhibit both solid and liquid like characteristics. The rate dependent nature is evident in context with the prey capture process. At high extension rates, such as when insect collides with the web, liquid like behavior by the glue generates high viscous adhesive forces that retains the captured prey for a longer time. At low extension rates, as when insect tries to free itself, glue behaves as an elastic solid preventing prey release. Single glue drop load-relaxation experiments have shown generation of a plateau like region corresponding to elastic behavior of glue (Figure 2.11).⁷⁰

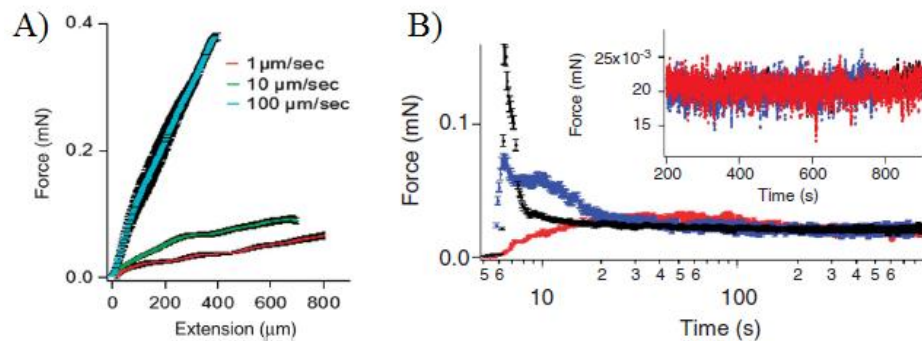


Figure 2.11 (A) Rate dependent pull-off forces for viscid glue droplets. (B) Load-relaxation analysis for viscid glue droplets at $100 \mu\text{ms}^{-1}$ (black), $10 \mu\text{ms}^{-1}$ (blue) and $1 \mu\text{ms}^{-1}$ (red). Inset is an enlargement of the plateau regions for the three conditions [Reprinted with permission from Ref. 70].

2.3.1.5 Humidity mediated adhesion

The adhesion of spider glue droplets is humidity responsive^{17,22,25,70-73} due to presence of hygroscopic salts.^{55,61,62,66} Glue droplets swell by an order of magnitude in presence of water and retain their shape at high humidity.²⁵ The interaction of the glue with water influences key adhesion parameters such as viscosity and droplet extensibility so that they adhere better as humidity increases. Glue viscosity decreases as humidity increases, making the droplets stretch further before they detach from the surface. This increase the work done in peeling until the glue modulus decreases at some very high humidity that little work is done during peeling.^{22,71} Single drop pull off measurements have shown glue droplets adhere weakly in low humidity, strongly in intermediate range and low at high humidity. In overly dry conditions, droplets behave as stiff or rigid materials and are unable to spread and make firm adhesive contact. The volume of the glue droplet also changes with humidity.^{25,72} With increase in humidity, the droplets absorb water and the volume of the glue droplet increases, leading to better spreading and contact on the surface. However, over lubrication in some cases can cause adhesion loss. Further, a recent study based on species belonging to diverse habitats highlighted the behavior of glue adhesion at different humidity environments. It was reported that maximum optimized adhesion always occurred at the foraging humidity of the species. One possible reason behind such behavior is the presence of diverse salts in glues of different species that may control adhesion.²² In another study, molecular and macro level evidence have demonstrated that salts help in water uptake and co-participate with glycoproteins in imparting adhesion in presence of humidity.⁶⁷

2.3.2 Gumfoot glue

The evolution of three-dimensional cobweb structures from more ancient two-dimensional orb web architectures was a major event in the evolution of spider diversity that is associated with an increase in the number and diversity of spider species⁷⁴ and enhanced protection against predators.⁷⁵ The evolution of cobwebs also resulted in novel uses of aggregate glue silk.^{51,74–77} Cobwebs are constructed by the spider family Theridiidae that includes the famous widow spiders in the genus *Latrodectus* (Fig. 2.12a).^{78–80} While the architectures of cobwebs are diverse across species and often behaviorally plastic⁸¹, black widows construct webs with two distinct regions (Fig. 2.12b).^{50,76,82–84} The upper part consists of numerous dry major ampullate (MA) silk fibers, termed ‘scaffolding silk’, that form a sheet structure suspended by supporting threads in a maze-like geometry.

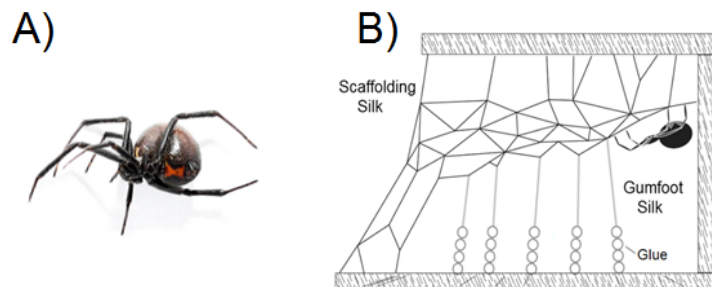


Figure 2.12 (A) Picture of a western black widow spider (*Latrodectus hesperus*). (B) Model structure of the three-dimensional cobweb prepared by *Latrodectus* spiders depicting the two regions: dry scaffolding silk (upper part) and gumfoot silk (lower part) consisting of glue droplets.

The lower part known consists of vertical MA silk, termed ‘gumfoot silk’, coated with adhesive glue droplets (~100 μm in diameter) extending 0.5cm to 2cm up from the

threads' attachment at the base of the web (Figure 2.13). Scaffolding silk mechanically supports the web, knocks down flying prey and provides an avenue on which the spider maneuvers. Gumfoot silk threads capture walking prey when the glue droplets adhere to the prey and the threads detach from their connection to the substrate – tension in the threads then pulls struggling prey up into the air.^{50,76,82–85}

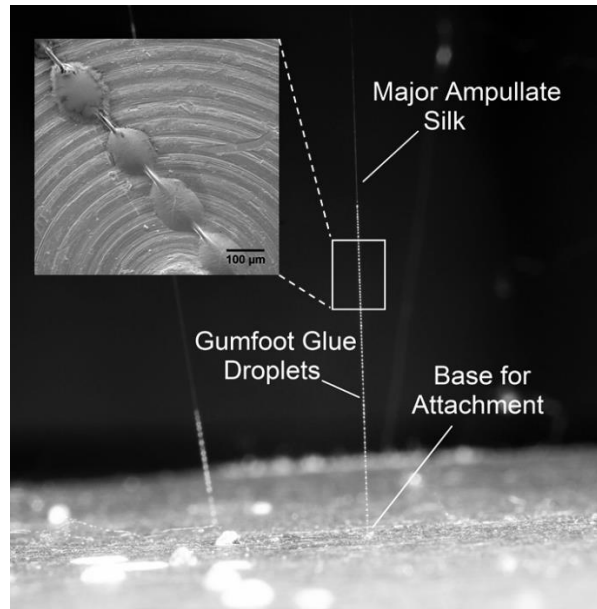


Figure 2.13 The real-time image depicts the structural arrangement of gumfoot silk in a cobweb. The strands are attached to the base and comprise of axial major ampullate silk thread coated with glue droplets. The inset is a SEM micrograph of a strand of gumfoot silk.

Black widow spiders are found in many different habitats^{78,80} and are popular species to study because of the toxicity of their venom. Widow venom generated by them contains a neurotoxin called α -latrotoxin that is active against vertebrate nervous systems and therefore holds biomedical potential.^{86–89} Widow spiders are also model species for the investigation of silk because they are easy to work with in the laboratory, the chemistry

and structure of many of their silks are well-characterized, and their silk gene expression is described at the genomic and transcriptomic levels.^{20,25,85,90–100} Most of this research focuses on MA silk, known for its excellent mechanical properties^{76,84,101}, with the goal of designing high toughness synthetic fibers. The chemistry and mechanism of adhesion of the gumfoot silk has only been a focus of investigation recently^{20,25,95}, but widow spider glue shows unusual performance properties compared to better-studied orb web spiders, which hold promise for application to synthetic adhesives.

2.3.2.1 Secretion mechanism

The aggregate glands produce glues in spiders.^{52,102} There are two pairs of such glands in the cobweb spiders: Typical and atypical. The sticky secretions on the silk strands are produced from the anterior pair of nodular ‘typical’ aggregate glands, which resemble the set of similar glands in orb web spiders.^{55,103,104} During cobweb construction, the glue is secreted from the typical gland after the spider attaches the first MA thread of the gumfoot thread to the substrate and begins moving back up to the sheet while spinning a second MA thread.^{50,76,84} The other ‘atypical’ aggregate gland is used in defenses and prey capture, producing a secretion that is combed out by setae on the tarsi of the fourth legs and subsequently hardens over a few seconds.^{55,103} Our focus here is specifically on the glue produced by the typical aggregate gland.

2.3.2.2 Chemical composition

Hygroscopic LMMCs: As described previously for viscid glue, salts present in glue are often termed as low molecular mass components.⁵⁵ Many of these compounds are also found in aggregate secretions for cobweb spiders. Atypical secretions from *Latrodectus*

mactans and *Latrodectus hesperus* contain GABA, GABamide, choline, proline, glycine and isethionic acid.^{55,103}

Water soluble peptides: Spider Coating Peptides (SCP's) are present in the water soluble extracts from the gumfoot glue.^{20,95} The peptides are classified as SCP-1 (36 amino acids) and SCP-2 (19 amino acids)⁹⁵ (Figure 2.14). While SCPs do not appear to be in the silk protein family, detailed analysis of the peptide sequences using MALDI-ToF revealed sequences, AVHHYEVVPR and TLFNQAADLLDHVV in SCP-1 and SCP-2, respectively, that have also been detected in the water-soluble fractions of egg case silks and scaffolding connection (pyriform) joints. The roles of these peptides in the glue is not clear, although SCP-1 exhibits metal-ion binding capabilities. Other hypothesized roles include participating in oxidation-reduction reactions, acting as anti-microbial agents and affecting the conformation of proteins.⁹⁵

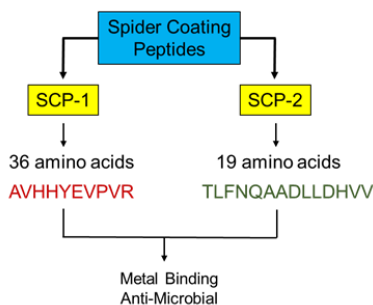


Figure 2.14 Types of spider coating peptides in gumfoot glue of *Latrodectus hesperus*.

Glycoproteins: Proteinaceous compounds have been detected in the combed secretions of *Latrodectus* spiders.^{55,103–105} However, they lack the visible core of adhesive glycoproteins seen in the centers of orb-weaver glue droplets. These results support previous histochemical evidence of glycoproteins in the typical aggregate glands of *Latrodectus* spiders.^{104,105}

Lipids: Lipids based molecules such as fatty acids, long chain methyl esters (1-methoxy alkanes) are in the non-polar solvent washings of webs and in glue droplets of some orb web spiders, including *Nephila clavipes*.^{106,107} Their origin from the aggregate glands is still not clear and they seem to be absent in other orb species.^{108,109} Similar compounds like 1-methoxy alkanes have been detected in cobwebs of *Latrodectus*, but again their presence in gumfoot droplets is debatable due to lack of evidence in the aggregate glands.¹⁰⁹ Nevertheless, it is suggested that lipids in the glue droplets may have anti-microbial properties^{106–108} and repel ants.¹⁰⁷ In addition, lipids may increase the spreading of glue on hydrophobic prey epicuticles and make prey more susceptible to toxic glue compounds by increasing cuticle permeability.^{55,107}

2.3.2.3 Viscoelasticity

The glycoproteins in viscid glue act as viscoelastic solids and this makes a key contribution to how spider orb webs capture prey.^{25,70} Gumfoot glue has strikingly different behavior because the glue droplets behave as viscoelastic liquids (Figure 2.15). When these glue droplets are subjected to a constant deformation, the stress relaxes to zero, indicating significantly reduced crosslinking in the gumfoot glue droplets and the absence of an anchoring core or granule in the droplet structure. The viscoelastic liquid nature of gumfoot glue is further supported by observations of the droplets coalescing, sliding or spreading over the fiber at high relative humidity.²⁵

2.3.2.4 Humidity mediated adhesion

The humidity response of cobweb glue droplets is notably different from orb-weavers. With increase in humidity, droplets of gumfoot glue, unlike viscid glue, coalesce and form bigger droplets that can flow/spread across the axial dragline fiber, but the overall

volume remains largely constant. The lack of a visible proteinaceous core and presence of viscoelastic liquid fluid, compared to orb spiders' viscid glue, likely enables the droplets to coalesce together. Cobweb glue adhesion is also largely invariant to humidity. Single droplet adhesion showed both adhesion force and adhesion energy to be constant with humidity, in contrast to all known orb spiders' glues, and humidity-dependence was seen only with the rate of pulling (Figure 2.16).²⁵

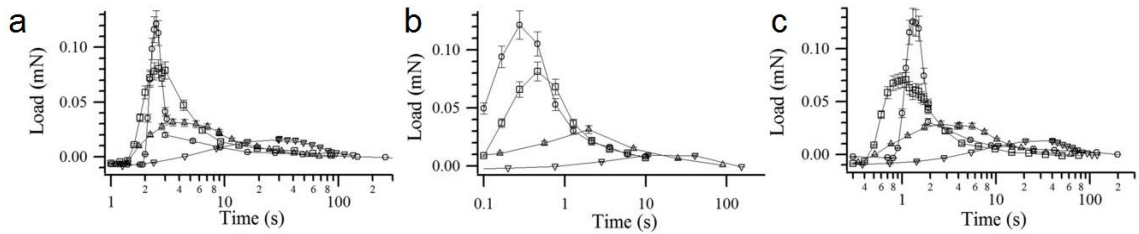


Figure 2.15 (a)-(c) are the load relaxation plots of single gumfoot glue droplet stretched by a constant length at 15% RH, 40% RH and 90% RH respectively. The different symbols represent pull off rates: 1 $\mu\text{m/s}$ (inverted triangles), 10 $\mu\text{m/s}$ (upright triangles), 50 $\mu\text{m/s}$ (squares) and 100 $\mu\text{m/s}$ (circles). [Reprinted with permission from Ref. 25].

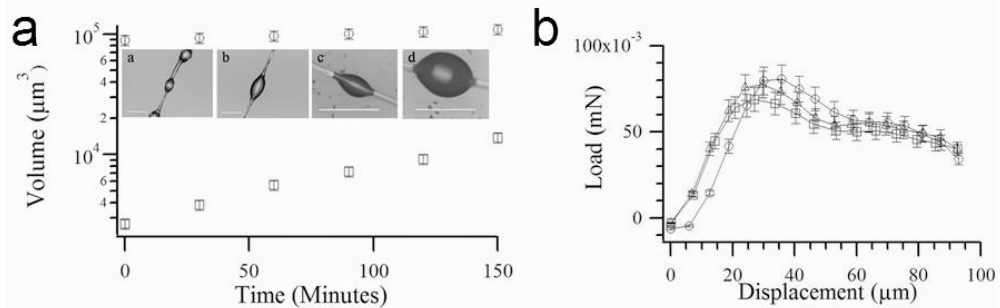


Figure 2.16 (a) shows comparison between gumfoot glue (circles) and viscid glue (squares) droplets for change in volume with time under high humidity conditions. (b) is the single droplet load vs extension at 50 $\mu\text{m/s}$ at 15% RH (circles), 40% RH (squares) and 90% RH (triangles). Reprinted with permission from Ref. 25].

2.4 Gecko setae

Geckos possess a fibrillar ‘smart adhesive’ in their foot pads.¹¹⁰ The sticky hairs are called ‘setae’, helping geckos to locomote on variety of natural surfaces in their dwelling habitats.¹⁹ This adhesive strategy in geckos finds its origin about 100 million years ago, is found in nearly thousand species and involves diverse morphological variations (Figure 2.17) including the presence of adhesive setae on the tails of certain species.¹¹¹



Figure 2.17 Diversity of foot pad architecture in different kinds of geckos [Reprinted with permission from Ref.111].

2.4.1 Characteristics of gecko adhesive system

a) Hierarchical structure

The gecko adhesive system is structurally organized in a hierarchical manner as depicted in Figure 2.18. At mesoscale, the foot pad comprises of adhesive lamellae or scansors (Figure 2.18b) with rows of uniformly distributed and oriented setae. Microscale arrangement comes in the form of arrays of setae that assume a tetrad grid-like pattern (Figure 2.18c). Setal dimensions vary across species with length, width and density being in the range of 78-120 μm , 1-4 μm and 11000-110000/ mm^2 respectively. At nanoscale, multi-level branching occurs in setae where each setae split at the tip into nanostructures called as ‘spatulae’ (100-1,000 in number) having a length and width of 200 nm at the tip.

Spatulae consist of a stalk connected to a thin plate-like triangular end which helps in making intimate adhesive contact with the surface on which geckos move.^{19,110,112,113}

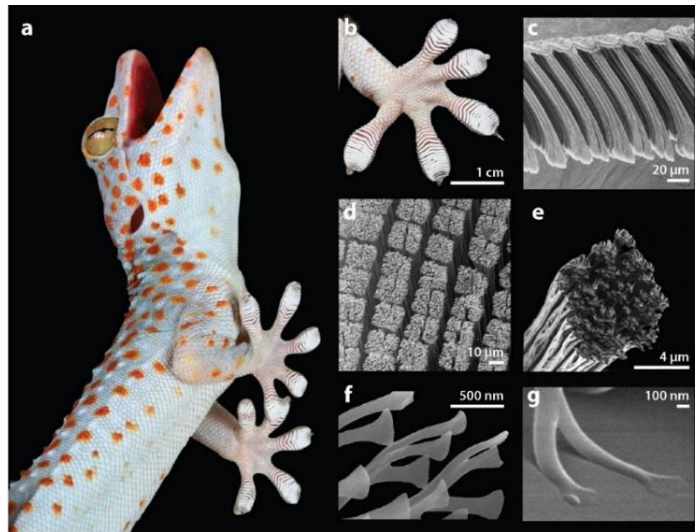


Figure 2.18 (a) A tokay gecko (*Gekko gecko*). (b) Foot of a tokay gecko highlighting scanners or adhesive lamellae (mesoscale) that are covered with rows of setae. (c) A cross sectional view of an isolated setal array. (d) Tetrads of setae present in the scanners (microscale). (e) Numerous branched spatular ends arising from single setae. (f) and (g) Flat and triangular spatular tips (nanoscale) responsible for adhesion to a surface [Reprinted with permission from Ref. 19].

b) **Chemical composition**

Setae are known to be composed of β -keratin and lipids. The detailed description for the two components is discussed in section 2.4.2.

c) **Attachment and detachment mechanism**

The gecko adhesive is a highly dynamic, directional and reversible system. The multi-level adhesive system attaches in a unique way. A single seta has been shown to produce pull off forces $\sim 40 \mu\text{N}$ when subjected to the “load-drag-pull” mechanism in the

following sequence of events: (a) a vertical preload, (b) micrometer scale drag parallel to the surface, (c) drag force in the direction of setae curvature and (d) maintaining setal shaft at an angle less than 30° . The combined effect of normal preload and drag force applied to an isolated seta works in a similar way as in the case of dynamics of gecko locomotion during climbing and thus produces significant adhesive forces.^{19,114} Geckos toes detach from surfaces in about 15 ms due to the factor of setal inclination angle (α). Spontaneous detachment is facilitated when the setal shaft makes an angle more than 30° with the substrate. This dynamic-directional attachment and detachment process seen in geckos often labels their adhesive foot pad as a 'programmable adhesive' that activates on preload and drag while deactivates with an increase in the shaft angle to 30° .¹¹⁴

d) **Microscopic/Molecular principles of setal adhesion**

Prior to the establishment of Van der Waals (vdW) forces in mediating gecko adhesion,¹¹⁵ setae had been hypothesized to adhere onto surfaces by mechanisms such as suction, glue, friction and mechanical interlocking, with all of them being dismissed with credible research investigations. VdW forces are weak intermolecular forces between two surfaces, that scale as $1/(\text{separation distance})^2$. It can be established between (1) a fixed dipole and a nondipolar molecule, (2) two rotating dipoles or (3) a rotating dipole and a nondipolar molecule. These forces increase with the bulk polarizability of surfaces in contact and are not directly related to the surface chemistry of surfaces.¹⁹ Also, VdW forces are the only forces known to make two hydrophobic surfaces stick in air. Evidence based on multiple studies related to strong adhesion of hydrophobic setae to hydrophobic surfaces including OTS and gallium arsenide cemented the fact that VdW forces control gecko adhesion.^{41,112}

Two more mechanisms that have come up now and then in the light of gecko adhesion are electrostatic and capillary forces. Electrostatic forces are active due to the movement of electric charges between two surfaces with one being positive and other negatively charged. The contact electrification hypothesis has been poorly understood and was first put forward in 1904 but turned down in 1934 when it was observed that geckos maintained adhesion in ionized atmosphere, an environment where electrostatic forces do not function. However, a recent study reiterated the importance of electrostatic forces in gecko adhesion.¹⁹ On the other hand, capillary forces that arise due to the formation of liquid bridges when surfaces are in contact has garnered attention and is being continuously studied (examples of studies in section 2.4.3).

e) **Anti adhesion/Superhydrophobicity**

The hierarchical nature of the gecko toe and the surface chemistry of the setae contribute to the superhydrophobicity of the gecko toe pad.¹¹⁶ The gecko toe pad has a water contact angle of approximately 150° and a contact angle hysteresis of 2°–3°.^{116,117} Experimental and theoretical studies relating water contact angle on a gecko setae reported angle between 70° and 90°.¹¹⁶ This means that the setae are neither strongly hydrophobic nor hydrophilic. The chemical and structural differences specific to the adhesive setae suggest that proteins and lipids, and their arrangement, have a functional role in the anti-adhesive system.^{23,118–120} The gecko toe is highly superhydrophobic and stable, even at pressures more than 12 kPa,¹¹⁶ agitation can change the wetting state from the Cassie–Baxter (heterogeneous solid–liquid and air–liquid interface) to the Wenzel (homogeneous solid–liquid interface) (Figure 2.19).^{116,121} In fact, the Wenzel state is the thermodynamically stable wetting state, as shown by wetting of the toe pad by water after

being kept in 100% RH for 3–4 days and by thermodynamic modelling.¹¹⁶ When the gecko toe pad transitions into the Wenzel state, the toe is no longer adhesive,^{121–123} though the gecko is capable of active self-drying by walking.¹²³

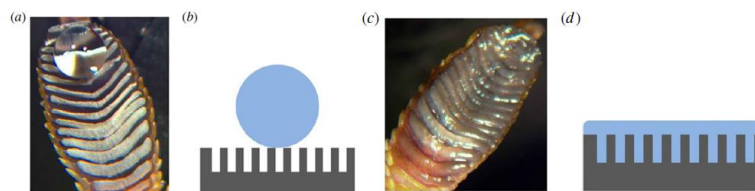


Figure 2.19 (a) The non-wetting Cassie Baxter state highlighting superhydrophobicity of gecko toe pad. (b) Schematic illustrating the non-wetting state. (c) Thermodynamically stable wenzel wetting state. (d) Schematic illustrating wetting of toe pad in wenzel state.

f) **Self-cleaning and anti-fouling properties**

Geckos frequently encounter contaminants in the environments they reside in. These unwanted particles can locate themselves into the fine structure of hairs and thus pose problems in adhesion. However, geckos setae are known to be self-cleaning and anti-fouling towards contamination. The unique cleaning property has been studied to work on the principle of digital hyperextension of toe pads and contaminant rolling (Figure 2.20). Moreover, the contact forces are less between particle-setae as compared to particle-surface, aiding in the cleaning process.^{19,124,125}

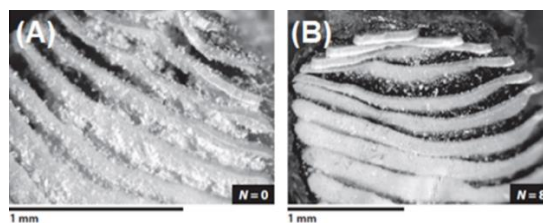


Figure 2.20 (A) and (B) are the images of toe with contaminants, before and after steps (~8) respectively taken on a clean surface highlighting self-cleaning property. [Reprinted with permission from Ref. 19].

2.4.2 Chemical composition of setae

2.4.2.1 β -keratin

In general, keratin is a structural protein that accounts for the most abundant biopolymer found in nature. The major properties of keratin^{126,127} are summarized as follows:

1. It is a complex protein resembling a fiber reinforced composite material having hierarchical structure comprising of polypeptide chains (with large amount of cysteine residues, thiol groups, -SH), filament-matrix structure (crystalline intermediate filaments and amorphous polymer), lamellar regions and a sandwich like arrangement.
2. Based on the arrangement of polypeptide chains, keratin can be divided into two types: α -keratin and β -keratin. α -keratin involves formation of helical structures corresponding to α -conformation while β -keratin consist of side-by-side anti-parallel pleated sheets assuming β -conformation (Figure 2.21). Table 2.2 highlights major features of the two types of keratins. The other classification is based on amount of sulphur crosslinks, categorized as 'hard keratin' which has higher crosslinks, more coherent structure and higher amounts of sulphur as compared weakly structured 'soft keratin' with less sulphur amounts.
3. Keratin possesses excellent mechanical properties and is among the toughest biopolymers with high modulus and toughness.
4. Keratin is found in different forms in nature including horns, nails, hairs and feathers that serve variety of functions such as a source of protection/cover (skin, hair, fur, quill), aggression/defense (nails, horns, claws, beak) and movement (feet, feathers).

5. It bears resemblance to the other important structural protein collagen in terms of having defined amino acid sequences α -helix polypeptide conformations and presence of glycine/alanine contributing to α -form but differs in terms of being a dead tissue that does not vascularize.

Table 2.2 Properties of two types of keratin [Reprinted with permission from Ref. 126].

Property	α -keratin	β -keratin
Structural Feature (Common in both)	Filament-matrix structure: IFs and beta-keratin filaments embedded in an amorphous matrix	
Diameters of filaments (nm)	IFs: ~ 7	Beta-keratin filaments: 3-4
Constituting proteins	The IFs consist of several kinds of low-sulfur proteins while the matrix consists of high-sulfur and high-glycine-tyrosine proteins	Do not have two different types of proteins; the filament and matrix are incorporated into one single protein
Characteristic structure	α -helical structure	β -pleated sheet structure
Molecular Mass	40-68 kDa	10-22 kDa
Examples	Wool, hair, quills, fingernails, horns, hooves; stratum corneum, reptilian epidermis, pangolin scales	Feathers, avian beaks and claws, reptilian claws and scales, pangolin scales

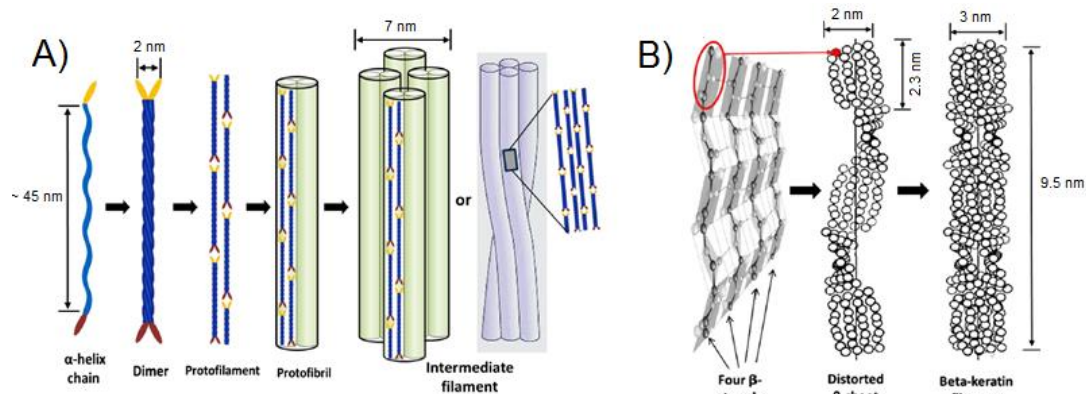


Figure 2.21 Structural arrangement of polypeptides chains in (A) α -keratin and (B) β -keratin [Reprinted with permission from Ref. 126].

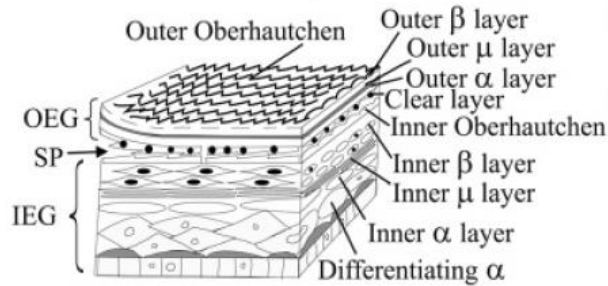


Figure 2.22 Different layers in the keratin based epidermis of a gecko [Reprinted with permission from Ref. 128].

In geckos, keratin is found as both α (inner soft layers) and β (hard outer layer) forms in the epidermal layers. The six different layers in the gecko epidermis (Figure 2.22) include oberhautchen, β , mesos, α , lacunar and clear layer. The cells present in the top two layers, oberhautchen and β -layer produce the hard corneous β -keratin while the cells in the inner layers are responsible for the accumulation of α -keratin. The epidermal layers are present as outer and inner generation forms. The inner generation layers are exposed as soon as the outer layers are shed as a part of the molting cycle.¹²⁸

The cells in the oberhautchen and β -layers produce two different types of structures on the epidermis of geckos (Figure 2.23). The first structure called as ‘spinulae’ is present on the normal scales (non-adhesive skin) and are 1-3 μm in length. On the other hand, the spinulae on the pad lamellae outgrow and form specialized ‘setae’ (20-100 μm long) having multiple ending structures known as ‘spatulae’ and responsible for adhesion of the foot pad. Before molting, the inner generation setae grows by accumulating beta keratin filaments to form longer elongations that constitute emerging new setae of the pad lamellae.^{120,129}

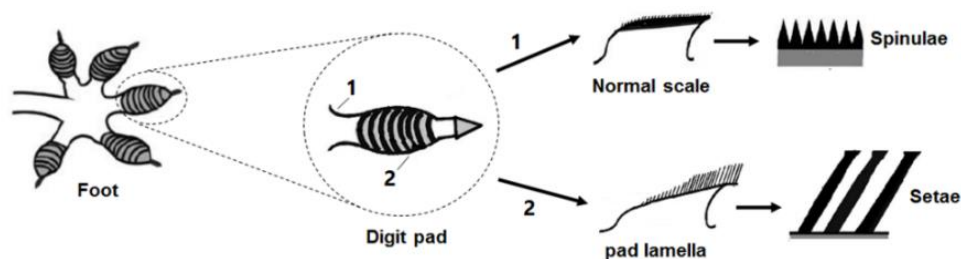


Figure 2.23 Structural features present on the epidermis of a gecko [Reprinted with permission from Ref. 129].

Apart from the two-alpha keratin based proteins (52-53 kDa), the proteins forming setae have been termed as keratin-associated beta proteins (KA β Ps) having a molecular mass of 10-21 kDa. The proteins have been characterized by western blotting, histological, immunocytochemistry, ultrastructural immunolocalization and molecular biology based techniques. The KA β Ps are classified as (1) HgG (high glycine), (2) HgGC (high glycine and cysteine), (3) HgC (high cysteine) and (4) LwGC (low glycine and cysteine) beta-proteins. Altogether three glycine rich beta proteins (17-21 kDa) and sixteen cysteine rich beta proteins (10 kDa) have been identified in the setae. Some examples include HgGC10, containing 13% glycine and 14.5 % cysteine and HgGC3 with 9% cysteine.¹³⁰

The β -keratin nature of the setae has also been established by: (1) Microbeam X-ray diffraction where the diffraction pattern of setae showed the presence of ordered protein structure similar to characteristic β -keratin signature, (2) Gel electrophoresis of extracted setal proteins showed the presence of β -keratin (14-20 kDa) protein and (3) Raman microscopy results for setae and its comparison with that of results for alpha keratin based sheep wool and other β -keratin system, bird feathers confirmed presence of proteins based on β -keratin. Structural characterization of setae by electron microscopy based methods

such as scanning electron microscopy (SEM) and transmission electron microscopy (TEM) have shown the presence of protein fibrils and matrix like region in the setal structure.^{131,132}

2.4.2.2 Lipids

Traditionally, lipids are defined as water-insoluble biological molecules that dissolve readily in organic solvents. The general structure of a lipid consists of two major parts: a polar head group and a non-polar hydrocarbon chain. The major classes of lipids (Figure 2.24) include: fatty acyls, glycerolipids, glycerophospholipids, sphingolipids, sterol lipids, prenol lipids, saccharolipids and polyketides.¹³³

These amphiphilic molecules serve different purposes in biological systems. In cell membranes, they are a source of fuel supply, act as reservoirs of energy storage and participate in signaling mechanisms. Other than these roles, they show active participation in membrane structures by forming bilayers, micelles and vesicles as well as non-covalently adhering with protein moieties to promote selective permeability in cell structure.¹³⁴ On a larger length scale, lipids are present in biological structures as a promoter for physical resistance and water barrier in epidermis,¹³⁵ hairs and feathers,^{136,137} as protective coating in dragline silk¹³⁸ and more recently as a key material component in biological adhesives in systems including plants, marine organisms and terrestrial organisms.^{8,11,118,139,140}

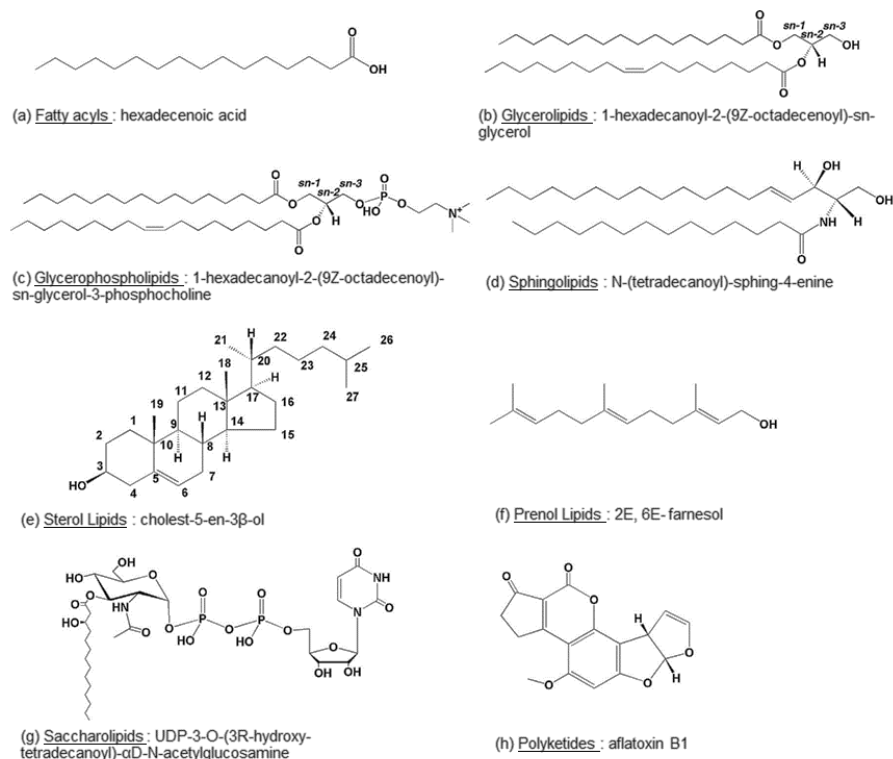


Figure 2.24 Different classes of lipids found in biological systems [Reprinted with permission from Ref. 133].

As outlined in the previous sections, gecko adhesive system is based on microscopic hairs made up of β -keratin,¹²⁰ works on van der waals forces. However, the recent discovery of gecko footprints¹¹⁸ bearing lipid signatures evoked interest and has been of interest lately in understanding both the material properties and adhesion mechanism of hairs with respect to lipids. Gecko adhesion has always been considered a dry phenomenon, and with lipids being present as in case of insect footprints, their role in gecko adhesion is intriguing. Apart from suggested role in wet adhesion, lipids in gecko setae have been hypothesized to serve a host of functions (Figure 2.25) that include contribution to the unique properties of self-cleaning and superhydrophobicity,

participation with β -keratin fibrils in the self-assembly of setal structure, acting as sacrificial layer to maintain the integrity of structure against wear related to the hairs and maintaining the hydration level of setae by acting as a barrier layer.

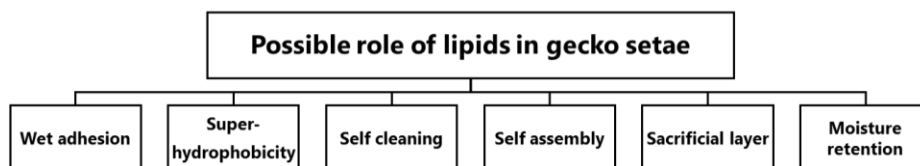


Figure 2.25 Schematic outlining various hypothesis for role of lipids in the gecko setae.

Lipids in setae have been characterized by several methods including visual observation of footprints using moisture condensation and staining methods,¹¹⁸ histochemical and ultrastructural analyses¹¹⁹ to establish presence and location of lipids in setae, surface sensitive Nano-assisted laser desorption-ionization mass spectroscopy (NALDI) to establish the types and spatial location of lipids and interface sensitive Sum frequency generation spectroscopy (SFG)¹¹⁸ to understand the interaction of lipids with water at the contact interface of a toe pad and substrate. Details of each are as follows:

1. Moisture condensation and footprint staining:

The invisible residues obtained on clean glass surfaces after Tokay geckos (*Gekko gecko*) stepped over them, were subjected to high humidity environments. Moisture condensation was observed on the region where gecko footprints were present (Figure 2.26a,b) while rest of the surface was wetted by a thin layer of water. This observation confirmed the presence of hydrophobic nature of footprints left by geckos as they walk. The footprints were also stained with a neutral lipid sensitive dye, Oil Red O as depicted

in Figure 2.26c. The image shows the presence of a lipid based material present across the footprint residue.^{118,141}

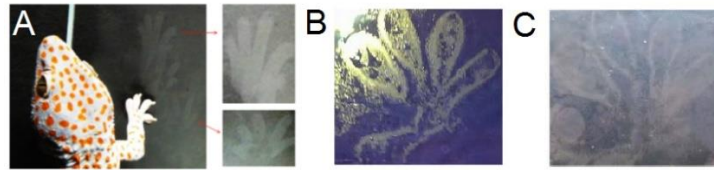


Fig. 2.26 (A) and (B) are moisture condensation images of a gecko (Tokay) footprint on clean glass substrate. The footprints in (A) were subjected to 98% humidity while those in (B) were first cooled with dry ice and then exposed to humid air. Hydrophobic regions were outlined with the droplets of water. (C) Gecko footprint stained with Oil Red O dye [Reprinted with permission from Ref. 141].

2. Histochemical and ultrastructural analysis of adhesive setae:

The presence and distribution and details in the adhesive setae was studied by Alibardi et al. for geckos, *Phelsuma dubia* and *Anolis carolinensis*. On staining the toe pad sections with Oil Red O, light microscopy images (Figure 2.27) showed lipids present in the spinulae stalks, vertically aligned outer setae (including horizontally extensive oberhautchen β -layer), growing inner setae and in dermis as lipid droplets and vesicles. The ultrastructural analysis found that lipids are spatially present in maturing setae during their renewal cycle of epidermal regeneration.¹¹⁹



Figure 2.27 Light microscopy image of scansor belonging to *P.dubia* showing the presence of lipids (indicated by orange staining) in outer setae (os), inner setae (is), oberhautchen layer (o), dermis (d). Scale bar: 200 μ m [Reprinted with permission from Ref. 119].

3. Nano-assisted laser desorption-ionization mass spectroscopy (NALDI)

NALDI experiments on footprints showed the presence of phospholipid and sphingolipid signatures. Spatial distribution of the detected lipids was analyzed by the footprint image where brighter regions corresponded to areas where hairs were in contact with the surface accompanied by higher concentration of the ion being detected. By means of additional tandem experiments, six-phosphocholine based molecules including 1,2-dipalmitoyl-sn-glycero-3-phosphatidylcholine (presence of m/z 184 corresponding to phosphocholine head group) and sphingomyelin containing D-erythrospingosine were detected in the footprints (Figure 2.28).¹¹⁸

4. Sum frequency generation spectroscopy (SFG)

The presence of lipids in setae was also confirmed by using an interface specific spectroscopy method called as SFG, that provides the molecular information of the chemical composition of the contact interface. In a SFG experiment, contact of the gecko toe with a dry sapphire prism showed the presence of exclusively methyl and methylene groups from lipids at the contact interface, confirming presence of hydrophobic signatures in the setal structure. Similar signatures were visible on peeling the toe from the surface and analyzing only the residual footprint. On a wetted sapphire surface, the contact of the toe still showed the presence of methyl and methylene moieties suggesting the gecko toe continuing being hydrophobic in presence of water. All spectra have been shown in Figure 2.29.

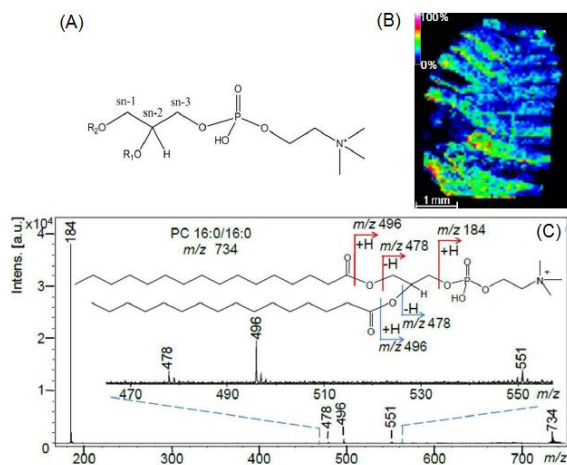


Figure 2.28 (A) General structure of phosphocholine based lipids. (B) Mapping image collected for peak m/z 184. (C) Tandem mass spectrum for the detection of m/z 184 [Reprinted with permission from Ref. 141].

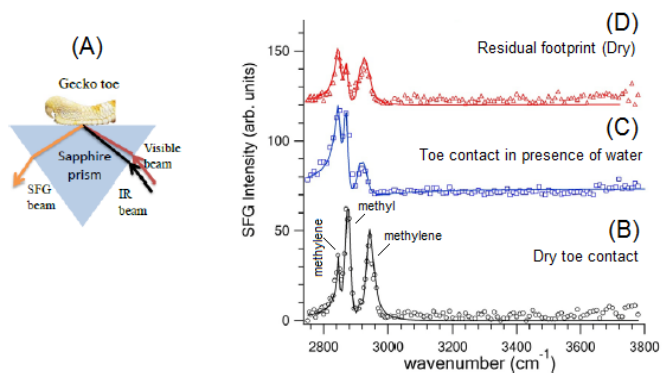


Figure 2.29 (A) Experimental set up for SFG of a gecko toe in contact with sapphire. (B)-(D) are the SFG spectra collected for dry toe contact, water wetted sapphire in contact with toe and dry footprint contact after peeling the toe from the sapphire surface respectively [Reprinted with permission from Ref. 141].

Based on the NALDI and SFG findings and work reported by Rizzo et al., Hsu et al. proposed two models for the arrangement of lipids in the gecko setae. In the homogenous model, the lipid layer forms an outer covering on the keratin spatulae. The

heterogeneous model accounts for either the lipid present between the keratin rods at the tips of spatulae or inter-dispersed with keratin in the spatula (Figure 2.30).¹¹⁸

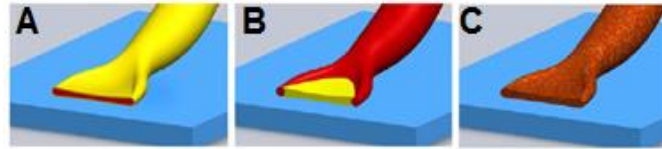


Figure 2.30 Models of arrangement of lipids (yellow) in setal hairs. (A) shows the homogeneous model where lipids cover keratin spatulae (red). (B) and (C) are the heterogeneous models where lipids are hypothesized to present between two spatular ends (B) or intimately mixed with keratin in the hairs (C) [Reprinted with permission from Ref. 141].

2.4.3 Gecko adhesion in presence of water

Geckos, about >1000 species encounter water in their natural environment such as tropical rainforests where water in the form of rains or due to high humidity makes the surfaces they move on, frequently wet.¹¹³ In the light of understanding gecko adhesion in environmentally relevant conditions, the mechanism of setal adhesion in presence of water has been of interest to researchers lately. The work on interaction of water has been investigated in two different ways. In first case, studies involve effect of surface water^{121-123,142-144} while the second set of studies concentrate on the role of high humidity on gecko adhesion.^{16,41,145-150} Adhesion of setae has been shown to enhance in presence of high humidity. Studies based on effect of humidity (in the form of adsorbed layers of water on setae) started off with clearing the perspective related to the mechanism (VdW or capillary forces) mediating adhesion in presence of humidity. At present, the gecko literature dwells

on the hypothesis of change in the mechanical properties of setae (setae softening) leading to enhancement of VdW forces in presence of humidity.

(a) **Surface water**

The relationship of surface water and gecko adhesion has been studied as a function of different parameters such as surface energy of setae, substrates (wetting conditions, surface energy, architecture, roughness) and presence of surfactants. In of the first attempts, change in surface wetting characteristics of setae on exposure to water was studied. Exposing a water droplet for about 20 minutes on a setal array converted the superhydrophobic cassie state (160°) to wetting wenzel state for the hairs. Water contact angle of the bulk keratin surface changed from 96° to 86° indicating change in the conformational state of amino acids constituting surface setal proteins. Adhesion of fully immersed setal arrays in water onto silica surface was seen to be reduced by about threefold due to the decrease in VdW forces in water.¹⁴⁶

The effect of surface water on shear adhesion of whole animal was studied on glass substrates for different wetting conditions (misted glass, submerged glass in water and soaked toe pads). It was observed that wetted and fully submerged toe pads showed lower adhesion on glass as compared to control dry toe pads. This observation is suggested to occur due to Cassie-Wenzel transition that renders the wetted toe anti-adhesive.¹²¹

Gecko adhesion as a function of surface wettability was tested for whole animal on four different surfaces (glass, polymethylmethacrylate (PMMA), octadecyltrichlorosilane self-assembled monolayer (OTS-SAM) and polytetrafluoroethylene (PTFE)) in dry and submerged conditions. Results showed (a) adhesion to be lower on submerged hydrophilic glass as compared to the dry condition, (b) no significant difference in wet and dry adhesion

on intermediate wetting (PMMA) and hydrophobic surface (OTS-SAM) and (c) adhesion on wet PTFE was significantly higher as compared to dry PTFE. These results were supported by a thermodynamic model of adhesion for different surfaces outlining ratios of shear adhesion in presence of water to that in dry air conditions. Also, in case of hydrophobic surfaces, higher adhesion in wet conditions was suggested to be due to the observed air plastron present near toe pads, aiding in expelling water surrounding contact interface and creating a dry environment.¹⁴²

Motivated by gecko locomotion on natural surfaces with different architectures, shear adhesion was tested on synthetic well-defined polydimethylsiloxane elastomer based patterned surfaces (Sharklet[®]) and smooth control surface in air and water. While geckos stuck equally well on surfaces in air, variability was seen in presence of water. The adhesion for smooth surface was much higher than the patterned surfaces in water which probably can be due to water seeping into the structured channels and reducing the available contact surface area as hypothesized in the study. Results were further explained by means of model based on nature of contact interface (dry or wet) between two adhering surfaces predicting the presence of water at contact interface for structured samples leading to lower forces in water.¹⁴³

The higher adhesion of geckos to wet PTFE (study discussed above in point 2) due to the hypothesized factor of roughness, triggered the basis of the study that involved testing gecko adhesion on a variety of smooth fluoropolymer based substrates (polytetrafluoroethylene (PTFE), fluorinated ethylene propylene (FEP), ethylene tetrafluoroethylene (ETFE)) and a non-fluorinated control (polyethylene terephthalate (PET)) in dry and wet conditions. The major findings included (a) higher adhesion on wet

fluoropolymers compared to dry as seen previously (b) higher adhesion in dry and wet conditions as compared to the previous PTFE study, due to elimination of the roughness factor, (c) dependence of adhesion on the degree of fluorination of substrate with effect being more prominent in dry conditions and (d) theoretical interfacial energies based on surface energy calculations for the substrates predicted wet to dry normal adhesion ratios complementing trend in adhesion based on fluorination.¹⁴⁴

The role of the air plastron in gecko adhesion was studied by the introduction of anionic and non-ionic surfactants (leading to decrease in surface tension and an unstable plastron formation) in testing adhesion of whole animals on glass, OTS-SAM and PTFE substrates in wet conditions. It was observed that air plastron was not formed in case of anionic surfactant leading to low adhesion on three substrates. In case of non-ionic surfactant, plastron was found to be more stable and thus adhesion was seen to be higher on substrates except glass. These results suggested that the combination of air plastron (necessary to render toes dry), contacting substrate and interfacial energies of surfaces involved control adhesion on wet surfaces.¹²²

The importance of surface chemistry of setae in adhesion was tested by tuning the toe pad molts from geckos to plasma based polar/hydrophilic (maleic anhydride) and non-polar/hydrophobic (perfluoro) coatings. The chemically modified sheds were then tested in dry and wet conditions on hydrophilic (glass) and hydrophobic (OTS-SAM) surfaces. Adhesion of the sheds was seen to be dependent on wettability of substrate with reduced adhesion on hydrophilic glass and consistent adhesion on hydrophobic OTS-SAM substrate. The surface chemistry of setae was seen to be inert towards dry and wet adhesion

across substrates indicating setal surface chemistry to be a less important factor in adhesion of hairs in air or water.¹¹⁶

(b) **Humidity**

In two separate spatular level studies by Huber et al.¹⁴⁵ and Sun et al.,¹⁴⁹ capillary forces were suggested to be the mechanism behind enhanced adhesion in high humidity. Huber et al. using surface force apparatus, tested adhesion of single spatulae on surfaces with varying degrees of hydrophilicities under different humidity environments. It was observed that adhesion of a spatula increased with increase in the hydrophilic nature of substrate and increase in humidity of atmosphere. These observations stressed upon the role of capillary bridges between spatula and substrate to enhance adhesion. Sun et al. tested the spatular adhesion on hydrophilic and hydrophobic cantilevers with atomic force microscopy in different humidities. They observed an increase in adhesion with hydrophilic surface as compared to hydrophobic, thus suggesting role of capillary forces as opposed to VdW forces. Niewiarowski et al. tested whole animal adhesion in environments of different humidities to observe an enhanced adhesion in high humidity. Temperature factor was also introduced in conjunction to humidity where the dual effect of both these factors enhanced adhesion at conditions of high humidity (80% RH) and low temperatures (12⁰C). Clarity about mechanism underlying these observations based on humidity-temperature effects were not clear.¹⁶ Kim and Bhushan numerically calculated the capillary contributions by considering attachment of single spatula with surfaces on different contact angles to find that hydrophilic surfaces enhance adhesion in presence of increasing humidity environments.¹⁵⁰ In a study by Pesika et al., apart from conducting adhesion of setal arrays in immersed state (discussed previously in surface water section),

performed it in a high humidity environment to observe enhanced adhesion. The reason was attributed to increase in surface energy (conformational energy of proteins) of setae on exposure to high humidity.¹⁴⁶

Puthoff et al. brought up the new hypothesis of setal softening in presence of high humidity governing VdW forces based enhanced adhesion. The hypothesis was supported by high humidity dynamic mechanical analysis (DMA) of setal arrays which showed a decrease in modulus and an increase in loss tangent. Additionally, shear adhesion of setal arrays tested on hydrophilic and hydrophobic surfaces in high humidity did not show any differences in adhesion, indicative of VdW forces and not capillary forces responsible for adhesion.⁴¹ Chen and Gao numerically modelled the vertical peeling process of a spatula by taking in consideration the experimentally found stiffness parameters for beta keratin in presence of humidity. Their results showed an increase in the pull-off forces of the pad under the influence of humidity.¹⁴⁸ Prowse et al. tested tensile deformations, fracture and dynamic mechanical response of individual setae and found a decrease in the mechanical properties in high humidity. Increasing humidity led to a decrease in stiffness, increase in failure to strain and a drop in the modulus of setae. These findings supported the hypothesis of setal softening responsible for enhanced adhesion in presence of high humidity.¹⁵¹ Tan et al. studied the effect of humidity component on adhesion of setal arrays on various surfaces by relating it to factors such as preload, sliding velocity and sliding direction. Adhesion was seen to enhance with humidity (about 60%) when setal arrays were subjected to a preload of 17.12 kPa but weakened when increased to 21.41 kPa and 34.32 kPa. Enhancement was suggested to occur on the account of softening of setae.¹⁴⁷

CHAPTER III

STICKY BUSINESS IN COBWEBS OF BLACK WIDOWS: DESIGN, HUMIDITY DRIVEN ADHESION AND MOLECULAR MECHANISMS OF GUMFOOT GLUE

This work has been previously published as

Jain, D., Zhang, C., Cool, L.R., Blackledge, T.A., Wesdemiotis, C., Miyoshi, T. and
Dhinojwala, A. *Biomacromolecules* **16**, 3373-3380 (2015).

and has been part of

Jain, D., Blackledge, T.A., Miyoshi, T. and Dhinojwala, A. in *Biological Adhesives*
(ed. Smith, A.M.) 303-319 (Springer International Publishing, 2016).

3.1 Introduction

Biological adhesives⁷⁻⁹ such as glues in a variety of aquatic animals^{11,13,14,152-155}, keratin hairs in gecko setae²³ and pollenkitt in pollen⁴² maintain adhesion in the presence of water or humid environments^{16,18,41} and in some cases even make strong bonds by displacing water from the contact interface^{152,153}, a feat that has been hard to match using synthetic glues.^{2,3,156-159} Hence, there is a strong need to understand the composition and mechanism of adhesion in biological materials with an ultimate goal to use those principles for fabricating synthetic adhesives that work in varying environmental conditions. Capture silks are produced by web building spiders to subdue their prey.^{17,50} In the case of orb web

spiders, the capture silk is known as ‘Viscid Silk’ and consists of a bead-on-a-string morphology, where the thread is spun from silk produced in the flagelliform gland and the glue in the beads comes from the aggregate glands.^{17,50,160} The aggregate secretions are a combination of glycosylated proteins^{55,56,58,59,69,70,161,162}, termed ‘Aggregate Spider Glue (ASG)’: ASG1 and ASG2,^{55,59} and a range of hygroscopic, low molecular weight organic and inorganic salts that constitute ~70-80 % of water soluble mass.⁵⁵ The salts, such as GABAamide, Betaine, Choline, N-acetyl taurine, KNO₃, KH₂PO₄, aid in water uptake that makes the silk tacky in humid conditions.^{55,61–67,163} The salts also directly interact with and stabilize the glycoproteins.⁶⁷

Many new web types evolved after the origin of aggregate glands that utilize viscid glue in novel ways.⁵¹ One of the most dramatically different web type is the cobweb, built by a family of spiders known as *Theridiidae*.^{76,80,84} The *Latrodectus* widow spiders belonging to *Theridiidae* family are distributed worldwide in a variety of geographical zones and include well-known spiders like black widows, Australian red-backs and brown widows.⁸⁰ *Latrodectus hesperus* (western black widow) constructs three-dimensional cobwebs (Figure 3.1a) that use gumfoot threads that act as spring loaded traps adhering to walking prey. The aggregate glue is found only in the 0.5-2 cm lower portion of the gumfoot thread (Figure 3.1a,b), which is composed of an axial core of major ampullate silk.^{50,76,84} This contrasts with the viscid silk of orb-weavers where the aggregate glue is distributed all along a highly elastic, two-dimensional spiral of silk that targets mostly flying insects.⁵⁰ The aggregate secretions¹⁰³ form of much larger glue droplets (Figure 3.1c) as compared to viscid silk.²⁵ The composition of the ‘gumfoot glue’ produced by

cobweb spiders, is relatively unknown although it does contain novel water soluble spider coating peptides (SCP-1 and SCP-2).^{55,95}

Cobweb spider glues appear functionally different from typical orb spider glues. Compared to the viscid silk produced by the orb spider *Larinioides cornutus*, *Latrodectus hesperus* gumfoot glue showed much weaker humidity response.²⁵ In addition, the viscid silk exhibited viscoelastic solid-like properties⁷⁰ where the stress did not relax completely with time while the gumfoot glue showed a viscoelastic liquid like properties, where the stress relaxed to values close to zero.²⁵ The glue droplets also lack the heterogeneous core that is visible at the centers of orb spider glue droplets. These differences in adhesive and structural properties suggest that aggregate secretions in cobwebs spiders may have evolved unique compositions. It is also unlikely that just a mixture of water and SCPs⁹⁵ are sufficient to impart strong adhesion in gumfoot glue. These observations raise several questions such as (1) What else is present in these large glue droplets of gumfoot silk? (2) Does the material properties of glue affect the humidity response towards adhesion?

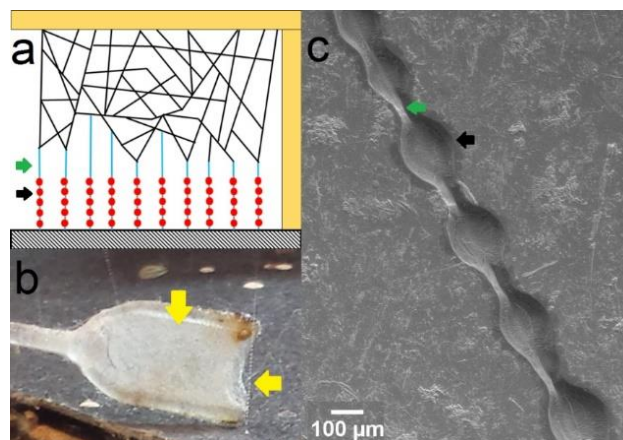


Figure 3.1 (a) Schematic of a cobweb built by the western black widow. The gumfoot silk thread is composed of beads of adhesive glue (black arrow) on a major ampullate silk thread (green arrow). (b) Collection of gumfoot threads (yellow arrow) from the base of web by using a glass fork. (c) SEM micrograph of a gumfoot silk thread (glue; black arrow and major ampullate silk; green arrow).

To answer these interesting concerns, we first used Solution and Solid-State Nuclear Magnetic Spectroscopy (NMR), Matrix Assisted Laser Desorption Ionization Mass Spectrometry (MALDI-MS), and staining to characterize and understand the design principles of gumfoot glue produced by black widows. Secondly, we correlated the compositional analysis with how the thread adhesion changes as a function of humidity for both pristine and washed gumfoot silk threads. Finally, we studied the molecular mechanism of glue to understand the role of its components in the humidity response. The goal is to understand the material properties of the glue and correlate it with its humidity response towards adhesion and molecular mechanism. The study will clear the understanding of functioning of capture glues and offer insights in new ways to design synthetic bio-inspired adhesives.

3.2 Experimental Section

Spider care/housing: In order to collect gumfoot silk for studying the material and adhesion properties of glue droplets, about 40 adult female *Latrodectus hesperus* (western black widow) were purchased from Bugs of America (Arizona, USA) and housed in custom-built plastic cages lined with cardboard frames to promote cobweb building.^{76,84} The spiders were fed with crickets twice weekly and cages were misted with water once every week.

Extraction of water-soluble components from gumfoot strands: To extract and analyze the water-soluble components from glue droplets, gumfoot silk strands were collected onto a custom built glass fork (Figure 3.1b). Silk threads were collected over a period of six months to yield five samples – 3000, 750, 450, 350 and 150 strands. Sample collections were done at room humidity (20-30% RH). The larger samples were used for Solid-State NMR while the smaller samples were used less-sample intensive techniques like Solution-State NMR. Each set of collected silk strands were washed with 10 ml of deionized water followed by lyophilization of the washed residue to procure the dried extract. The water-soluble extract was weighed and refrigerated until it was used for Solution-State NMR and MALDI experiments. The washed gumfoot silk (silk after the removal of water soluble components) was dried and preserved for the microscopy experiments.

Solution-State NMR: Solution-State NMR measurements were used to trace the presence of salts in the water-soluble extract. A part of the water-soluble extract was dissolved in 99.96% deuterated water (~1 ml) (Cambridge Isotope Laboratories) and packed in the 5mm NMR tube (Norell) for analysis. To identify the peaks in the NMR spectra of water soluble extract for salts, commercial standards of GABA, Isethionic Acid and Choline Acetate

(Sigma Aldrich), and GABamide (provided by Dr. Townley, University of New Hampshire) were solubilized in deuterated water and packed in NMR tubes. Proton spin-lattice relaxation (T_1) measurements were carried to determine the appropriate recycle delay for quantification experiments. The longest relaxation time (4 s) was for isethionic acid triplet peak around 3.8 ppm. The recycle delay was set to $5 * T_1 \sim 20$ s for further natural extract experiments. ^1H NMR experiments were conducted for all samples at 298 K on a Varian Mercury 300 MHz spectrometer. The experiments were recorded with 128 scans for natural water-soluble extract with a delay of 20 s and a 90° pulse-width of 15.20 μs and acquisition time 3 s. The commercial salts spectra were recorded with 32 scans. The peaks were integrated using ACD/NMR software to calculate the relative composition.

Matrix Assisted Laser Desorption Ionization Time-of-Flight Mass Spectrometry

(MALDI-ToF-MS): We used mass spectroscopy to identify rare compounds in the glue. The water-soluble extract was dissolved in minimal amount of water (Fisher, Optima grade), and 1 μg of trypsin (Sigma Aldrich) was added to the solution. The samples were digested overnight at 37°C . A solution of the matrix (α -Cyano-4-hydroxycinnamic acid, CHCA) was prepared in methanol (Fisher, Optima grade) at a concentration of 10g/ml. A layer of CHCA solution was added to the MALDI plate. The sample solution was filtered with a ZipTip (Millipore, C18) directly onto the MALDI plate. The water was allowed to evaporate before an additional layer of CHCA solution was applied. A Bruker Ultraflex III (Billerica, MA) MALDI ToF/ToF mass spectrometer was used for analysis. The mass spectra were acquired in positive mode. Tandem mass spectrometry (MS/MS) was performed using LIFT mode.⁹⁵

Glycoprotein staining studies: Periodic Acid-Schiff (PAS) stain (Sigma Aldrich) was used to determine where glycoproteins were present in the gumfoot strands. The standard protocol outlined by the supplier of the staining kit was followed for the experiments. The pristine gumfoot silk, pristine viscid silk, and reeled major ampullate silk threads were individually placed on glass slides. The slides were immersed in Periodic Acid solution for five minutes at 25⁰C followed by rinsing in distilled water. Next, the slides were immersed in the Schiff's reagent for fifteen minutes at 25⁰C. After that, they were washed in running tap water for five minutes. The slides were counterstained in Hematoxylin solution Gill No. 3 for 90s and then again washed with tap water. Finally, the samples were dehydrated and mounted to observe under the light microscope at different magnifications (Olympus BX60).

Solid-State NMR: To trace the glycoprotein signatures and to study the molecular effect of humidity on the glue composition, Solid-State NMR experiments were performed on pristine and washed silk samples. The sample for pristine silk consisted of ~3000 gumfoot strands (collected on glass fork from the cobweb). For washed silk sample, a sample set of 1400 strands were collected separately and were washed with deionized water and dried. Major Ampullate silk acted as a control sample and was collected by forcibly reeling the silk directly from the gland of the spider (without any isotope feeding) as described by Jenkins et al.⁹⁹ All samples were collected at 30-40% RH and were refrigerated until used for the NMR experiments. *Pristine Gumfoot Silk:* The glass fork wrapped with the gumfoot strands (~3000) was crushed in a mortar pestle. Depending on the experiment, the crushed silk sample was subjected to different humidity conditions (30% RH for glycoprotein analysis and 10%,60% or 90% RH for humidity effect analysis) in a custom-built humidity

chamber assembly for an hour at temperature of 25⁰C. After the humidity optimization, it was subsequently packed in the 4 mm Solid-State NMR rotor and sealed with Teflon tape and then loaded in the NMR set up for analysis. *Washed Gumfoot Silk*: The 1400 dried and water-washed gumfoot strands were crushed and subjected to similar procedure for humidity optimization and packed in NMR rotor as described above. *Major Ampullate Silk*: The collected spool of silk (~ 23 mg) was exposed to 30% RH as described earlier and packed in the NMR rotor to make it ready for analysis. All experiments were performed on a Bruker AVANCE 300 MHz NMR equipped with a 4 mm double resonance VT CPMAS probe at 298 K. The ¹H and ¹³C carrier frequencies were 300.1 and 75.6 MHz, respectively. The MAS rate was set to 6000 ± 3 Hz. The ¹³C chemical shift was referenced to the CH signal of adamantane (29.46 ppm) as an external reference. The 90° pulses for ¹H and ¹³C were 4 μs while the recycle delay and contact time were 2 s and 2 ms, respectively. High-power Two Pulse Phase Modulation (TPPM) decoupling with a field strength of 56 kHz was applied to the ¹H channel during an acquisition time of 41 ms. In order to improve the S/N ratio, the data presented (glycoprotein analysis) was processed by truncating the FIDs after 20 ms and zero filling up to 8192 points.

Thread adhesion: Fresh individual silk strands of gumfoot were collected from the cobweb of *Latrodectus hesperus* directly onto cardboard cutouts across 5 mm gaps and adhered using Elmer's glue. Experiments were conducted using an MTS NanoBionix (Agilent) with a custom designed environmental chamber. The silk was fixed on the upper clamp perpendicular to a 3 mm wide glass substrate placed on the lower clamp (Figure 3.2). To determine how adhesion changed as a function of humidity, the gumfoot silk was equilibrated at the desired humidity (10%, 30%, 50%, 70% and 90% RH) for 3 minutes

and then brought in contact with glass substrates. The preload force was fixed at 50 mN and, after contact for 6 seconds, the silk was pulled away at a rate of 0.1 mm/s and the detachment work/work of adhesion (stickiness) was calculated from the force-displacement measurements. A total of 15 samples were tested for each set of humidity condition for pristine gumfoot silk threads. To determine how water-soluble compounds, influence adhesion, pristine silk was immersed in a water dish to remove the salts and peptides (water-soluble components) and dried in air overnight to produce washed gumfoot threads. Next, washed gumfoot threads were tested for the adhesion in different humidity environments as described above (5 threads for each humidity).

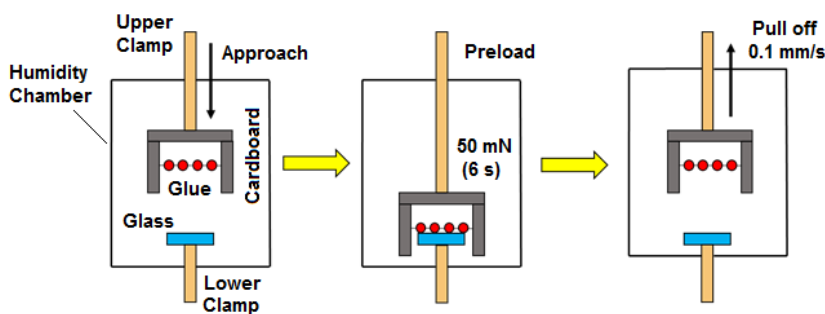


Figure 3.2 Schematic of gumfoot thread pull-off experiments.

Optical and Scanning Electron Microscopy (SEM) Imaging: Gumfoot silk (pristine and washed) was imaged using optical and electron microscopy to see how removal of aqueous components affected morphology. Optical images were collected using Leica DM LB2 and Olympus SZX16 at different magnifications. SEM micrographs were taken using a JEOL JSM-7401F field emission scanning electron microscope at different magnifications. The washed silk samples were sputter coated with silver particles and were placed on the aluminum stubs lined with conductive carbon tape.

3.3 Results

Composition of gumfoot silk: The water-soluble extract constituted $\sim 56 \pm 12$ wt. % of the mass of the collected gumfoot strands. Solution-State ^1H NMR (Figure 3.3a) showed the presence of organic salts which made up ~ 75 -85 wt.% of the water-soluble extract while the remaining portion was found to be made up of water (~ 15 -25 wt.%, calculated using mass of the pristine gumfoot strands, washed gumfoot strands and water-soluble extract). The salt signatures consisted of GABamide ($\sim 64 \pm 8$ wt.%), Isethionic acid ($\sim 20 \pm 3$ wt.%), and Choline ($\sim 14 \pm 5$ wt.%). In one of five samples, traces of GABA ($\sim 3\%$ wt. %) were found. The NMR assignments were confirmed by analyzing commercially available salts as well as from NMR spectra in the published silk literature.^{61,62,66,67} SCPs (spider coating peptides)⁹⁵ were not detected in the water-soluble extract using ^1H NMR, indicating that they must be less common even than the GABA salts.

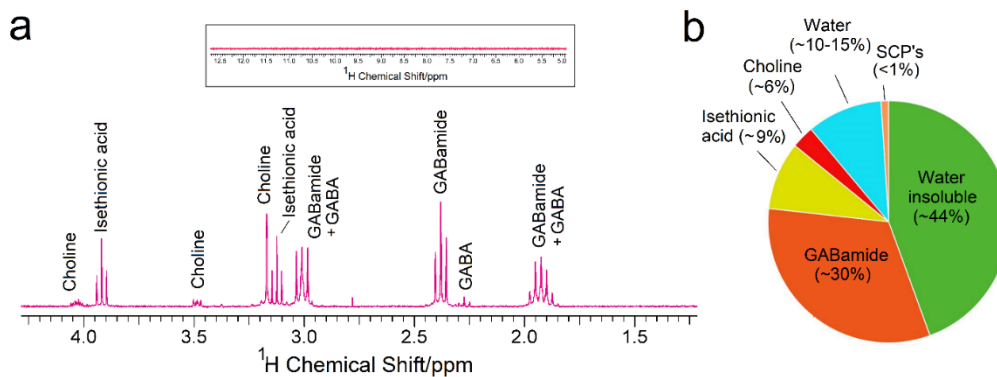


Figure 3.3 (a) ^1H NMR spectrum for the water-soluble extract from gumfoot threads. Inset in (a) shows the extended chemical shift range (5-12 ppm) depicting the absence of peptide peaks (SCPs) in the amide region. (b) Different material components in the gumfoot silk relative to the total mass of collected gumfoot.

The presence of an insoluble residue on the water-washed gumfoot silk thread (Figure 3.4) was striking and had not been reported in the published literature. This indicated an additional novel component in the gumfoot silk, besides previously reported SCPs⁹⁵ and presently discussed hygroscopic salts. However, the amount of the water insoluble residue couldn't be precisely determined due to the presence of major ampullate threads in the sample (the remaining ~44 wt.% water insoluble part contains both insoluble residue and major ampullate silk). A summary of the various components present in the gumfoot silk is shown as a pie chart in Figure 3.3b.

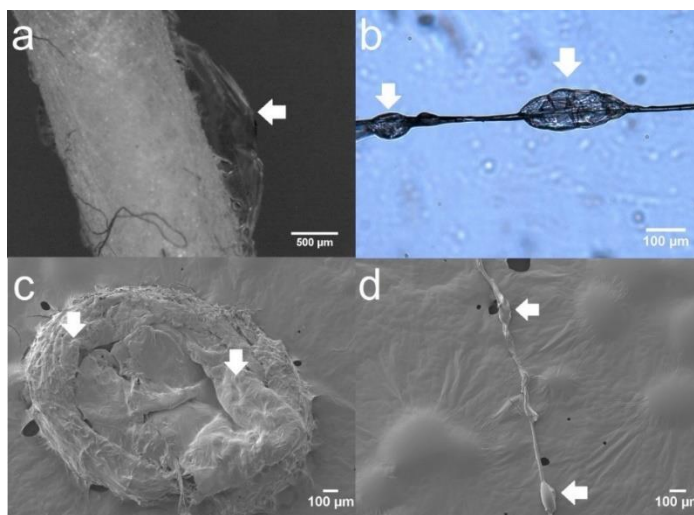


Figure 3.4 (a) Bundle of washed gumfoot threads. (b) Single washed gumfoot silk thread. (c) and (d) SEM micrographs of number of washed threads scraped from the collection rod single washed gumfoot silk thread respectively.

MALDI-ToF-MS of water soluble extracts from gumfoot silk: We used MALDI-ToF-MS (Matrix Assisted Laser Desorption Ionization Time-of-Flight Mass Spectrometry) to confirm the presence of SCPs in the water-soluble extract because it is a more sensitive technique than Solution-State NMR. Figure 3.5a shows the MALDI-ToF spectrum of

trypsin-digested, washed-solution of the gumfoot silk of *Latrodectus hesperus*. Many peptides identified were consistent with the earlier study by Hu et al.⁹⁵ The prominent peaks include m/z 812.2, 826.2, 979.3, 1206.4 and 1555.5 corresponding to sequences TVHHYR, TIHHYR, HGLLNNVGR, AVHHYEVPR, and TLFNQAADLLDHVV, respectively. Figure 3.5b is the MS/MS spectrum of the prominent peak (m/z 1206.4) detected in the extract. Upon fragmentation, several product ions such as 109.9, 307.9, 370.9, 416.9, 444.9, 470.0, 608.0, 737.1, 762.1, 808.1, 836.2 and 899.2 were detected that correspond to different fragments of the AVHHYEVPR peptide (as labeled in 3.5b).

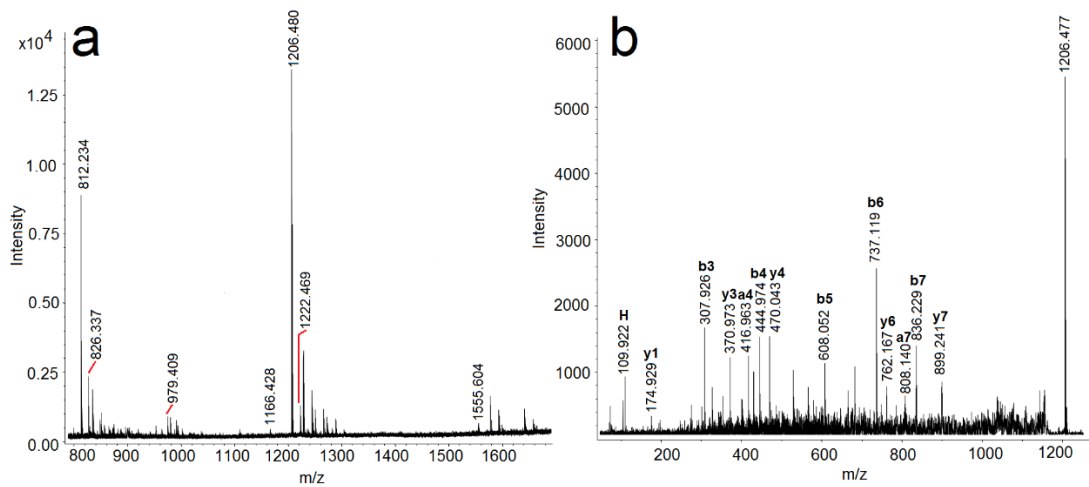


Figure 3.5 (a) Trypsin digested water-soluble extract from gumfoot silk of *Latrodectus hesperus* highlighting the presence of peaks related to spider coating peptides (SCPs) particularly at m/z 812.2, 826.3, 979.4, 1116.4, 1206.4, 1222.6 and 1555.5. (b) CAD MS/MS of the 1206.4 peak showing the different fragments of AVHHYEVPR.

The absolute concentrations of the peptides could not be determined because of lack of controls to calibrate the mass spectrometry analysis. Although all these sequences of SCPs have been detected before⁹⁵, this analysis shows that the SCPs are present in the washed-solution and, because the Solution-State NMR is unable to detect them, the SCPs are much rarer than the quantity of organic salts present in the gumfoot silk.

Analysis of water insoluble residue: The large quantity of water-insoluble fraction in the gumfoot silk was surprising and had not been reported before. All the samples showed this residue (Figure 3.4) on the washed gumfoot silk, indicating the presence of water-insoluble material in the gumfoot silk. This residue was also visible in the SEM analysis (Figure 3.4c,d). To establish the chemical nature of the residue, we characterized it using staining analysis and Solid-State NMR.

(i) **Staining analysis:** Since the viscid silk of orb-weaving spiders has glycoproteins that are responsible for adhesion, we checked the water-insoluble fractions of the gumfoot silk using stains positive for glycoproteins. PAS staining is used to detect polysaccharides as well as glycans and glycoproteins.^{161,164} Figure 3.6a-d shows the immobilized silk threads (gumfoot, viscid, major ampullate) stained with PAS. The gumfoot silk (Figure 3.6a,b) shows the presence of dark pink to magenta color (PAS positive) over the silk thread and at the ends of the thread where the insoluble residue collects after water washing. Viscid silk threads (*Larinoidea cornutus*) (Figure 3.6c) stain similarly, confirming the presence of glycoproteins. The glycoproteins in the immobilized viscid silk threads, unlike the gumfoot silk assume a circular shape and maintain their geometrical structure after washing. This observation supports the hypothesis that there are structural differences between the

gumfoot and viscid silk due to physical/chemical crosslinking in the later.²⁵ Major ampullate silk (Figure 3.6d) stained positively because it has a thin layer of glycoprotein.¹⁶⁵

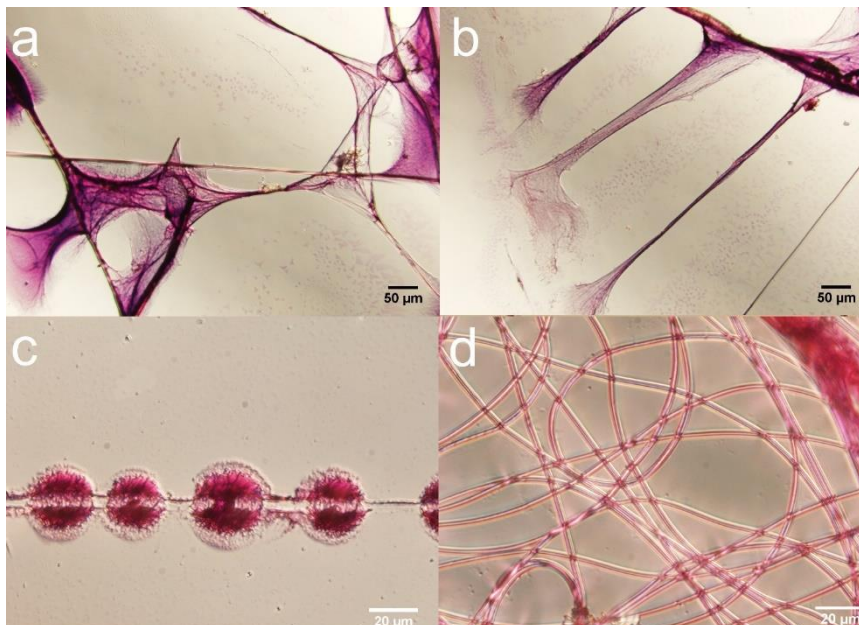


Figure 3.6 Periodic acid Schiff (PAS) staining. (a) and (b) Washed gumfoot silk from *Latrodectus hesperus*. (c) Washed viscid silk from the orb weaver *Larinioides cornutus*. (d) Major ampullate silk from *Latrodectus hesperus*.

(ii) **Solid-State NMR:** To further identify the chemical nature of the water-insoluble residue, we compared the CP/MAS spectra for pristine gumfoot silk, washed gumfoot silk and pristine reeled MA silk (Figure 3.7). If gumfoot glue was comprised solely of salts and SCPs (water soluble components), then the washed gumfoot silk spectrum should resemble that of the major ampullate silk⁹⁹ (since the glue adheres to MA silk, Figure 3.7, schematic inset). But, key differences were observed in the spectrum of washed gumfoot silk. The heightened shoulders around 50-65 ppm and 25-30 ppm in the pristine and washed gumfoot silk (Figure 3.7, spectrum inset) corresponding to the C_{α} and C_{β} signatures for amino acids

respectively¹⁶⁶, hinted at the presence of additional protein-based molecules in the gumfoot silk as compared to major ampullate silk. Further an unidentified peak around 70-75 and 105 ppm was present in the spectra for pristine and washed gumfoot silk but absent in the major ampullate silk. Recent studies on caddisfly larval silk¹⁵⁴ using Solid-State NMR showed these regions correspond to carbohydrate/glycosylated signatures. These observations confirm the presence of protein-based molecules, specifically glycoproteins, that are unique to the gluey regions of gumfoot threads.

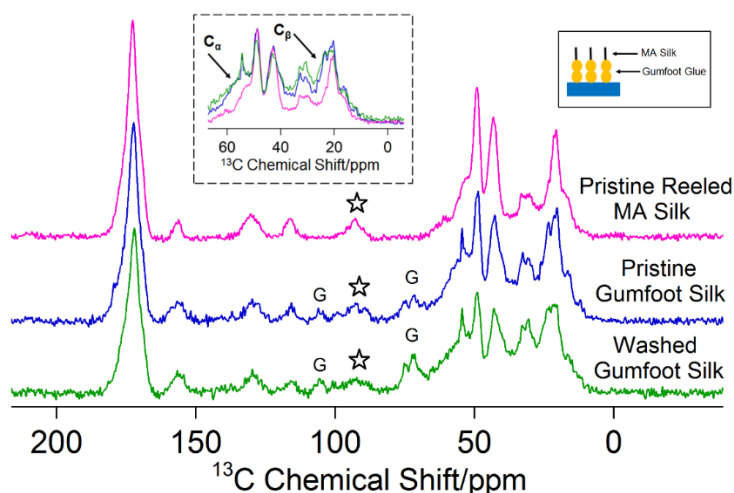


Figure 3.7 CP/MAS spectra for pristine reeled major ampullate (MA) silk, pristine gumfoot silk and washed gumfoot silk. Inset schematic shows the arrangement of gumfoot silk (glue and MA silk). Ideally after washing, gumfoot silk and MA silk spectrum should match if they are chemically identical, but the presence of heightened shoulder around 25-35 ppm (C_{β} for amino acids), 55-60 ppm (C_{α} for amino acids) (inset spectrum) and peaks related to glycoproteins (75 ppm and 105 ppm, labeled as G) indicates the presence of additional proteinaceous residue in gumfoot silk that is absent in the control major ampullate silk sample. The starred peak refers to a spinning sideband. All spectra are measured at 30% RH, 25^oC and MAS frequency ~ 6 kHz.

Adhesion of gumfoot silk threads: Adhesion of pristine (Figure 3.8a) versus washed (Figure 3.8b) gumfoot threads on a glass substrate was compared across 10-90% RH. The adhesion at 10% RH is lower than other humidity conditions (p-values, 10%&30%: 6.31×10^{-8} , 10%&50%: 4.54×10^{-8} , 10%&70%: 1.16×10^{-9} , 10%&90%: 2.25×10^{-6}) due to the silk being dry and unable to spread and adhere to the substrate. Above 30% RH the adhesion was insensitive to humidity (p-value: 0.78) (Figure 3.8c). When the pristine silk is water-washed, the washed threads show no measurable stickiness across the humidity range as compared to the pristine threads, indicating that the removal of water and water-soluble components drastically reduces the adhesive capability of gumfoot silk threads (Figure 3.8d).

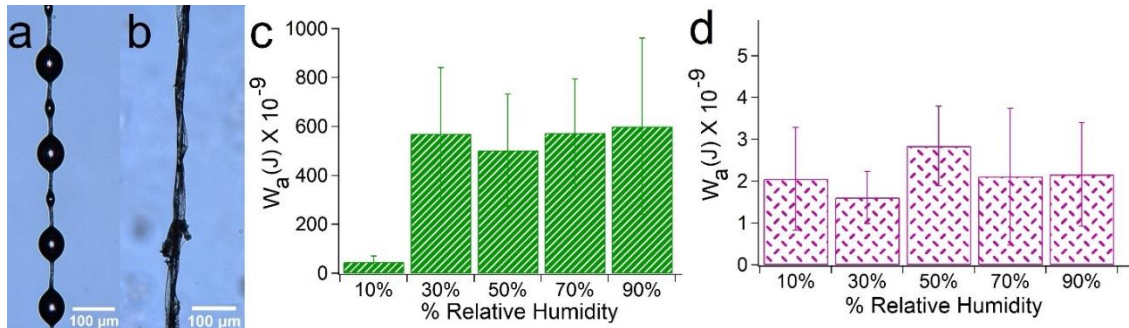


Figure 3.8 (a) Pristine gumfoot silk. (b) Washed gumfoot silk. (c) and (d) Variation of work of adhesion (W_a) with relative humidity (% RH) ranging from 10%-90% for pristine and washed threads respectively.

Molecular mechanism in presence of humidity: As described previously, the major components of gumfoot glue are organic salts and glycoproteins, and the presence of both is critical in adhesion in presence of humidity. Here, we present novel molecular evidence that the organic salts in the glue absorb water and become mobile with increase in RH and

affect the hydration behavior of the glue proteins. We directly measure the molecular level mobility of the gumfoot silk strands produced by the western black widow *Latrodectus hesperus* using Solid-State Nuclear Magnetic Spectroscopy CP/MAS and Direct Polarization/Magic Angle Spinning (DP/MAS) were performed on pristine and washed gumfoot silks exposed to different humidity environments (10% RH, 60% RH and 90% RH) to understand the dynamic behavior of the glue constituents (salts and glycoproteins) in presence of humidity.

Detecting gumfoot glue peaks: The samples used for the solid-state NMR analysis were gumfoot silk strands that combined both the axial major ampullate thread and the gumfoot glue. To identify the peaks specifically related to glue (salts and glycoproteins) we measured the ^{13}C CP/MAS spectra for forcibly reeled major ampullate silk threads as a control and compared it with the pristine gumfoot silk spectrum (Figure 3.9). The peaks corresponding to the major ampullate silk match with the earlier reported assignments.^{99,167} Pristine gumfoot silk spectra, apart from the major ampullate peaks, show additional peaks related to the organic salts, specifically at 23 ppm (GABamide, Choline), 33 ppm (GABamide), 40 ppm (GABamide), 53 ppm (Isethionic acid, Choline) and 55-58 ppm (Isethionic acid, Choline). These peak assignments were confirmed by studying the ^{13}C Solution State NMR spectra for pure organic salts (results not shown). Glycoproteins in the gumfoot glue have been detected previously and described in Section 3.3.3. Additionally, salts form a major component of the gumfoot glue, the observations of similar salt peaks (GABamide, Isethionic acid and Choline) in the Solid-State NMR analysis confirms that these peaks must originate from the gumfoot glue.

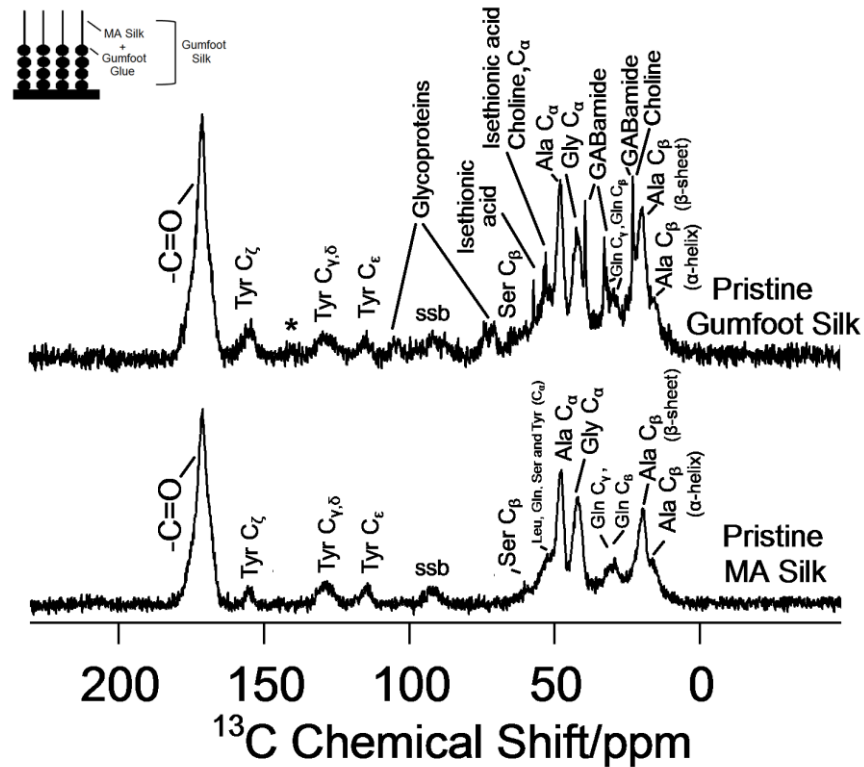


Figure 3.9 Comparative CP/MAS spectra of pristine gumfoot silk and major ampullate silk. Inset depicts the gumfoot silk arrangement. All spectras were recorded at MAS frequency of 6 kHz, 60% RH and 25⁰C. Starred peak is unidentifiable component and ssb refers to the spinning sideband.

Effect of salts on the humidification of glue proteins: Figure 3.10 shows the CP/MAS spectra for pristine (Figure 3.10a) and washed (Figure 3.10b) gumfoot silk at different RH (10%, 60% and 90%). Poor signal to noise ratio (due to lack of ¹³C labelled and less sample) limits our efficiency in glycoprotein analysis. However, in the case of pristine silk,

increased humidity softens the silk. The salt peaks (GABAamide, Isethionic acid and Choline) are visible at 10% RH and 60% RH but they seem to become lower in intensity/disappear at higher RH (90%), indicating higher mobility. However, the glycoprotein peaks at 75 ppm and 105 ppm do not show a dramatic change in intensity with as humidity increases, in contrast to previous observations with viscid glues.⁶⁷ The reason behind this behavior is not, but the observation may explain why gumfoot glues are largely inert to humidity. Other protein moieties in the gumfoot silk, such as amino acids constituting major ampullate silk¹⁶⁷ and also hypothesized proteins present in glue, are affected by water. Decrease in the intensity (Figure 3.10a, inset) of the peaks related to amino acids of these proteins, as the humidity increases, indicates enhanced protein backbone and side-chain mobility.¹⁶⁷ This effect is especially visible in the aliphatic C_α region with amino acid signatures – Leu C_α, Ser C_α, Gln C_α, Tyr C_α (shoulder near 55 ppm), Ala C_α (49 ppm), Gly C_α (40 ppm) – showing lower peak intensities with increase in RH. Other aliphatic peaks such as Gln C_{γ,β} (30 ppm) and Ala C_β (random coil, 17 ppm) are also affected. The peak intensity of more hydrophobic Ala C_β (22 ppm) segments shows no effect because these amino acids are mostly in the antiparallel β-sheet conformation¹⁶⁷, which does not get perturbed by water. In case of washed gumfoot silk, it is evident that the salts are not present and their removal decreases the overall water uptake and mobility of the gumfoot silk. The change in intensity for regions corresponding the amino acids of MA and glue proteins is not dramatic as in case of pristine silk. The glycoprotein peak at 75 ppm shows increased intensity as compared to pristine silk indicating rigidity in the absence of salts. Overall this result suggest that the presence of salts is important for the water uptake by the proteins in glue and MA silk.

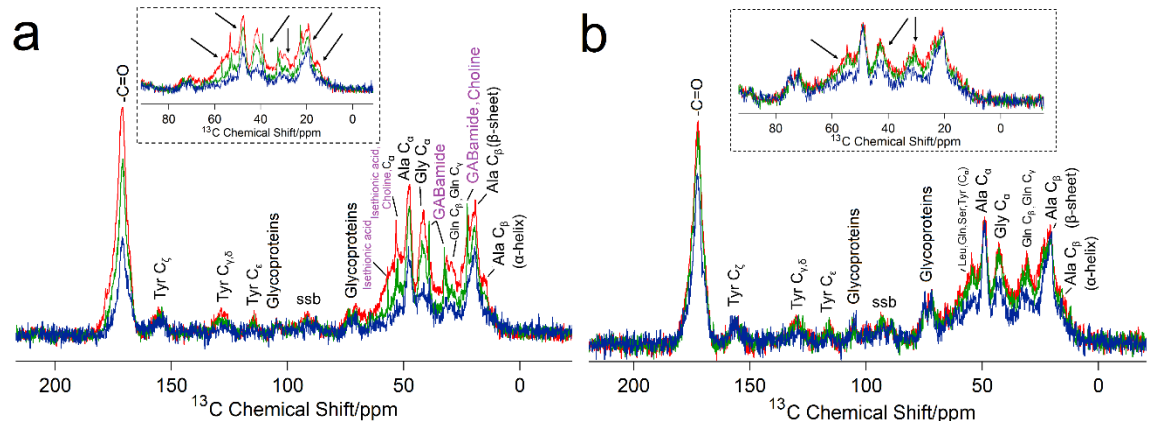


Figure 3.10 (a) and (b) CP/MAS spectra of pristine and washed gumfoot silk spectra respectively at 10% RH (red), 60% RH (green) and 90% RH (blue). Insets in each spectrum shows the peaks affected in aliphatic region with humidity exposure. All spectras were recorded at MAS frequency of ~6 kHz and 25⁰C. ssb refers to the spinning sideband.

Effect of humidity on salt mobility: To identify the mobile components in gumfoot glue, DP/MAS experiments were carried out for pristine (Figure 3.11a) and washed (Figure 3.11b) gumfoot silks at different RH (10%, 60% and 90%). For the pristine silk (Figure 10a), clear NMR peaks are identified for three different salts, GABAamide (24.5, 35.3 and 40.2 ppm), Isethionic acid (55.5 and 59.6 ppm), and Choline (the signal at 23.1 ppm, which overlaps with one at 24.5 ppm from GABAamide, 53.8 ppm, 55.6 ppm, and 67.4 ppm). The carbonyl resonance from GABAamide shows a peak at 182 ppm. Peaks related to glycoproteins (70 and 105 ppm) were not observed in the aliphatic region spectra over the range of RH studied here, indicating that they are not as mobile as the organic salts. Also, there were two unidentified peaks (156 and 177 ppm) in the aromatic/carbonyl region. Clearly, these peaks are not from the major ampullate silk present in the gumfoot silk and

possibly belong to the glycoprotein glue. The peak width decreases as the RH increases suggest that the salts are absorbing water and becoming more mobile. Second, choline is the only hygroscopic salt^{61,66} among the three at low RH and it shows a clear single sharp resonance at 55.6 ppm at 10% RH. All of the salts peaks are absent in washed silk, as expected. These results show salts to be the mobile component in the glue that is responsible for absorbing moisture from the environment with increase in RH.

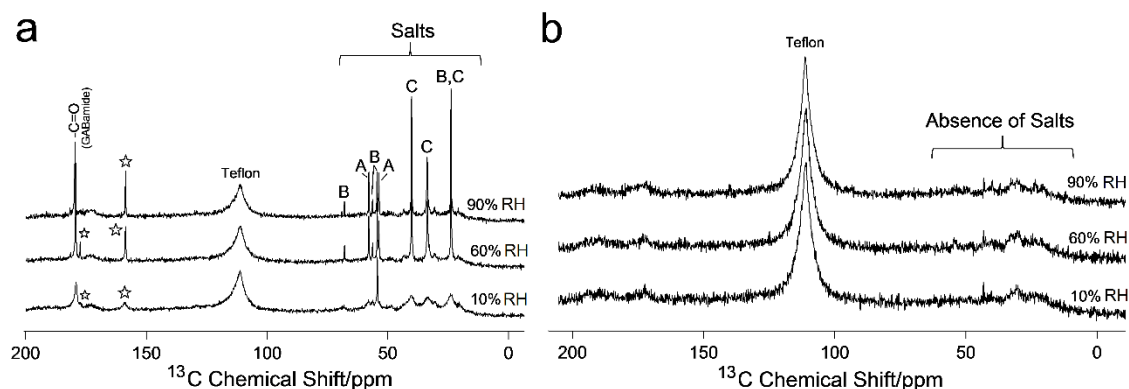


Figure 3.11 (a) and (b) DP/MAS spectra of pristine and washed gumfoot silk at 10% RH, 60% RH and 90% RH. (A: Isethionic acid, B: Choline and C: GABamide) Starred peaks in (a) are unidentified peaks. Spectras were recorded at MAS frequency of ~ 6 kHz and 25°C .

3.4 Discussion

Spiders use the adhesive silk in their webs to capture prey.^{17,50} The aggregate glues of orb spiders are complex mixes of glycoproteins^{55,56,58,59,69,70,161} and cocktails of hygroscopic salts^{55,61-67} that make the glues highly humidity responsive.^{25,67,72} But, aggregate glues are used in new ways in many of the webs that evolved from orb-weaving ancestors.⁵¹ Here, we report for the first time significant chemical similarities in the aggregate glues of cobweb spiders compared to their orb-weaving relatives. Water soluble organic salts are a major component of the glue (~ 45 wt % salts + ~ 10 wt. % water) of the

gumfoot silk of *Latrodectus hesperus* (western black widow) while the previously reported SCP's⁹⁵ are found to be present in low amounts. These salts are necessary for adhesion and make gumfoot silk adhesion humidity-responsive, but only at very low RH compared to orb spiders. Glycoproteins are also present in the gumfoot glue droplets. Thus, evolution maintained the basic structural and functional design of aggregate glue across a major ecological transition in web construction highlighting the interplay between salts and glycoproteins for generating strong adhesion.

In addition to the water-soluble components (salts and SCPs), we detected a water insoluble residue on the washed gumfoot threads (Figure 3.4). The presence of residue was surprising and not discussed in the published literature.^{55,103} The insoluble residue was analyzed using glycoprotein-sensitive staining (Figure 3.6) and Solid-State NMR (Figure 3.7) studies and consisted of carbohydrate based signatures, specifically glycoproteins. This is reminiscent of other biological adhesives where glycoproteins form an important part of sticky secretions (as seen in insects, starfish, limpets, ticks, velvet worms, caddisfly).¹⁵⁴ The presence of glycoproteins in the gumfoot silk is also supported by the detection of glycoproteins in other aggregate secretion known as Black Widow Defensive Secretion (BWDS) in genus *Latrodectus*.^{55,103} BWDS produced from the 'atypical' aggregate gland¹⁰³ during response to predators or prey capture, comprises of high and intermediate (8-100 kD) molecular glycoproteins. One of the glycoproteins (Glycoprotein A) is rich in N-acetylgalactosamine, threonine, serine and proline.¹⁰³ Similar observations have been made for the viscid silk, where residue is left after washing threads with water. The residue has been well characterized in the past and is composed of

glycoproteins.^{55,56,58,59,69,70,161} However, more detailed analysis will be required in the future for establishing the identity of this protein-based residue in gumfoot silk.

The importance of water-soluble components for adhesion is indicated by the comparison of whole thread adhesion for pristine and washed silk (Figure 3.8c and 3.8d). Pristine threads show two orders of magnitude higher adhesion than washed threads, where the SCPs and salts were removed. This highlights the interaction between proteins, SCPs and salts in maintaining the stickiness of spider silk glues. Glycoproteins alone present in the washed threads fail to adhere to the glass substrate and do not respond to humidity. Instead, the hygroscopic salts absorb water from the atmosphere and interact with glycoproteins to make the silk adhesive. There is a significant increase in adhesion around 30% RH and the adhesion remains constant from 30% RH to 90% RH. At 10% RH, the silk is rigid and dry and fails to make contact and spread, leading to poor adhesion. At 30% RH and higher, the salts absorb water and make the glycoproteins tacky and sticky. Thus, the gumfoot adhesion of black widow spiders is insensitive to humidity after 30% RH.

Solid-State NMR provides direct molecular information of how gumfoot silk components interact with humidity and directly correlates with the macro-level adhesion observations. CP/MAS results for pristine silk demonstrates that the glue responds to humidity and softens due to water uptake by salts with increase in RH (Figure 3.10a) Thus, at the macro-level the glue is able to spread and adhere to the substrate. On the other hand, washed silk shows the inability of the glue to absorb water without the presence of salts (Figures 3.10b and 3.11b), ultimately rendering it non-sticky. The low adhesion at 10% RH (Figure 8a) points out that the salts are dry and the glue does not have sufficient water

to plasticize and make it flow and spread on the substrate. Direct molecular evidence of this behavior can be seen in DP/MAS spectrum of pristine silk (Figure 3.11 a), where salts at 10% RH exhibit broad peaks indicating rigidity. Increases in RH leads to increase in water uptake of salts and sharpening of peaks, again indicative of enhanced adhesion when RH is greater than 10%.

The relative independence of adhesion from changes in humidity is consistent with the foraging habitat of Black Widows since they reside over a broad range of varied environments including dry to moist microhabitats.⁸⁰ The importance of water-soluble components in controlling adhesion is similar to our previous results for washed viscid silk (*Larinioides cornutus*).⁶⁷ For viscid silk produced by orb-web weaving spiders, it has also been observed that across the various species of spiders including *Larinioides cornutus* that the silk adhesion is optimum at a particular humidity condition. This optimum humidity where the adhesion is maximum correlated with the optimum foraging conditions of that particular species of spiders.²² These results point out that the material composition of the water-soluble components is important for adhesion.

Our findings show that natural selection maintained the basic ground plan for spider aggregate glue over more than 200 million years and across a major ecological transition in web spinning.⁵¹ Cobweb spiders originated from an early orb weaving ancestor in the Jurassic, but elaborated the two dimensional orb web into a three-dimensional cobweb that uses gumfoot threads to target walking, rather than flying, insect prey.⁵¹ Gumfoot silk is a composite arrangement of glue secreted on stiffer major ampullate thread^{50,76,84}, compared to the relatively elastic flagelliform silk present in the axial fiber in orb spiders' viscid silk.¹⁶⁰ The glue in gumfoot silk appears homogeneous, coalesces, and

spreads easily, behaving more like a viscoelastic liquid²⁵ at different levels of humidity, hinting at the absence of crosslinking in the system. On the other hand, the viscid silk acts as a viscoelastic solid⁷⁰, shows a dense central core, suggesting physical and chemical crosslinking in the silk.²⁵ Despite these differences, we find here major similarities between the gumfoot and viscid silk. Like viscid silk⁵⁵, the gumfoot silk has a mixture of soluble hygroscopic organic salts and insoluble glycoproteins in the glue. Gumfoot silk loses its adhesion when those salts are washed away, like viscid silk.⁶⁷ Finally, we also found that adhesion increases significantly with humidity, as seen in viscid silk, but only at low RH so that gumfoot adhesion is mostly invariant to humidity across a broad range of potential microhabitats.

The constant adhesion of gumfoot silk above 30% RH is a key difference to orb spiders' viscid silk, which typically improve in their adhesion as humidity increases initially but then declines above some species-specific optimum humidity.²² The whole thread adhesion results for gumfoot threads are consistent with the single drop pulling measurements where Sahni et al.²⁵ observed that adhesion was independent of humidity (15%, 40% and 90% RH). This stark variation in the adhesive behavior between gumfoot and viscid silk can be possibly due to the difference in chemical nature of the salts and glycoproteins. Gumfoot silk from *Latrodectus hesperus* contains salts like GABamide (~70%), isethionic acid and choline. Choline is relatively hygroscopic but present in the lowest concentration while GABamide and isethionic acid are hygroscopic only above 50% RH.⁶⁶ In contrast, viscid silk often contains substantial quantities of highly hygroscopic salts. The glycoproteins^{55,56,58,59,69,70,161} in viscid silk hold potential sites for glycosylation and are anticipated to play important role in water retention, elasticity, adhesion properties

of viscid silk.⁵⁹ It is likely that the glycoproteins in gumfoot silk have similar domains but that differences in composition and structure of glycoproteins and their interaction with salts results in the differences in adhesion between the two types of silk glues. A detailed analysis of the protein sequence is necessary to understand the differences in the glycoproteins in the gumfoot and viscid silks.

3.5 Conclusion

We studied the adhesive gumfoot glue from the cobweb of *Latrodectus hesperus* (western black widow) to understand how its composition correlates with adhesion and molecular mechanism, in presence of humidity. Solution-State NMR showed the water-soluble component is mostly composed of organic salts like GABAamide, Isethionic acid and Choline, with only low concentrations of Spider Coating Peptides (SCPs). A water insoluble residue on water washed silk threads was characterized using staining and Solid-State NMR and consisted of glycoprotein. Whole thread adhesion measurements showed the importance of water soluble components in adhesion and optimization of silk adhesion across a broad range of humidity >30% RH. Molecular findings confirm the importance of salts in making glue humidity responsive. Our study highlights the recurring observation of how salts and proteins interact to produce the adhesion of spider capture silk and how that interactions modulates adhesion in different humidity environments, a lesson that provides clues for developing humidity responsive synthetic adhesive systems.

CHAPTER IV

ROLE OF HYGROSCOPIC LOW MOLECULAR MASS COMPOUNDS IN HUMIDITY RESPONSIVE ADHESION OF CAPTURE SILK

4.1 Introduction

Water, in bulk or vapor form has always been a roadblock in the performance of adhesive based synthetic systems.^{2-5,157,168,169} On the other hand, nature provides us with a number of biological adhesives that stick well in the presence of water^{8,170} or high humidity.^{16,18,22} Apart from their structural design, the material composition contributes to their exceptional performance in presence of water or humidity. Hence, there is an immense need to understand the design strategy of such natural systems so as to improve the existing challenges in adhesion of synthetic systems as well as fabricate adhesives that can work in presence of humidity.

Prey capture adhesives produced by spiders¹⁷ is a good system for investigation because of they routinely function at fluctuating or high humidity.^{22,72,73,171} The sticky capture silk used by araneoid spiders for trapping walking and flying insects, consists of an axial thread of either stretchy flagelliform (orb web) or a major ampullate (cobweb) silk coated with microscopic drops of glue (viscid in orb webs and gumfoot in cobwebs) made

up of a mixture of organic/inorganic low molecular mass compounds (LMMCs), glycoproteins, and water.^{55,56,61–66,161,172} Glycoproteins make the glue viscoelastic,⁷⁰ which implies that there is an increase in adhesion at high peeling rates to trap struggling insects and lasting elasticity to trap insects over longer period of time.^{50,70} The complex mixture of hygroscopic LMMCs^{55,61–66,172} collect water from the environment and makes the glue tacky enough to stick to natural surfaces including insect cuticles.¹⁷³ Because of the hygroscopic LMMCs, glue has sufficient water to spread efficiently upon contact but also maintain high enough viscosity to resist cohesive failure and thereby maximize the adhesion strength.²²

Volume and the extensibility of the glue droplets increases with increase in humidity.^{25,70–73} Till an optimal relative humidity (RH), an increase in volume leads to faster spreading of the glue upon contact while the extension contributes to the suspension bridge mechanism of glue droplet detachment and increases the energy required to detach the thread.^{25,71–73} Glue viscosity varies over five orders of magnitude as atmospheric humidity changes for many species of spiders, but maximum adhesion always occurs within a narrow range of that variation when comparing different species of spiders from dry and wet habitats. Thus, viscid glue maximizes adhesion at an “universally optimal” viscosity.²²

The humidity response of the capture silk is frequently associated with the presence of water soluble LMMCs that are present in very large quantity, about 30-60 wt.% of the total mass of the dry web.⁵⁵ Organic LMMCs form about 60% of water soluble components⁵⁵ and compose of mostly polar aliphatic compounds such as glycine, betaine, choline, putrescine, GABamide, isethionic acid bearing amine, sulfonate, or acetate

functionalities.^{55,61–66,172} Inorganic LMMCs, though not characterized extensively as their organic counterparts, comprise of 10-20% of the water soluble mass from the webs and are known to have Ca^{2+} , H_2PO_4^- , NO_3^- , Na^+ and K^+ ions.⁵⁵

There are number of hypotheses for explaining the presence of a complex cocktail of LMMCs in the glue droplets.^{55,62} It has been shown that inorganic/organic LMMCs play a critical role in solvating the glycoproteins.⁶⁷ When the LMMCs are washed off, the glue is no longer sticky even after adding external water to the glue droplet.⁶⁷ Other suggested roles include acting as neurotransmitters, imparting anti-UV and antimicrobial properties, inhibitors for crystallization of the axial flagelliform silk proteins and as toxic agents for prey capture.^{55,62} The primary tested hypotheses are for water absorption and retention, and for increasing adhesion.^{20,67} However, it is still not clear why such a wide variety of LMMCs are present in glue. Past efforts relating the composition, hygroscopicity and adhesion of capture glue constituents have been limited. Vollrath et al. discovered the LMMCs in the glue droplets and have shown that these LMMCs are hygroscopic.⁶⁶ Townley et al.⁶¹ have studied the water uptake for a specific family of araneid spiders (*Argiope aurantia*, *Argiope trifasciata* and *Araneus cavaticus*) and have shown that the LMMCs are more hygroscopic than the insoluble protein components of the web.

The recent study emphasizing the optimum viscosity for glue adhesion suggested that the spiders in dry habitat may have LMMCs that absorb water at low relative humidity compared to spiders from wet environments.²² This leads to two possible, non-mutually exclusive hypotheses of role of LMMCs that results in similar viscosity at very different humidities to maximize adhesion for spider species: (1) Controlling the ‘hygroscopic strength’: It has been well established that there is a significant variation in the chemistry

of the LMMCs present in capture glue across species.^{20,55,61,62,65} On an individual basis, the diverse LMMCs may vary in hygroscopic response across different humidity environments. When present as mixtures in the glue droplet, their combined hygroscopic activity can tune the overall water uptake of the capture glue and impart the observed viscosity/adhesion response. (2) Optimizing interactions with glycoproteins : Although glycoproteins of spiders have not been sequenced extensively, significant established differences in their composition^{59,60} may be necessary for the variation in the chemical composition of the organic LMMCs to interact with them leading to chemistry specific interactions, to generate the humidity response.

The current study takes a step forward from the earlier studies^{61,66} and explores the role of LMMCs present in capture glue in terms of controlling the maximum adhesion and optimal viscosity, by taking in account four spiders spread across diverse habitats with each of their glues exhibiting different adhesion responses in presence of humidity (*Latrodectus hesperus*, *Argiope trifasciata*, *Larinioides cornutus* and *Tetragnatha laboriosa*). We hypothesize that differences in the hygroscopicity of LMMCs compositions across species controls variation in by determining water content, and hence viscosity, of the glue droplets at different humidities. To test this hypothesis, we study the hygroscopic properties of the glue and its individual components. Firstly, we present the chemical composition of organic LMMC's of four species from different habitats. Secondly, we discuss the water uptake of suspended pristine glue droplets (glue in its native form consisting of LMMCs and glycoproteins) in presence of humidity. Thirdly, we decouple the glue components (LMMCs and glycoproteins) and switch our analysis to first to study the humidity response of 'LMMCs' in three different sample types: (a) individual synthetic organic LMMCs

found in glue droplets and (b) LMMCs mixtures extracted from capture glue threads and (c) synthetic salt mixtures mimicking salt compositions in capture glue. Lastly, we analyse the other glue component, ‘glycoproteins’ obtained after washing of the LMMCs from capture glue threads and studied its hygroscopic response.

4.2 Experimental Section

Procurement of Capture Silk Threads: We choose four spider species belonging to different habitats: *Argiope trifasciata* (open fields; Blacksburg, Virginia), *Larinioides cornutus* (near water bodies; Akron, Ohio), *Tetragnatha laboriosa* (above water; Akron, Ohio) (all three are orb weavers)²² and *Latrodectus hesperus* (widespread across various geographical habitats^{21,80}; Bugs of America, Arizona) (cobweb weaver). Other than belonging to different habitats, the orb web weavers *Argiope trifasciata*, *Larinioides cornutus* and *Tetragnatha laboriosa* were selected because each of their glues show maximum adhesion at different humidity conditions (30%, 50% and 90% RH respectively).²² On the other hand, cobweb weaver *Latrodectus hesperus* is selected as it shows a constant adhesion across a range of humidity conditions (30%-90% RH).^{20,21} The difference in the adhesive response of each provides us with the criteria to check our hypothesis of water uptake by organic LMMCs dictating maximum adhesion. *Larinioides cornutus*, *Argiope trifasciata* and *Latrodectus hesperus* procured from above mentioned locations were housed in custom built cages in the laboratory to aid web building and subsequent web/thread collection while freshly built capture silk from the webs of *Tetragnatha laboriosa* was collected by directly winding whole webs on cardboard frames and glass pipettes from their natural habitat near the Cuyahoga river (Akron, Ohio), since *Tetragnatha* were unable to build webs in the laboratory setting.

Solution-State NMR Measurements: The composition of LMMCs present in the capture silk of the spiders in the study was measured using Solution State NMR. Individual glass pipettes covered with whole orb webs (*Argiope trifasciata* ~10, *Larinioides cornutus* ~ 60 and *Tetragnatha laboriosa* ~25) were collected. In case of cobweb weaver *Latrodectus hesperus*, the sticky capture glue present in lower part of the web as individual vertical strands known as gumfoot silk. About 750 of gumfoot strands were collected for analysis.²⁰ The collected capture glue from each of the species was washed with deionized water for ten minutes followed by lyophilization of water washings to get LMMCs. A part of the extracted salt mixtures for each spider silk was dissolved in 99.96% deuterated water (1 ml) (Cambridge Isotope Laboratories) and filled in the 5 mm NMR tube (Norell) for chemical characterization. All ¹H experiments were carried at 298 K on Varian Mercury 300 MHz spectrometer. For quantification, proton spin-lattice relaxation experiments were performed and the longest relaxation time was about 4 s for each of the extract sample. So, accordingly ¹H experiments were conducted by setting the recycle delay to 5*T₁~ 20 s respectively. The ¹H experiments were conducted with scan size ~ 512, acquisition time ~2.9 s and pw90 ~ 15-22 μs The peaks were analyzed and integrated with ACD/NMR software to calculate the relative composition of each salt compound in the glue.

Hygroscopicity of suspended pristine glue threads: The hygroscopic water uptake of the suspended pristine capture glue threads was measured through change in volume using imaging with Olympus BX53 microscope with 20X and 50X objectives and Photron FASTCAM SA3 camera to under different humidity.²² A custom-built humidity chamber controlled the ambient humidity around the capture silk mounted on a glass fork. The same glue droplet was observed as the humidity was increased from 10%, 30%, 60% to 90% RH.

At each humidity, the droplet was observed to equilibrate quickly but pictures were taken after 5 minutes for consistency. The droplet volume calculated by the formula defined by Liao et. al.¹⁷⁴ The change in volume in the glue droplet is assumed to be only because of the water uptake and hence, the increase in glue droplet volume is measured at different humidities. Please note that the volume measurement from imaging is the actual glue volume increase which includes the effect of glue compositions, size and droplet curvature. 12-20 glue droplets from 3-5 spiders were tested for each spider species. Two sample t-test was used to compare the change in volume.

Hygroscopicity of synthetic organic LMMCs, natural LMMCs extracts, synthetic LMMCs mixtures, washed glue threads and pristine immobilized glue threads: In order to understand the hygroscopic nature of different components of glue, we measured the water uptake of a variety of samples using a Cahn Microbalance (Figure 4.1) Samples included (a) Synthetic organic LMMCs, in order to establish the individual hygroscopic response of various LMMCs present across glues of diverse species of spiders (b) Natural extracted LMMCs mixtures from whole webs, to understand the hygroscopic nature of the cocktail of LMMCs based on the composition they are found in the capture glue (c) Synthetic LMMCs mixtures prepared based on the composition found in glue, to compare the activity with natural extracts (d) Washed capture silk to study the trend in water uptake of capture silk threads in presence of only glycoproteins and (e) Pristine immobilized glue threads, to compare with washed capture silk and separate the hygroscopic response of LMMCs from glycoproteins. *Method of measurement:* The hygroscopicity of the five different types of samples described above was established by studying the water uptake using a cahn microbalance attached to a custom-built humidity set up. The microbalance

was fitted with an acrylic sheet that served as inlets for hygrometer (VWR) and humidified/dry air. The sample placed on pre-weighed aluminum foil was loaded on the suspended pan in the microbalance. In order to confirm there was negligible uptake by aluminum foil, control experiments were performed with empty foil throughout the range of conditions (30%, 60% and 90% RH). The sample was dried at 10% RH until a constant reading displayed on the readout. This mass subtracted from the aluminum foil mass was taken as the mass of the sample. Next, the humidity was increased to 30%, 60% and 90% RH and at each humidity after the desired environment was equilibrated, readings were taken at every five minutes for a total of twenty minutes. In case of individual synthetic LMMCs, the sample was kept in oven at 50⁰C-60⁰C for thirty minutes to expel water and then immediately transferred on the pan in microbalance and dried again at 10% RH followed by steps discussed previously. The final reading at each humidity (30%, 60% and 90% RH) was taken for calculating the % water uptake in each case. The water uptake was normalized to the weight measured at 10% RH condition. A set of three measurements were done for each type of sample. The statistical analysis was carried using ANOVA.

Sample Preparation: (a) *Synthetic organic LMMCs:* The LMMCs included N-acetyl putrescine, Betaine, GABA, Isethionic acid, Choline Chloride, Taurine, Putrescine, l-Proline, β -Alanine (all from Sigma Aldrich), N-acetyl taurine (synthesized in laboratory), GABamide (provided by Dr. M.A. Townley, University of New Hampshire) and Glycine (Calbiochem). About 1-2 mg of LMMCs was taken on a pre-weighed aluminum foil and analyzed for the uptake. (b) *Natural LMMCs extract from webs:* Whole webs collected on glass pipettes from *Larinioides cornutus* (~20 webs), *Argiope trifasciata* (two sets of samples with 25 and 17 webs each respectively), *Tetragnatha laboriosa* (~20 webs) and

Latrodectus hesperus (two sets of samples with 725 and 380 gumfoot strands each respectively) were washed as per procedure described in the Solution State NMR section. The extract was then placed on previously weighed strip of aluminum foil to initiate the measurements. (c) *Synthetic LMMCs mixtures*: Two set of synthetic mixtures based on the compositions of *Argiope trifasciata* and *Tetragnatha laboriosa* were prepared by mixing the individual synthetic organic LMMCs described above. Both these spiders were selected because their adhesion shows maximum at drastically opposite humidity values) *Argiope* ~ 30% RH and *Tetragnatha* ~90% RH). So, these systems become ideal choices to test whether compositions dictate adhesion differences. The recipe of each mix was based on the composition found by NMR analysis in the present study. About 10 mg of mix was prepared by weighing the respective LMM and dumping them in a glass petridish. The petridish was then placed overnight in a small humidity chamber to initiate homogeneous mixing of salt. After a clear liquid pool was formed, a drop of mixture (~1 -2 mg) was taken with a micropipette and placed on a pre weighed aluminum foil followed by conducting the water uptake measurements described previously. (d) *Washed capture silk*: Two to three webs of *Larinioides cornutus* and *Argiope trifasciata* were collected on glass pipette and given repeated washes in deionized water to remove the water soluble compounds. The pipette with the washed silk on it was then allowed to dry overnight in air. Later, the dried silk was scrapped from the pipette and used for measurements. (e) *Pristine immobilized capture silk*: Freshly spun pristine sticky silk threads were collected on a strip of aluminum foil directly from the webs of *Argiope trifasciata* and *Larinioides cornutus* and used for measurements. All biological samples were stored in refrigerator and synthetic LMMCs in desiccator until measurements were done.

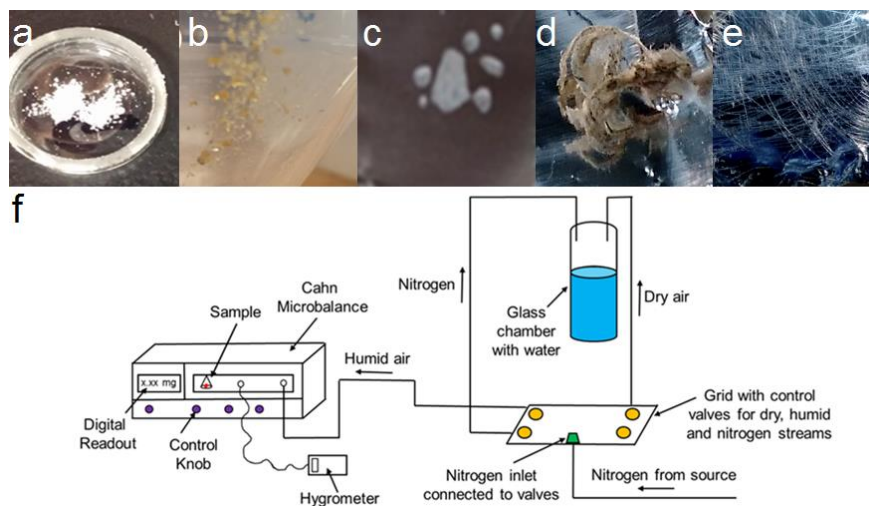


Figure 4.1 (a)-(e) Different types of samples for water uptake measurements. (a) Synthetic organic LMMC (l-proline shown here). (b) Extracted LMMCs in a centrifuge tube after lyophilization. (c) Synthetic LMMCs mixture mimicking recipe from glue of *Tetragnatha laboriosa*. (d) Washed capture silk. (e) Pristine immobilized glue threads on an aluminum foil. All natural samples shown are related to the capture silk from the webs of *Larinioides cornutus*. (f) Set up for water uptake experiments showing different parts including the custom built humidity controller and Cahn Microbalance.

4.3 Results

Solution-State NMR of LMMCs extracts from webs: The water soluble LMMCs extracts (Figure 4.2) from the capture silk threads of *Latrodectus hesperus*, *Argiope trifasciata*, *Larinioides cornutus* and *Tetragnatha laboriosa* were analyzed for the presence of organic LMMCs and their respective compositions by ^1H Solution-State NMR. The spiders selected belong to different habitats and clearly glue from each species is a combination of distinct organic LMMCs combinations ranging from three in *Latrodectus*

hesperus, five in *Tetragnatha laboriosa*, six in *Argiope trifasciata* to seven in *Larinioides cornutus* (Figure 4.3). Across species, LMMCs differ not only in the chemical properties but also in their composition. One or two LMMCs dominated the composition, but their identity differed among species (*Latrodectus hesperus*: GABamide ~69%, *Argiope trifasciata*: N-acetyl putrescine ~34% and Isethionic acid ~27%, *Larinioides cornutus*: GABamide ~56%; *Tetragnatha laboriosa*: N-acetyl taurine ~46% and Betaine ~39%). Hence, there is tremendous diversity of the LMMCs present in the glue of spiders.

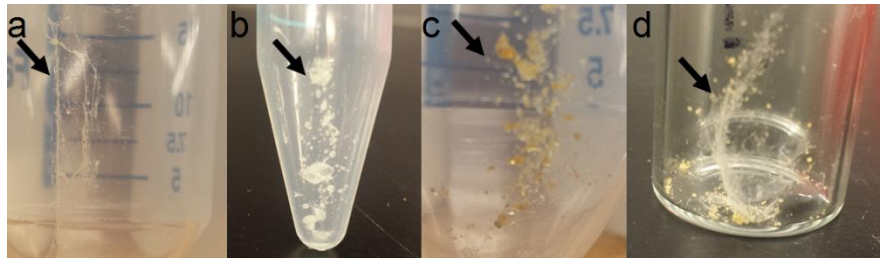


Figure 4.2 (a)-(d) Water solubles LMMCs (black arrow) extracted from the webs of *Latrodectus hesperus*, *Argiope trifasciata*, *Larinioides cornutus* and *Tetragnatha laboriosa* respectively.

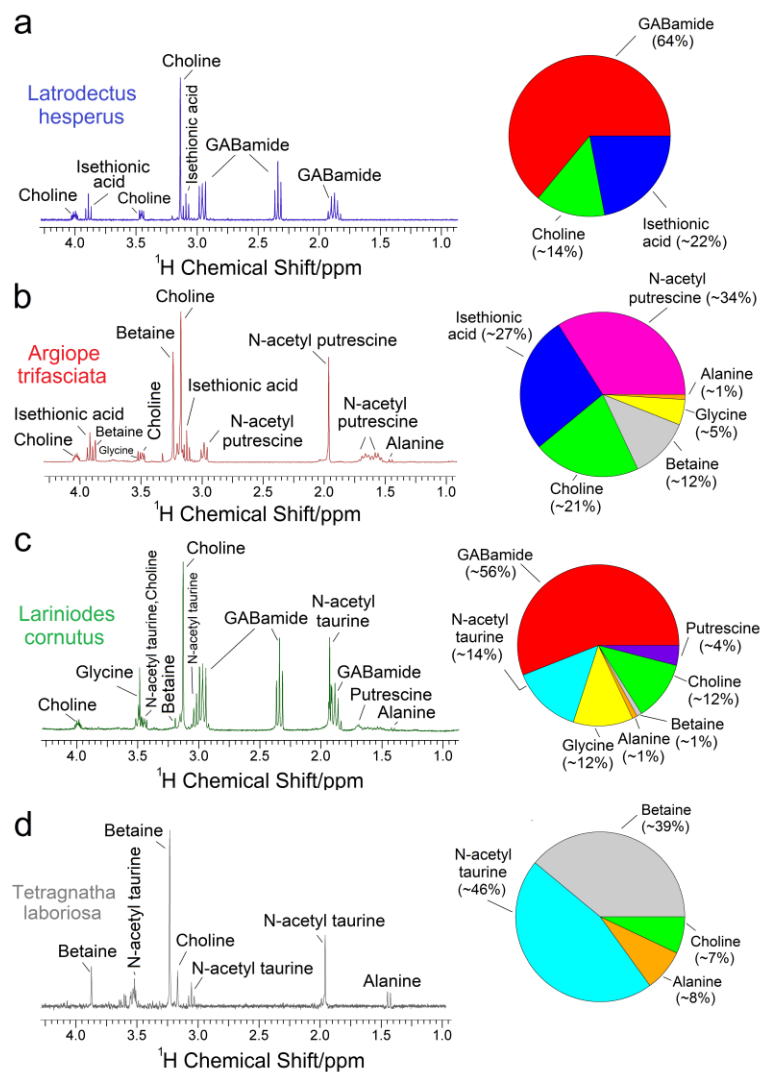


Figure 4.3 (a)-(d) ^1H Solution-State NMR spectra of the extracted LMMCs mixtures from the webs of *Latrodectus hesperus*, *Argiope trifasciata*, *Larinioides cornutus* and *Tetragnatha laboriosa*, respectively. Each spectrum is accompanied with a color coded pie chart (each color representing a distinct LMMC) showing the details of relative composition of each LMMC component in different capture silks.

Water uptake of suspended pristine silk threads: After establishing the differences in organic LMMCs compositions among the capture silks of species, we started with the series of water uptake studies. The capture silk in its native state is in suspended form where water uptake is a result of a combination of factors: hygroscopic material, droplet geometry, and exposure surface area of glue droplets. Immobilizing the glue droplets on the substrate may change the rate and extent of water uptake. Hence, we used microscopy of suspended glue droplet to measure the water uptake by glue droplet. We calculated the glue volume using formula described by Liao et al.¹⁷⁴ and plotted the increase in volume of pristine glue at each humidity with respect to volume at 10% RH, in suspended state for the four spider species. Figures 4.4 shows a single glue droplet of *Latrodectus hesperus* under increasing humidity. Notice that the glue droplet size increases significantly with an increase in humidity. Clearly, glue of *Tetragnatha laboriosa* absorbs significantly less moisture at 90% RH than the other three species (Figure 4.4). This observation supports the spreading and viscosity observation where the *Tetragnatha laboriosa* glue appears more viscous than the species from wet habitat shows higher viscosity than other species tested at 90% RH. The normalized increase in volume of the other three species tested is similar (Appendix A) but given that the glue of some species, specially *Argiope trifasciata* that shows maximum adhesion around 30-50% RH, probably has water present at 10% RH. Our other experiments related to ATR-IR measurements show bound water even at 0-10% RH. *Latrodectus hesperus* glue is unique because although it absorbs moisture and shows a ~1000X drop in viscosity with an increase in humidity, the adhesion is constant over the 30%-90% RH.²⁰ This is unlike the other orbweb spider species, where adhesion changes with a change in glue viscosity. Hence, we see a difference in the water uptake of

native glue threads among species of different habitats. Next, based on the results of differences in LMMCs compositions and water uptake of glue threads among species, we tested whether the diverse LMMCs composition (Figure 4.3) modulates the water uptake of glue that matches the adhesion performance.

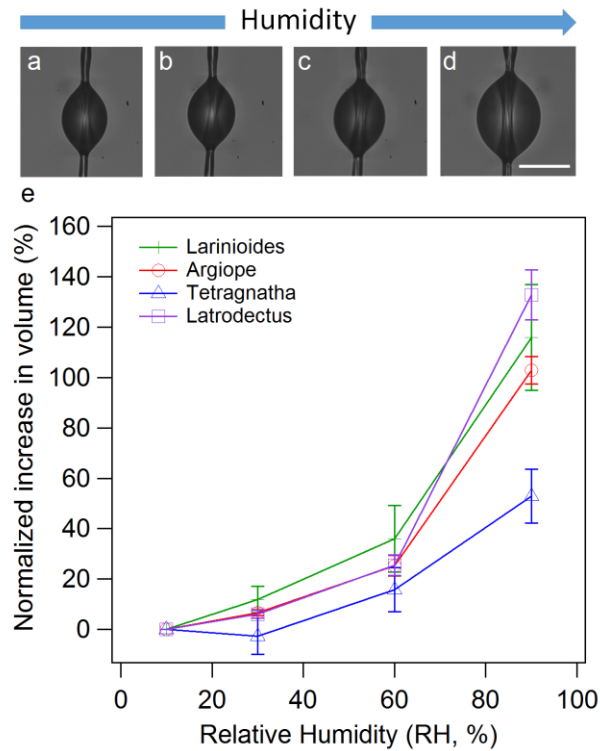


Figure 4.4 (a)-(d) Optical images of the single capture glue droplet of *Latrodectus* exposed to 10%, 30%, 60% and 90% RH respectively. Scale bar is 50 μ m. (e) Normalized increase in volume (%) of pristine capture silk glue belonging to *Latrodectus*, *Argiope*, *Larinioides* and *Tetragnatha*, as a function of relative humidity. The error bars show $\pm 95\%$ confidence interval, and sample size is ≥ 15 .

Hygroscopicity of LMMCs: Water uptake studies for LMMCs were performed in three different ways (Figure 4.1). Firstly, to establish the individual hygroscopic response of the various LMMCs present in glue, water uptake by twelve synthetic organic LMMCs was measured. There have been past attempts done in this direction but they were limited to specific LMMCs, took in account humidity range till 60% RH.^{61,66} Here, we present an extensive analysis of the hygroscopic response of organic LMMCs from 30% to 90% RH. Figure 4.5 show the normalized water uptake of various organic LMMCs found in capture silk. The water uptake was normalized to the weight of the sample at 10% RH. Control sample (aluminum foil) did not show a significant increase in water uptake upon increase in environment humidity. The common organic LMMCs detected in the capture silks across species (Figure 4.3 and unpublished results by Townley and Tillinghast) varied in hygroscopic response and were broadly classified as low, moderate and high (Figure 4.6) on the basis of their total water uptake capacity at 90% RH . Overall, the water uptake by LMMCs increases with increase in the humidity, with total water uptake ranging widely 6-120% at 90% RH for different organic LMMCs. Low hygroscopic activity LMMCs including glycine, taurine and alanine are described as LMMCs which overall show inertness to water absorption with low water absorption (< 20% water uptake by mass wrt mass at 10% RH) at higher humidity (90% RH). Moderately active LMMCs include putrescine, choline chloride and GABA, absorb in the range of 40-70 % by mass at 90% RH. Highly active LMMCs include n-acetyl putrescine, n-acetyl taurine, betaine, GABamide, isethionic acid and l-proline that absorb between 80-120% by mass (wrt mass at 10% RH) at 90% RH. Hence, we find a diversity in hygroscopicity of the organic LMMCs present in glue . It is observed that upon exposure to 90% RH, non-active LMMCs

maintain their powder form and do not turn into a liquid pool as seen in case of all of the active LMMCs. Also, among the active LMMCs only choline chloride and putrescine turn into liquid pool as soon as they are exposed to the external environment (observed at 20-30% RH).

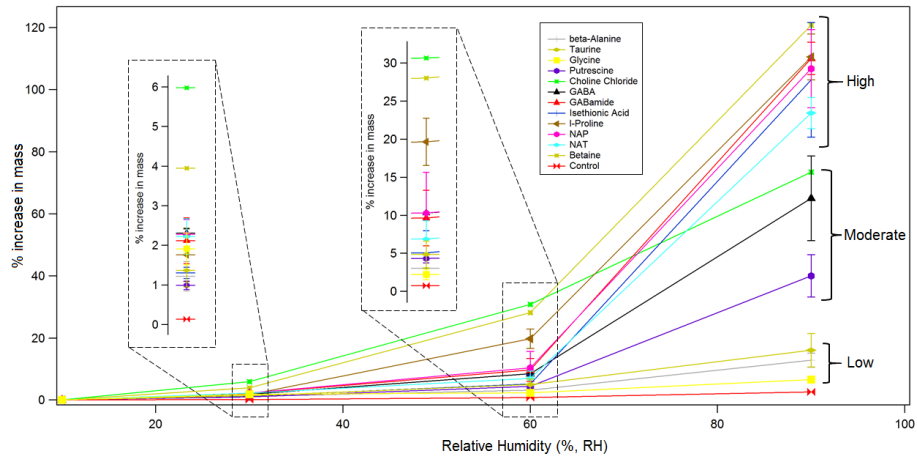


Figure 4.5 Normalized percent increase in mass of different synthetic organic LMMCs over the range of humidity conditions (30%, 60% and 90% RH). Insets are the zoomed in regions for 30% and 60% RH. The data is represented as mean \pm standard deviation from a set of three measurements.

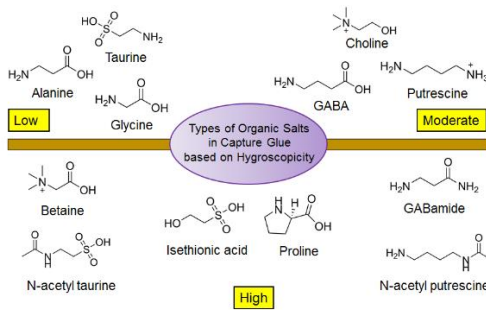


Figure 4.6 Schematic illustrating the major organic LMMCs in the glue droplets across various species. The LMMCs are divided into less active, moderately active and highly active based on the total water uptake of synthetic LMMCs at 90% RH.

In second set of experiments, we probed the hygroscopic strength of natural LMMCs mixtures extracted from capture silk. Figure 4.7a shows the water uptake by natural LMMCs extracts of the four spider species, *Latrodectus hesperus*, *Argiope trifasciata*, *Larinioides cornutus* and *Tetragnatha laboriosa*. The mixtures present in glue are hygroscopic and show an increase in water uptake with increase in humidity. However, at each humidity studied, we do not see any significant differences in the water uptake behavior of natural LMMCs mixtures among different species, unlike the trend observed in pristine silks's water uptake (Figure 4.4) (see Appendix A for statistical analysis). Firstly, *Argiope trifasciata* is active at low humidity and its glue has the least viscosity at 30% RH. But its extracted LMMCs do not show any difference in hygroscopic water uptake at 30% RH as compared to other species. Secondly, unlike suspended glue droplets, we did not observe a reduced water absorption for *Tetragnatha* LMMCs at 90% RH. Also, *Latrodectus hesperus* LMM extract does not show a consistent uptake behavior similar in case of its adhesion over different relative humidity conditions.²⁰ The trend in the normalized water uptake is challenging to interpret as we are normalizing with respect to the dry weight at 10% RH. From our other spectroscopic data, bound water is present at even at low humidities in the pristine glue of *Argiope trifasciata*. Based on the composition found by NMR analysis and hygroscopic performance of synthetic LMMCs, we calculated the theoretical mass uptake for each mixture recipe (Figure 4.8) and found no significant differences among the hygroscopic performance of mixtures across species in a set of humidity conditions.

In the last set of LMM based experiments, in order to counter check the observed trend in the water uptake of natural extracts, we formulated synthetic salt mixtures related

to the compositions of *Argiope* and *Tetragnatha*. As stated earlier, *Argiope* shows maximum adhesion at 30% RH while *Tetragnatha* shows at 90% RH. Clearly no distinction in the water uptake properties for synthetic salt mixtures is seen between the two species across the humidity conditions (Figure 4.7b, see Appendix A for statistical analysis). The trend is similar as seen in the natural extracts of the glue belonging to the species of spiders (Figure 4.7a). Results pertaining to natural and synthetic mixtures suggest that the water uptake by LMMCs alone does not control the glue viscoelasticity and ultimately adhesion. We further probed the water uptake by the glycoproteins.

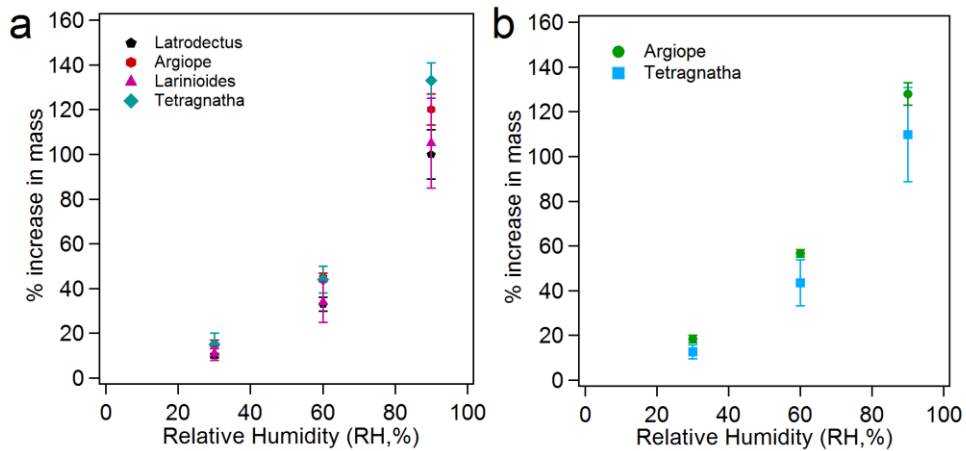


Figure 4.7 (a) shows normalized increase in mass (%) of natural LMMCs extracts obtained from webs of *Latrodectus*, *Argiope*, *Larinioides* and *Tetragnatha* as a function of humidity. (b) shows the comparison of normalized increase in mass (%) for synthetic LMMCs mixtures species from extreme habitat: *Argiope* and *Tetragnatha*.

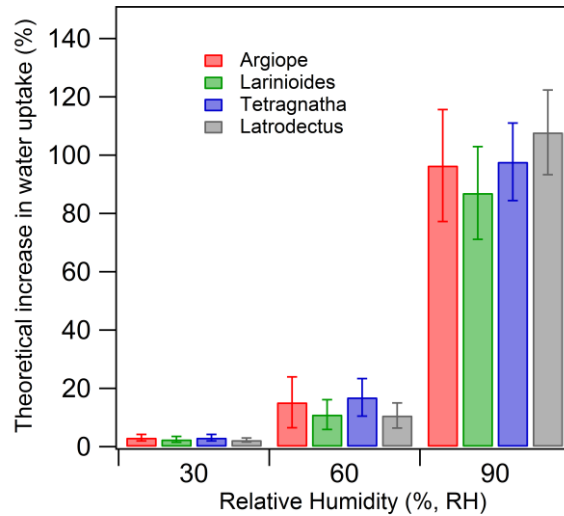


Figure 4.8 Theoretical water uptake of LMMCs mixtures

Hygroscopicity of glycoproteins: To understand the role of glycoproteins in mediating viscoelasticity, we studied the water uptake of washed capture silk threads and compared it with the behavior of pristine silk threads in presence of humidity. Washing silk with water removes the LMMCs and leaves the residual glycoproteins.^{20,67} In absence of LMMCs, glycoproteins lose adhesion as seen previously in our macro and molecular level studies.^{20,21,67} Figure 4.9 depicts the comparison of the hygroscopic behavior of pristine immobilized silk threads with washed silk threads of *Argiope trifasciata* and *Larinioides cornutus*. It is clearly evident that the water uptake is drastically reduced (<20% at 90% RH) for both the species and clearly glue with glycoproteins alone does not take up water as much as in presence of LMMCs (pristine sample). The behavior of washed glue in

presence of humidity relates to the loss in adhesion and reiterates the synergistic play of both LMMCs and glycoproteins in preserving adhesion of capture glue.

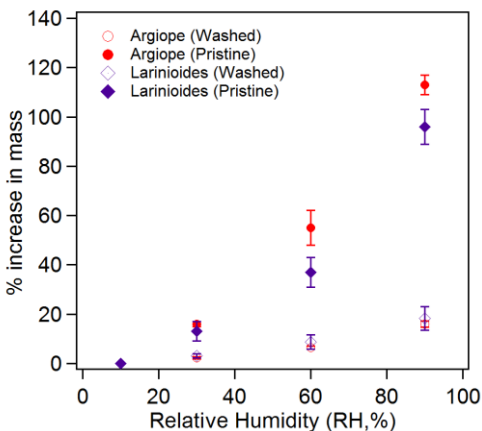


Figure 4.9 Normalized increase in mass (%) of washed glue (residual proteins) vs pristine glue for *Argiope* and *Larinioides* as a function of relative humidity.

4.4 Discussion

The adhesion of capture silk threads in spider webs is humidity dependant such that adhesion is maximized when the glue absorbs enough water that viscosity optimizes the contributions of both spreading and bulk dissipation.²² The humidity response of capture silk is often linked to the presence of a cocktail of organic and inorganic hygroscopic LMMCs that form ~50%-60% of the dry mass of the adhesive capture spiral. The humidity at which viscosity is optimized varies greatly across species and this argues for the hypothesis that the diverse LMMCs in the capture silk explains differences in the the humidity response across species by optimizing glue properties. We found diversity in organic LMMCs (Figure 4.3) across species spanning different habitats. Qualitatively, these differences in composition coupled with available LMMCs literature^{61,66} (unpublished results by Townley) for these species and hygroscopic response of synthetic

LMMCs (Figure 4.5 and 4.6) point at possible inter species differences in the hygroscopicity of glues. For instance, glues of *Argiope* and *Lariniodes* are made up of ~70-75% ‘high’ hygroscopic compounds while *Tetragnatha* glue is ~ 85-90 % ‘high’ hygroscopic compounds (majorly two highly hygroscopic LMMCs, betaine and N-acetyl taurine). This difference in *Tetragnatha* LMMCs composition may correlate with its novel adhesion response at 90% RH as compared to other species. The big question though is does the diversity in LMMCs compositions reflect quantitative differences in macroscopic water uptake of glue? Hygroscopicity results of suspended native glue droplets (composed of both glycoproteins and LMMCs) showed no significant differences in uptake of water between species at 30% and 60% RH. However, at 90 % RH *Tetragnatha* glue volume increased only ~40% as compared to ~100-140% increases for the other species (*Argiope trifasciata*, *Larinioides cornutus* and *Latrodectus hesperus* (Figure 4.4) . This correlates well with the behavior of *Tetragnatha*’s glue, which maintains a higher viscosity and doesn’t reach maximum adhesion until 90% RH. Further, narrowing our focus exclusively to contribution of LMMCs, we studied the water uptake of the natural LMMCs extracts (Figure 4.7a), synthetic mixtures (Figure 4.7b) and calculated theoretical water uptake (Figure 4.8) for LMMCs recipes on the basis of NMR compositions and individual organic LMMCs hygroscopicities. For natural mixtures, there was not any significant difference among species for water uptake across different humidity ranges (all extracts showed ~10% for 30% RH, 35-40% for 60% RH and 100-130% at 90% RH). No particular trend is observable specially in case of *Tetragnatha* LMM, whose uptake at 90% RH looks similar to the activity of LMMCs extracts of other species. Previous work on hygroscopicity of water soluble LMMCs extracts based on *Argiope aurantia* and a comparison between

Argiope aurantia, *Argiope trifasciata* and *Argiope cavaticus* have also reported the water uptake numbers in the similar range over humidity ranging from 20%-60% RH.^{61,66} Moreover, the work by Townley et al.⁶¹ reported the water soluble extract of the three species differed in the LMMCs compositions, but it was difficult to distinguish between the web hygroscopicities. Exploring the hygroscopicity of synthetic mixtures (Figure 4.7b) for the dramatically opposite (in terms of adhesion and viscosity) *Argiope* and *Tetragnatha*, showed an increase in mass with increase in humidity but pattern of change was similar between two species (same as in the case in the natural extracts). Finally, theoretical water uptake calculations for salt mixtures (Figure 4.8) also depict the absence of any differences between species throughout the humidity range under investigation. Thus, we found that while LMMCs composition does cause differences in hygroscopicity, these are insufficient on their own to explain the humidity response of different spider species. Instead we found evidence for an interaction between LMMCs composition and glycoproteins determining glue hygroscopicity and ultimately variation in adhesion.

A host of previous studies support the role of LMMCs in interacting with glycoproteins in controlling the humidity responsive adhesion of glue. Glycoproteins present in glue are sticky only in the presence of LMMCs.^{20,21,67} If the LMMCs are washed away, glycoproteins became rigid and fail to take in water (less than 20% at 90% RH) (Figure 4.9). Apart from these observations, there are two major factors that provide support to the interaction hypothesis: (a) variation in glycoprotein chemistry : Glycoproteins present in the capture glue are composed two proteins ASG1 and ASG2 deduced based on cDNA studies.⁵⁹ Recently, a ~10% variation has been observed in the sequence of proteins sequence from three species.⁶⁰ One of the evidences for their diversity

include the optical images of the capture threads published by Opell et al.⁵⁷ for seventeen species orb web weavers indicating the differences in glycoprotein granule morphology (appearance, shape, length, width, area and volume). Also, when studying the comparison between capture silk produced by orbweb weavers (viscid glue) versus cobweb weavers (gumfoot glue), we found differences in the morphology of the glycoproteins with viscid glue assuming core shape structure and gumfoot glue being fluid like and spreading over the underlying fiber.^{20,25} Isolation of glycoproteins from capture threads is tedious as compared to the LMMCs as the glue proteins tend to stick to the underlying axial thread. Devising strategies to remove them from capture threads and characterize their material properties should form basis of a potential area of study in future. Nevertheless, the published observations provide speculative clues for variations in glycoproteins, which might be important in interacting with diverse LMMCs functionalities in glue and ultimately tuning the adhesion response. (b) glue viscoelasticity: During peeling test of glue, energy is spent in breaking/deforming both interfacial bonds and bulk polymer network.¹⁷⁵ For viscoelastic adhesives, such as spider glue, the energy spent in the bulk can be significantly higher than the energy spent in breaking interfacial bonds. The viscoelasticity of the glue determines the energy spent in the bulk during peeling. We believe that spider glue viscoelasticity is constant at the maximum adhesion conditions across spider species. The glue viscoelasticity is dependent on multiple variables, including the LMMCs-glycoprotein interactions and also LMMCs/glycoprotein concentrations. Direct measurement of salt and glycoprotein concentration for glue droplet for each species is challenging due to limitations in glue sample collection. However we used a combination of gravimetric and optical measurements to infer the protein

concentration. The calculated protein concentrations vary widely with humidity and are not similar at the maximum adhesion condition for the four species. This finding again supports the hypothesis that these diverse LMMCs are not just for water uptake but also for specific interactions with glycoproteins to modulate viscosity and ultimately adhesion.

Protein-LMMCs interactions form an important part of various biological mechanisms. Proteins in presence of LMMCs or osmolytes or compatible solutes are known to have stabilized conformational structures.¹⁷⁶ LMMCs also mediate the ‘salting in’ and ‘salting out’ mechanisms by interacting with proteins, leading to precipitation or crystallization.¹⁷⁷ It is likely that the organic LMMCs are acting as ionic liquids for the solubilization and stability of glycoproteins. The commonly used functional moieties for the synthesis of ionic liquids bear similar chemical structures (amines) as the organic LMMCs in the glue. Importantly, ionic liquids based on choline have been extensively used for protein dissolution. On the other hand, it is been shown that inorganic LMMCs hold importance in interacting with adhesive proteins produced by marine organisms such as oysters, mussels and caddisflies as well as in functioning of synovial fluids based on glycoproteins. Synthetic systems such as hydrogels¹⁷⁸, electrospun fibers¹⁷⁹, polymer brushes¹⁸⁰, membranes¹⁸¹ and more recently adhesive joints¹⁸² have also been shown to function on the basis of interaction of LMMCs with macromolecular structures such as polymers. These literature findings supporting protein-LMMCs interactions point at possibility of the LMMCs in the glue interacting with glycoproteins. Among the diverse LMMCs present, some LMMCs may preferentially interact strongly with the glycoproteins as compared to others in presence of water. 2D Solid-State NMR based techniques provide a pathway to understand the such interactions between individual components in a system.

Efforts in this direction should be made in future, however precautions should be taken related to degradation of humidified sample (separation of LMMCs from glue) due to longer acquisition times at fast NMR spinning rates (personal observation). Understanding individual LMMCs interactions with glycoproteins will not only help decoding glue adhesion mechanism but also non-linear response of glue viscosity in humidity.

4.5 Conclusion

The present study aims at establishing the role of LMMCs in capture silk adhesion. We hypothesized that the combination of diverse LMMCs present in the glue droplet tune their water uptake capacity to optimize the viscosity and maximum adhesion. We found that the glues of *Latrodectus hesperus*, *Argiope trifasciata*, *Larinioides cornutus* and *Tetragnatha laboriosa*, each belonging to a different habitat, varies widely in the chemical composition of organic LMMCs. The water uptake of pristine suspended glue droplets indicated differences in water uptake with humidity, with *Tetragnatha* glue taking up less water at 90% RH as compared to other species and matching the adhesion performance. The contribution of LMMCs was assessed by quantifying the hygroscopic performance of individual synthetic LMMCs, natural mixtures and synthetic mixtures. The synthetics were found to be hygroscopic and were classified as low, moderately and highly active. On their own, the water uptake behavior of LMMCs mixtures, both natural and synthetic were found to be inadequate to explain the humidity responsive adhesion. Finally, glycoproteins in absence of LMMCs showed a reduced water uptake activity. These results reiterate the role of LMMCs in interacting with glycoproteins to mediate capture silk adhesion. Understanding these interactions of individual LMMCs moieties with glycoproteins may add to the current knowledge of role of diverse LMMCs in capture silk, the natural design of capture silks, silk adhesion mechanism and fabrication of similar synthetic mimics.

CHAPTER V

LIPIDS IN GECKO SETAE: TRACING THEIR PRESENCE AND ASSOCIATION WITH β -KERATIN

This work has been previously published as

Jain, D., Stark, A.Y., Niewiarowski, P.H., Miyoshi, T. and Dhinojwala, A.

Sci. Rep. **5**, 9594 (2015).

5.1 Introduction

Lipids form an integral part of various biological systems.^{135,136} One of the key examples, the epidermis (mammalian, reptilian or avian), consists of lipids surrounding dead keratinous cells in the upper region of the skin known as stratum corneum.^{137,183} Lipids help in maintaining physical resistance and serve as an epidermal water barrier.^{184,185} Besides acting as a skin barrier, lipids have been associated with a variety of biological attachment strategies such as the hairy structures on the chitin-based cuticle of insects^{140,186,187}, podia in sea stars¹⁸⁸ and cement secretions in barnacles.¹¹ Other roles include their presence as a protective coating in dragline silk in spiders,¹³⁸ as well as in self-assembly of the proteins in mussel byssal threads.¹⁸⁹ Thus there is increasing interest in lipids from multiple fields, but little work has been focused specifically on them.

One system of great interest recently has become the gecko adhesive system, where lipids have also been confirmed in the small hair-like adhesive structures¹¹⁹ and in invisible footprint residue that is left behind as they walk.¹¹⁸ In general, geckos have historically been known for their popular ‘smart’ keratinous fibrillar adhesive,¹¹⁰ which is comprised of highly organized similarly oriented and uniformly distributed microscopic hairy structures known as setae (Figure 5.1a), which further branch at the tips into spatula.^{110,190,191} In addition to the numerous ultrastructural, immunological and histological analyses^{120,130,192–194}, the use of Microbeam X-ray diffraction and Raman spectroscopy¹³² have confirmed that the main constituent of setae is stiff keratinous material. Keratin is a fibrous and structural protein that finds a prominent role in mammals (hair, wool, horn, fur, nail and skin), reptiles (scales and claws), birds (feather, beak and claw) and fish (teeth and slime).^{127,195} Various biochemical analyses^{120,130,192–194} suggest that during development, gecko setae incorporate keratin at their base, which is further deposited into long bundles oriented along main axis of setae. The adhesive setae consists of specific keratin associated beta proteins (KAbetaPs) and various forms of α -keratin.^{120,130,192–194} The keratin-based adhesive setae have a high elastic modulus, which is likely used to maintain the robustness of the setal structure during repeated attachment and detachment.¹¹⁰ However, the recent discovery of phospholipid footprints, and their potential to be at the adhesive contact interface¹¹⁸ has puzzled many and given a new dimension to existing keratin-based models of the gecko adhesive system.

Nano Assisted Laser Desorption Ionization (NALDI) mass spectrometry measurements confirmed the presence of the phospholipid ‘dipalmitoylphosphatidylcholine’ (DPPC) (Figure 5.2) in the traces of the footprint residue,

while Sum Frequency Generation (SFG) spectroscopy showed the presence of hydrophobic methyl and methylene groups at the contact interface between the gecko toe pad and substrate.¹¹⁸ Additionally, histochemical studies have shown the presence of lipids packed with the keratin material in the adhesive setae.¹¹⁹ The presence of lipids and their potential association with the keratin in the gecko setae calls into question their possible function in self-assembly of keratin bundles,¹³⁶ adhesion (dry and wet),^{16,121,142} self-cleaning,^{124,125} superhydrophobicity,¹⁹⁶ ductility and wear of the system.¹³⁸ Since the setal structure is a combination of keratin and lipids, one of the key questions is how the keratin and lipid components are associated in the setal structure. Hence, there is a need to study the assembly of these constituent materials, identify the interaction between them, and understand the structure and dynamics of this essential feature at a molecular level, all of which has been severely lacking in gecko adhesion literature.

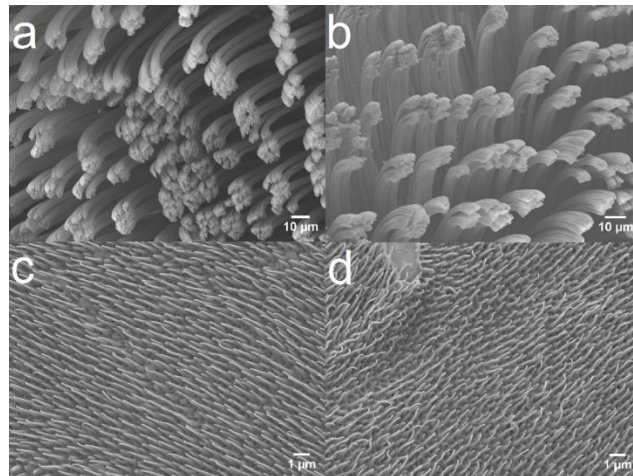


Figure 5.1 Scanning electron micrographs (SEM) for pristine (a) and delipidized (b) toe sheds, showing the adhesive hairy features known as ‘setae’ and pristine (c) and delipidized (d) skin sheds, showing the ‘spinulae’ structures respectively.

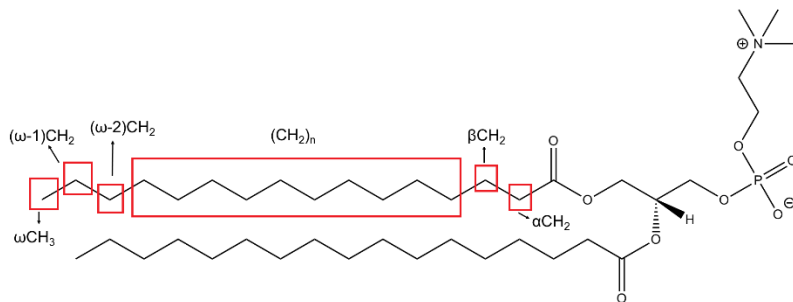


Figure 5.2 The phospholipid structure shows the positions of various methylene (CH_2)_n, $(\omega-1)\text{CH}_2$, $(\omega-2)\text{CH}_2$, αCH_2 and βCH_2 and methyl ωCH_3 groups. These signatures are detected in the NMR experiments. The structure is shown as a model example to understand the different peaks in the NMR results.

Motivated by Solid-State NMR studies of α -keratin^{197–204} focused on relating the macro properties of the material with the structure and dynamics of the molecules,²⁰⁵ we report the first ever Solid-State NMR analysis done on the molts (sheds) of the Tokay gecko (*Gekko gekko*) (Figure 5.3). In addition to the rows of setae in the toe pad shed (~ 65-70 % of the shed, see Appendix B for calculations), the molt is also comprised of several other layers of epidermis.¹³⁰ In order to confirm that the NMR signal is dominated by setae, skin sheds from the non-adhesive epidermis (Figure 5.1) have also been studied to present a comparative view. Based on the finding of phospholipid footprint residue,¹¹⁸ the current work hypothesizes that (a) the lipids are present in the setae, and (b) the lipids in the setae are loosely bound and are mobile at the NMR timescale. To test this we first removed unbound lipids off the sheds (chloroform methanol exposure)²⁰⁶ and used Solution State NMR²⁰⁷ and TLC^{208,209} to analyze and confirm the presence of lipids in both the toe and skin shed. Second, we used Solid-State NMR based Magic Angle Spinning (MAS) techniques (Cross Polarization (CP/MAS), Direct Polarization (DP/MAS) and Proton

($^1\text{H}/\text{MAS}$), to establish the keratin and lipid related peaks as well as to probe the dynamic behavior of the two components present in the shed.

Our results help to clarify the lipid-keratin association in both the adhesive gecko setae and non-adhesive skin, as well as provide insight to improve fabrication designs for synthetic adhesives.



Figure 5.3 (a) Removal of freshly molted gecko toe shed from *Gekko gecko*. (b) Removed shed from the toe region.

5.2 Experimental Section

Collection and preparation of samples of sheds: Freshly shed toe and skin molts were collected from *Gekko gecko* and preserved at -20°C . Precautions were taken to prevent the sheds from coming into contact with the hand while collecting (Figure 5.3). The collected toe sheds were carefully examined and cut with a blade and a tweezer under an optical microscope to remove the skin surrounding the shed.¹¹⁶ All procedures involving live animals were approved by the University of Akron IACUC protocol 07-4G and are consistent with the guidelines published by the Society for the Study of Amphibians and Reptiles (SSAR 2004).

Lipid extraction: Pre-weighed samples of toe/skin sheds from *Gekko gecko* were treated with a solvent mixture for removal of unbound lipids. The samples were placed in 60 ml chloroform and methanol (Sigma Aldrich) mixtures successively (2:1, 1:1 and 1:2) for 2 hours. Each treatment was then repeated again for 1 hour. Thereafter the delipidized sheds were separated from the solvent mixture and dried in vacuum to remove traces of solvent. The solvent extract was collected and subjected to rotary evaporation under reduced pressure to procure the dried lipid.²⁰⁶

Thin Layer Chromatography: The dried extracted lipid from the sheds (toe and skin) was dissolved in chloroform and applied to a 5 cm x 2 cm silica plate column with a micropipette. Lipid standards (1-palmitoyl-2-oleoyl-*sn*-glycero-3-phosphocholine (PC) and N-Nervonoyl-*D-erythro*-Sphingosylphosphorylcholine (SM), Avanti Lipids) dissolved in chloroform were also applied on the same plate. The plate was then dried in air for few minutes and developed in a small vial. A solvent mixture of chloroform-methanol-water (25:10:1, v/v/v) (Sigma Aldrich) (AOCS, Lipid Library) was used to develop the chromatograms and allowed to run through the plate for 10 minutes. After that, the plate was dried with a hair dryer and sprayed with either ninhydrin, 40% sulphuric acid or primuline (spot detection agents). The acid or ninhydrin sprayed plates were then heated at 110°C in an oven to char the lipids and observe the separated lipids as colored spots, while the primuline treated plates were observed under UV to view the spots.^{208,209}

Scanning Electron Microscopy: Images were taken using a JEOL JSM-7401F field emission scanning electron microscope at different magnifications. The pristine or delipidized toe/skin sheds were sputter coated with silver particles and were placed on the aluminum stubs lined with conductive carbon tape.¹¹⁶

Sample preparation for Nuclear Magnetic Resonance (NMR) Spectroscopy: *Solid-State:* Pristine or dried delipidized sheds (toe and skin separately) were weighed (~ 0.05 g) and packed in the 4mm solid state rotor (Bruker). Teflon tape was inserted to pack the sample tightly. *Solution-State:* $^1\text{H}/^{31}\text{P}$ NMR: The dried extracted lipid (from the toe and skin sheds separately) was dissolved in a 2:1 mixture of deuterated chloroform and deuterated methanol (Cambridge Isotope Lab.) for ^1H NMR, or deuterated water (Cambridge Isotope Lab.) containing 250 mM sodium cholate (Alfa Aesar) and 5 mM EDTA (Calbiochem) for ^{31}P NMR.¹⁶⁶ Samples were then packed in a 5 mm solution NMR tube for analysis.

NMR Measurements: *Solid-State:* All experiments were carried out with a Bruker AVANCE 300 MHz NMR equipped with a 4 mm double resonance VT CPMAS probe at 298 K. The ^1H and ^{13}C carrier frequencies were 300.1 and 75.6 MHz, respectively. The MAS rate was set to 6000 ± 3 Hz. The ^{13}C chemical shift was referenced to the CH signal of adamantane (29.46 ppm) and ^1H chemical shift with tetrakis(trimethylsilyl)silane (0.2 ppm) as an external reference. The 90° pulses for ^1H and ^{13}C were 4 μs while the recycle delay and contact time were 2 s and 2 ms, respectively. High-power Two Pulse Phase Modulation (TPPM) decoupling with field strength of 88 kHz was applied to the ^1H channel during an acquisition time of 55 ms. ^{13}C DPMAS spectra were obtained with a recycle delay of 15 s. ^1H MAS spectra were obtained by a simple single pulse with a receiver delay of 6.5 μs and a recycle delay of 2 s. *Solution State:* ^{31}P and ^1H NMR spectra were recorded at 313 K and 298 K respectively on a Varian INOVA 400 MHz spectrometer. Chemical shifts were recorded in ppm (δ) relative to 85% orthophosphoric acid (Phosphorus) and CDCl_3 (Proton). ^{31}P NMR spectra were recorded for 1648 scans with a 1 s delay using a

90° pulse width of 7.6 μ s and an acquisition time of 1.6 s. ^1H NMR spectra were recorded for 16 scans with a delay of 3 s, acquisition time of 1.6 s and a 90° pulse width of 9.75 μ s.

5.3 Results

Delipidization: The hydrophobic lipid footprint residue¹¹⁸ is anticipated to be unbound lipid associated with the setal structure. To test this hypothesis, we carried out the lipid extraction technique described by Swartzendruber et al.²⁰⁶ to remove the unbound lipids. The technique has been used previously to extract lipids from lizard skin²¹⁰ the results of which match our current lipid extracts from skin (~10-12 wt% of the mass of the sheds). Interestingly, the amount of extractable lipid material from the toe shed was found to be around ~ 8-10 wt %, slightly less than the skin. Keratin is insoluble in organic solvents¹⁹⁵ hence, we do not believe keratin is being removed by the treatment. Furthermore, when investigating the pristine and delipidized samples, we did not see any obvious change in morphology of the setae and spinulae (Figure 5.1).

Analysis of lipid extract: Standard lipid characterization techniques such as Thin Layer Chromatography (TLC) and Solution-State NMR were used to analyze the lipid extracts from toe and non-adhesive skin sheds. Table 5.1 lists the TLC results (R_f values of the lipids) using primuline as the detection agent. Lipids including phospholipids such as sphingomyelin (SM), phosphatidylcholine (PC), and phosphatidylethanolamine (PE) as well as non-polar lipids (probably glycerides, fatty acids and cholesterol) were seen in the toe and skin extracts. In addition to the R_f values available in literature,²¹¹ the presence of SM and PC was confirmed by comparing with standard sample spots. PE was confirmed by spraying the plate with ninhydrin. Spots were also visualized with 40% sulphuric acid spray.

Table 5.1 Retention factors for extracted lipids from toe and skin sheds measured using Thin Layer Chromatography

Retention Factor (R_f)				
Lipid	Literature Values	Toe Extract	Skin Extract	Standard Lipids
<i>Sphingomyelin(SM)</i>	0.11-0.15	0.12-0.15	0.11-0.16	0.14-0.15
<i>Phosphatidylcholine(PC)</i>	0.26-0.30	0.27-0.32	0.24-0.29	0.28-0.30
<i>Phosphatidylethanolamine(PE)</i>	0.50-0.54	0.53	0.53-0.55	N/A
<i>Non-Polar Lipids</i>	0.80-1	0.82-1	0.87-1	N/A

In addition to TLC, we used Solution-State NMR to further probe the extracted lipid solution. Standard samples of PC and SM show peaks at -0.64 ppm and -0.04 ppm respectively (Figure 5.4a). The toe shed extract shows peaks at -0.64 ppm and -0.08 ppm (Figure 5.4b), which confirms the presence of phospholipids PC and PE (as detected in TLC).²⁰⁷ The SM peak lies near the PE peak and we anticipate it to lie within the shoulder of the broad PE peak (Figure 5.4b). Similar peaks are seen in the skin shed extract (Figure 5.4c). Clearly, non-polar lipids cannot be detected with this technique due to the absence of a phosphorus moiety in their structure. In general, the reptilian epidermis is associated with non-polar lipids such as free fatty acids, cholesterol and triglycerides (as shown in the TLC results) as well as polar lipids like phospholipids and sphingomyelin (TLC and NMR results),²¹⁰ although it is possible that there are other lipid species present in the setae. Our

work here however is the first to report that in addition to the phospholipids detected in the NALDI study¹¹⁸ (PC and SM), other lipid types are also in the adhesive toe pad extract. We confirmed that the delipidization treatment did not remove keratin from the sheds using ¹H NMR (Figure 5.4d). Peaks at 0.8 ppm (ω CH₃) and 1.1 ppm ((CH₂)_n) in addition to other lipid based peaks (inset Figure 5.4d) further confirmed the presence of lipids in the extract.²¹² Proteins usually show a crowd of peaks in the range of 1-5 ppm in ¹H NMR,¹⁶⁶ which is absent in the lipid extract spectra, suggesting that keratin was not removed from the toe or skin shed during the delipidization treatment and thus will not affect our analysis.

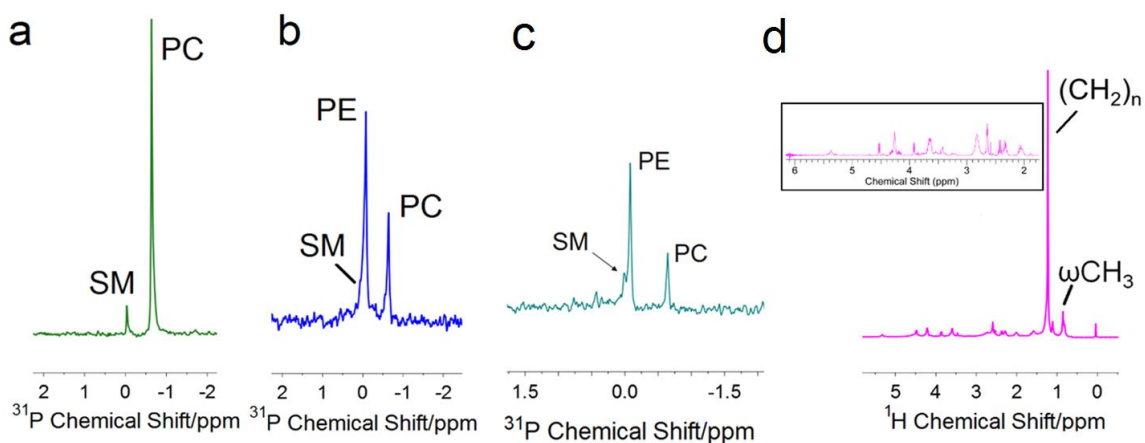


Figure 5.4 (a) ³¹P NMR for standard phospholipids (PC and SM). (b) ³¹P NMR for extracted phospholipids. (c) ³¹P Solution NMR of lipid extracts from skin shed. (d) ¹H NMR for lipid extract from toe sheds. Inset in (d) is the enlarged spectrum from 2-6 ppm.

Solid State NMR: (a) *Cross Polarization/Magic Angle Spinning (CP/MAS)*: Figure 5.5 shows the ¹³C CP/MAS spectra of pristine and delipidized sheds for *Gekko gekko*. Since this Solid-State NMR technique is sensitive to molecules with slow dynamics,²⁰³ the keratin dominated spectra reveals that the amino acids forming the structural protein

keratin are rigid at the frequency less than ~ 10 kHz.²⁰³ Peaks were assigned by taking into consideration previous studies on keratin-based systems using solid-state NMR,¹⁹⁷⁻²⁰⁴ as well as biochemical results for amino acids specific to the proteins constituting setae and skin.^{192,213} The spectra can be divided into four regions: carbonyl, aromatic, C_α and aliphatic.^{197,199-201} The carbonyl region shows a distinctive peak including signatures from the carbonyl backbone present in amino acids comprising the keratin. The aromatic region shows peaks from amino acids such as tyrosine and phenylalanine. The C_Z for arginine is the only exception which despite being aliphatic appears in the aromatic region. The broad peak between 46-60 ppm consists of C_α resonances from amino acids (except glycine) in keratin. The alpha carbon for glycine is conspicuous around 43 ppm.^{197,199-202} The aliphatic region is dominated with signatures from cysteine, proline, isoleucine and alanine. Similar peaks are seen for the non-adhesive skin (Figure 5.5b). Amidst the keratin dominated spectra, it was interesting to observe the peaks related to lipids in the aliphatic region (33 ppm, 30 ppm and 14 ppm) for toe and skin sheds (Figures 5.5). Such peaks have been observed previously in keratin-based systems.¹⁹⁹⁻²⁰³ Generally, lipids (DPPC as an example, Figure 5.2) show distinctive peaks at 33 ppm and 30 ppm corresponding to the CH_2 repeating units, and another peak at 14 ppm due to the terminal methyl (ωCH_3) in their structures.¹⁹⁹⁻²⁰³ The lipid peaks observed in NMR would be a contribution from both the unbound lipids as well as esterified bound lipids present in the toe or skin sheds. To confirm we were removing unbound lipids using the method described previously,²⁰⁶ lipid peak intensities in delipidized sheds were observed. The reduction in the lipid peak intensities (33 ppm and 30 ppm $\sim (CH_2)_n$ and 14 ppm $\sim \omega CH_3$) in delipidized toe and skin sheds

confirms the removal of loosely bound lipids (Figure 5.5). Post delipidization we do still see a small peak in lipid regions, which is likely from the esterified lipids.

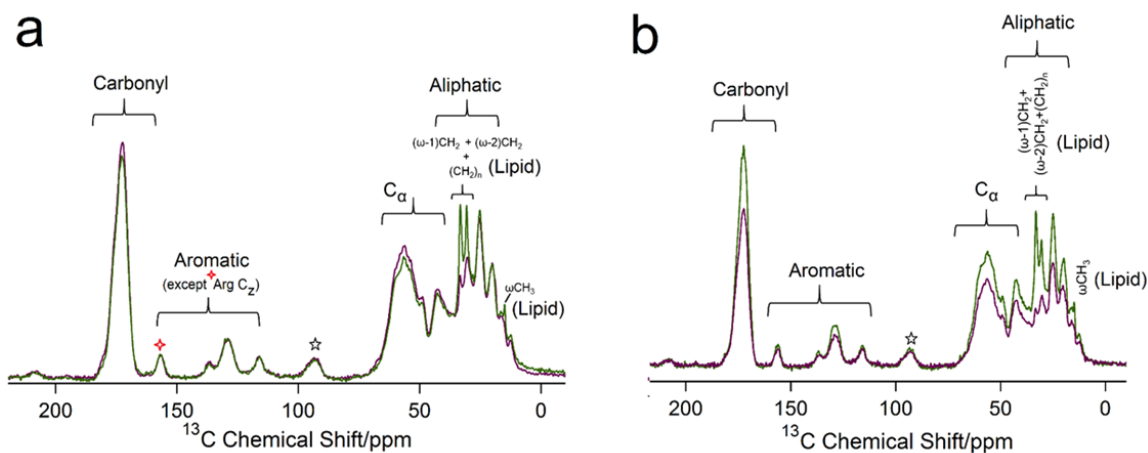


Figure 5.5 CP/MAS spectra shows the pristine (green) and delipidized (purple) for toe (a) and skin (b) sheds. The spectra are measured at MAS frequency ~ 6 kHz. Star labelled peak refers to spinning sideband.

Direct Polarization/Magic Angle Spinning (DP/MAS) and ^1H /Magic Angle Spinning ($^1\text{H}/\text{MAS}$): To assess the mobility of the lipids present in the sheds, DP/MAS (Figure 5.6) and $^1\text{H}/\text{MAS}$ (Figure 5.7) techniques were used. Sharp signals in these techniques indicate the presence of mobile molecular segments in the sample, contrary to CP/MAS. The majority of the signal in pristine toe and skin shed spectra is concentrated in the aliphatic range (Figure 5.6 inset, 0-50 ppm), which is the lipid dominant region, indicating lipids are more mobile than the keratin in the toe and skin sheds.²⁰³ In addition, the carbonyl region shows a broad peak and most of the amino acid peaks seem to be absent except the broad peak in the aliphatic region and few sharp signatures in the aromatic region, again indicating that the keratin constituent is rigid compared to the mobile lipid material in the

toe sheds. The sharp keratin signatures detailed above in CP/MAS (Figure 5.5), further confirms the rigidity of keratin and compliments the DP/MAS results. In detail, sharp lipid signatures in the DP/MAS results can be seen at 37.9 ppm, 32-33 ppm, 30.5 ppm, 25.2 ppm, 23.4 ppm and 14.7 ppm corresponding to αCH_2 , $(\omega-2)\text{CH}_2$, $(\text{CH}_2)_n$, βCH_2 , $(\omega-1)\text{CH}_2$, and ωCH_3 respectively²⁰³ (Figure 5.6 inset). Upon delipidization, these prominent peaks, specifically the CH_2 and ωCH_3 region, reduce in intensity.

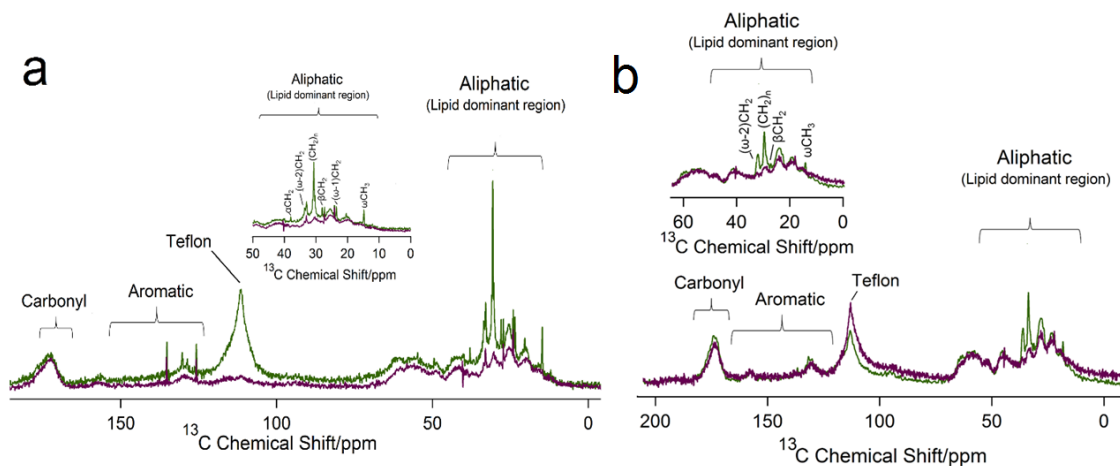


Figure 5.6 DP/MAS spectrum for the pristine (green) and delipidized (purple) toe (a) and skin (b) sheds respectively. The inset is enlarged aliphatic region (0-50 ppm) showing lipid signatures $(\text{CH}_2)_n$, $(\omega-1)\text{CH}_2$, $(\omega-2)\text{CH}_2$, αCH_2 and βCH_2 and ωCH_3 . All spectra are measured at MAS frequency ~ 6 kHz.

Figure 5.7a shows the ^1H MAS spectrum for pristine and delipidized toe sheds. Considering the phosphatidylcholine (DPPC) structure as an example (Figure 5.2). The peaks ranging from 1.1 ppm to 1.4 ppm corresponds to $(-\text{CH}_2-)_n$, $(\omega-1)\text{CH}_2$ and $(\omega-2)\text{CH}_2$; 0.7 ppm corresponds to terminal alkyl protons (ωCH_3); and 1.8-2.5 ppm covers protons at α/β positions next to carbonyl group.²¹⁴ The broad peak seen at 3.9-4.7 ppm encompasses the alpha protons from the amino acids²¹⁵ constituting the keratin in the toe

shed. This range can also include signatures from other protons in the lipid structure.²¹² The appearance of the sharp peak at 4.8 ppm riding over the broad peak may be potentially attributed to the presence of water in the sample. After the toe shed sample was delipidized, the reduction in the intensity of the lipid peaks is evident in the spectra. Again, the peak intensities for 1.1 ppm ($(-\text{CH}_2)_n$, $(\omega-1)\text{CH}_2$ and $(\omega-2)\text{CH}_2$) and 0.7 ppm (ωCH_3) regions are affected by delipidization, confirming the removal of unbound lipids. Similar peaks can be seen in skin shed both prior to and after removal of unbound lipids (Figure 5.7b).

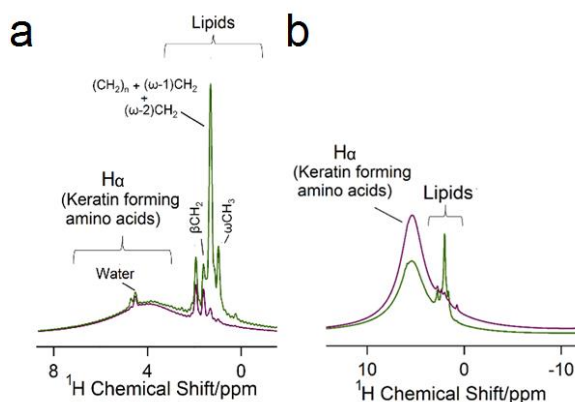


Figure 5.7 (a) and (b) are the ^1H MAS NMR spectra for toe and skin sheds respectively. The sheds have been analyzed in both pristine (green) and delipidized (purple) forms. All spectra are measured at MAS frequency ~ 6 kHz.

5.4 Discussion

Reptilian epidermal lipids playing an important role as a barrier to water loss¹⁸³ are primarily of two types: polar and non-polar. Polar lipids include phospholipids such as phosphatidylcholine, phosphatidylethanolamine, phosphatidylserine, phosphatidylinositol, lysophosphatidylcholine and sphingomyelin, while non-polar lipids include cholesterol, diacylglycerols, alcohols, free fatty acids, aldehydes, wax esters and sterol esters.²¹⁰

Although it was known that these lipids are present in the mesos and alpha layers of the reptilian epidermis,¹¹⁹ it was surprising to detect them also in the oberhautchen layer and maturing setae being formed during regeneration cycles¹¹⁹ and in gecko footprints.¹¹⁸

Solution-State NMR and TLC in this study confirm first that unbound lipids exist and further, were successfully removed from the sheds. Lipid components are similar in the toe and skin sheds (Figure 5.4 and Table 5.1). Solid-State NMR results on the adhesive toe pad and skin sheds (¹³C CP/MAS, DP/MAS and ¹H/MAS; Figure 5.5 , 5.6 and 5.7) confirm the presence of lipids. Upon extraction of unbound lipids,²⁰⁶ the presence of the residual peak in the lipid region of the delipidized spectra indicates that there may be bound lipids present in the sheds.²⁰² Interestingly, major phospholipids found in the gecko footprints (PC and SM), are present in the toe shed extracts, consistent with the observation that geckos leave footprints on surfaces.¹¹⁸

Although we see sharp signatures for lipids in the ¹³C CP/MAS spectra, overall it seems the lipids are mobile compared to the rigid keratin proteins in the sheds. The appearance of a sharp lipid peak (33 ppm) in the ¹³C CP/MAS is due to the methylene group of the crystalline all-trans hydrocarbon chains present in general lipid structure.²⁰³ Conversely, in ¹³C DP/MAS the liquid like trans/gauche conformation appears at 30-31 ppm, thus the sharp peak observed in the ¹³C DP/MAS at around 30 ppm is more strongly supported.²⁰³ While the difference in mobility of keratin and lipids is intriguing, it is important to remember that the sheds from the toe pad are not exclusively comprised of setae; they are attached to several layers of epidermis. However, the setae account for ~65-70% of the total mass (Appendix B).

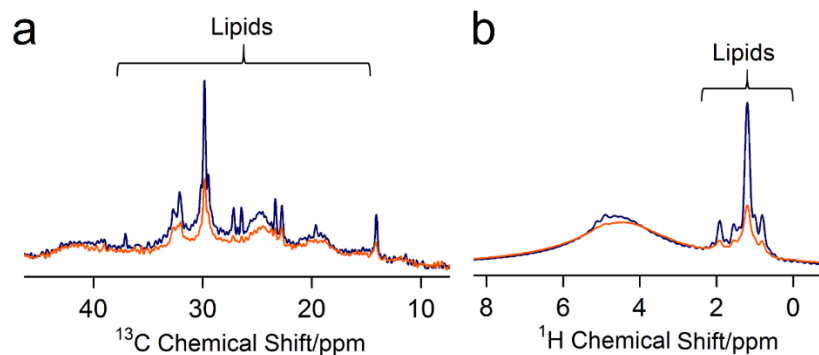


Figure 5.8 (a) and (b) are the direct polarization and proton magic angle spinning spectra respectively for pristine toe (blue) and pristine skin (orange) sheds. The nature of the lipid region differs in the toe and skin shed samples highlighting the difference in the lipid mobility between the two types of sheds from the gecko epidermis. All spectra are measured at MAS frequency ~ 6 kHz.

There are clear differences in lipid mobility between toe and non-adhesive skin (Figure 5.8). Pristine toe sheds show sharper lipid peaks compared to the pristine skin, indicating that lipids are more mobile in the setae than the skin. Interestingly, another major difference between the skin and toe shed samples is seen in their response to delipidization. Visually, after delipidization clear differences are seen in the texture of the toe and skin sheds. While the toe sheds seem to be intact, the skin sheds seem to become rough and break after the treatment (small skin pieces are seen in the solvent mixture post treatment). Interestingly however, we do not see a similar behavior in the adhesive toe pad sheds. This contrasting behavior, in addition the difference in lipid mobility between toe and skin sheds may not be surprising as it is consistent with previous observations of the differential organization of lipids and keratin in the adhesive setae and in the skin of a gecko and an anole.¹¹⁹ Indeed, recent analyses of specialized regions of epidermis in lepidosaurs like the

adhesive setae of geckos¹³⁰ or the ventral scales of snakes,²¹⁶ suggest that protein and lipid distribution may vary in response to functional roles of the epidermis. For example, even though an alpha and mesos layer may be conserved in structure and function across species and region of the epidermis, outer layers such as the beta and oberhautchen may differ in protein and lipid content organization.²¹⁷ Moreover, it may be important to distinguish how variation in protein-lipid interactions could be driven not only by function in the mature epidermis, but also in the development of the tissue itself.

Our observations of different responses in NMR hints that there are differences in keratin and lipid associations (chemical or physical) in the two types of epidermal sheds. Past immunological and ultrastructural studies involving characterization of keratin shows the presence of two major beta proteins Ge-cprp-9 (cysteine rich) and Ge-gprp-6 (glycine rich), as well as alpha keratin proteins, Alfa1 and Alfa2 in the gecko setae.¹⁹² Raman spectroscopy also confirmed the presence of alpha and beta keratins in the setae with primarily cysteine/phenylalanine/tyrosine signatures.¹³² These signatures were detected in the ¹³C CP/MAS spectrum for the toe sheds (Figure 5.5). On the other hand, the non-adhesive skin is comprised of the proteins Ge-gprp-1, Ge-gprp-3, Ge-gprp-4, Ge-gprp-6, Ge-gprp-7 and Ge-gprp-8 with amino acids glycine, serine and proline being the most abundant,²¹³ all of which could be seen in ¹³C CP/MAS results for skin sheds. The ¹³C CP/MAS spectra for both toe and skin sheds show amino acid peaks dominating the spectra, indicating the rigid nature of the keratin. Our TLC and Solution State NMR results report that there is little to no difference in lipid composition between the adhesive toe pad sheds and the skin, yet clearly the keratin components do differ, specifically in the dominance of particular amino acids. It may be these differences that result in the

difference in lipid mobility between toe pad shed and skin shed. Another possibility is the difference in the physical arrangement of lipids with the keratin in the toe and skin sheds. It is known that the lipids in the skin shed (brick and mortar layer) (Figure 5.9) may be arranged in an orderly manner (orthorhombic or hexagonal),²¹⁸ thus being less mobile. In contrast, lipids in the toe shed are also present in the setae as a part of the matrix,^{119,131,132} surface coating¹¹⁸ and/or spatulae¹¹⁸ (Figure 5.9). In these locations lipids are likely in a more disordered manner and are thus more mobile. We believe that the difference in lipid mobility in the skin shed and toe pad shed is either: 1. related to the chemical association of keratin components with lipids, where lipids in the toe pad sheds are more mobile by association with the cysteine and glycine rich keratin,¹³⁰ as opposed to the lipids in the skin shed which are associated with glycine, serine and proline rich keratin²¹³ or 2. due to the difference in the physical association between the keratin and lipid components.²¹⁸ Clearly further investigation is necessary to fully understand this complex relationship but NMR results provide evidence that the setal structures on the gecko toe pad are not just morphologically specialized but also perhaps chemically specialized, where unbound lipids are weakly associated with the rigid keratin proteins. This hypothesis is further supported by the relatively easy and routine deposition of lipid footprints by the gecko as it moves across surfaces.¹¹⁸

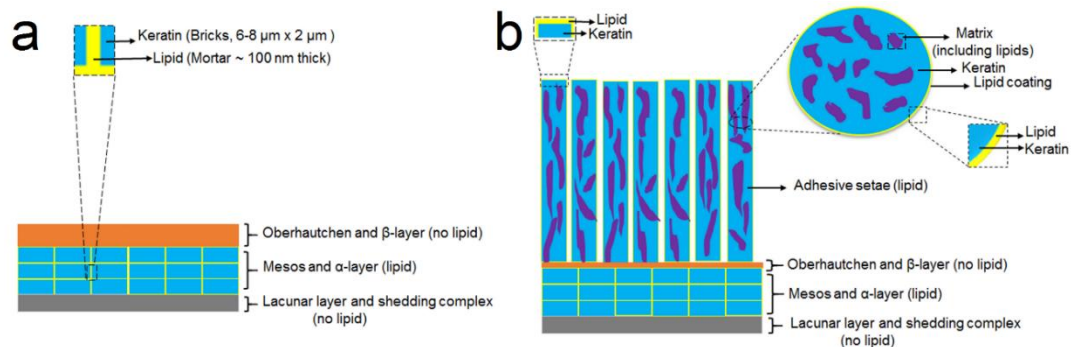


Figure 5.9 (a) Layers of skin shed including the brick and mortar-based mesos and alpha layer rich in lipids. (b) Layers in the toe pad shed, where setae (lipid rich) are added to the skin layers described in (a). The setae likely contains lipids in the form of a thin coating, in the adhesive spatulae (not shown) and matrix. The matrix is a combination of lipids (yellow) and unknown material (purple). The figures have not been drawn to scale and the spatula have not been included in the rendering of (b).

Finally, we can use results above to compare proposed models for keratin-lipid association in the setae.¹¹⁸ The toe sheds consist of outer keratinized setal hairs and several inner layers of cells that may contain lipids (Figure 5.9). The α -layer present underneath consists of “brick and mortar” pattern, where keratinocytes form the “bricks” and the lipids form the “mortar”.^{218,219} Based on the amount of lipid extracted from the toe sheds and the dimensions of the bricks and mortar reported in previous publications, we can estimate that ~ 11 wt.% of the setal hairs are composed of lipids (Appendix B). The models¹¹⁸ where lipids are only present as an outer thin layer on setal hairs or as a major component in the spatula seem unlikely because the mass of lipid extracted is far greater than that predicted based on the amount of lipids extracted from the setal hairs. A more realistic model is the heterogeneous model,¹¹⁸ where the lipids are distributed with the keratin throughout the

setal hairs. However, the Solid-State NMR results suggest that spatial proximity of keratin and lipids has to be larger than 0.5 to 1 nm,²²⁰ this is because after lipid extraction the protein peaks were unaffected. Therefore, a more realistic model of lipid distribution within the setae would be similar to the transmission electron microscopy (TEM) cross-section images published by Rizzo et al.¹³² and Huber et al.¹³¹ In this region of specialized epidermis, keratin is not organized into lamellar blocks as in coenocytes, but instead into long filaments of uncertain nano-construction.²²¹ Huber et al.,¹³¹ showed that the darker-colored keratinized regions (69% by volume, 80-100 nm in diameter, and microns in length) are separated by lighter-colored 'matrix' region (31% by volume).¹³¹ The TEM images did not provide the chemical composition of the matrix and we propose that part of that matrix is composed of unbound lipids (almost 37% of the matrix based on the amount extracted, see appendix), as has been proposed for the lipid-keratin association in mammal stratum corneum.²²¹ A physical model illustrating the association of the lipids with keratin is shown in Figure 5.9. In this model, we have included the possibility that the outer thin layer is still composed of lipids. In addition, it is also possible that there are bound lipids associated directly with keratin. Upon removal of unbound lipids, the structure of the setal hairs is still intact in contrast to the extraction of the lipids from the skin. In the case of skin, the extraction affects its physical integrity. Although further work is required to confirm this model organization, it is intriguing to consider a specific keratin and lipid architecture in the setae, perhaps for use as a specialized controlled wear component, where lipids are sacrificed at the adhesive interface by being more mobile than those same lipids in the non-adhesive skin.

5.5 Conclusion

In summary, we detected lipids in the adhesive setae of gecko toe pad sheds using NMR-based techniques. First, the sheds were delipidized to remove loosely bound surface lipids, the removal being evident in the NMR results. Additionally, the lipid extract was characterized using Thin Layer Chromatography and Solution-State NMR. Second, Solid-State NMR was used to investigate the association and dynamics of the lipid and keratin components of both toe and skin sheds. Analysis on the non-adhesive skin was primarily done to differentiate between the two types of material in the toe pad sheds (setae and underlying skin). Similar lipid associations were found in the toe pad shed and the non-adhesive skin shed but clear differences were seen in the dynamic behavior of the respective lipid regions. Lipids in the toe shed were more mobile than those in the skin sheds, suggesting that the specialized adhesive setae are chemically or physically structured differently than the rest of the epidermis. These findings have important implications for understanding the assembly of lipids and keratin in the adhesive setae as well as in fabrication of gecko-like adhesives using a mixture of materials. We also believe that the presence of lipids in multiple natural adhesive systems, ranging from barnacles¹¹ to geckos^{118,119}, highlights an important role of lipids in these systems, which needs to be more fully appreciated and investigated. Clearly our work here provides evidence that the lipid-keratin association in the specialized adhesive structures of the gecko is specific to those structures and thus may be relevant to their function.

CHAPTER VI

ROLE OF SURFACE LIPIDS IN ADHESIVE AND ANTI-ADHESIVE PROPERTIES OF GECKO SETAE

This work has been adapted from a previously published article,
Stark, A.Y., Subarajan, S., Jain, D., Niewiarowski, P.H. and Dhinojwala, A.

Phil. Trans. R. Soc. A. **374**, 20160184 (2016).

6.1 **Introduction**

Despite their complexity, hierarchically structured surfaces are surprisingly prevalent in the natural world.²²² Examples of hierarchical surfaces span taxonomic phyla (broad groupings of biological organisms), suggesting that these structures have a specific functional role for the organism. These functions include the production of colour in the butterfly wing and bird feather,²²³ the self-cleaning of dirt from the lotus leaf,²²⁴ or even the layering of filaments and fibrils in mechanically resilient biological materials like bone, nacre and chitin.²²⁵ While the structure–function relationships of these common examples appear to be well resolved, most are only studied with one specific relationship in mind, rather than taking into account a system- level series of relationships and possible trade-offs.²²⁶

The adhesive gecko toe pad is another well-known example of a biological hierarchically structured surface. The gecko toe pad consists of thousands of fine, hair-like structures which often branch and terminate into flattened tips that make millions of contact points with the surface a gecko clings to.²²⁷ Over the past 15 years, the hierarchal gecko toe pad has been intensely studied, and the adhesive mechanism, via this complex hierarchy, has been well resolved.¹⁹ Interestingly, in addition to being adhesive, the structured surface of the gecko toe is also anti adhesive, that is superhydrophobic and possessing a low contact angle hysteresis.^{116,117} We do not fully understand if this anti-adhesive behaviour of the toe pad is (i) relevant for adhesion or some other function, or (ii) if it is a non-functional remnant of the development of an adhesive made out of the materials available to the gecko (i.e. proteins and lipids) and its requirements (i.e. multiple contact points). We believe the answer to this question can only be resolved by investigating the complex interaction between adhesion and anti-adhesion jointly, and in an ecological context.

Since the discovery of invisible lipid footprints left behind by geckos as they walk,¹¹⁸ we have questioned what the role of lipids is in adhesion, if any role exists, and if they relate to a higher-level interaction between adhesion and anti-adhesion. While it appears lipids likely contribute to anti-adhesion,¹¹⁶ if and how they relate to adhesion is unknown. Narrowing our focus to surface lipids on the adhesive setae of the gecko toe, the most obvious role these lipids may play is in adhesion directly. It is unclear how a soft, wearable, fat-like layer helps adhesion, and rather, it intuitively seems like it would impede it. However, it is our common misconception to assume that all adaptations in biological systems like the gecko are related to a single function, without considering system-level

concerns and trade-offs.²²⁸ For instance, if the setae were completely hydrophilic and lacked this lipid layer they may be more adhesive, increasing the likelihood of self-adhesion and fouling. Directionality of the setae and the intimate contact made by spatular tips have been shown to be imperative for successful attachment;^{114,229,230} thus, reducing self-adhesion or adhesion of dirt by adding a non-sticky lipid surface layer could benefit the gecko at a system level. Furthermore, consider the repeated use of the setae. Geckos shed their skin and replace the adhesive setae every few months. Until then, the setae are used over and over on a variety of surfaces. Of all the microscopic images of gecko setae in the literature, none document obvious evidence of wear. In fact, the only wear appears to be in the form of the lipid gecko footprint.¹¹⁸ Perhaps, it is the wear of this fine lipid layer that protects the larger setal structure against constant abrasion in the gecko's natural environment. This again points to a system-level requirement. With regards to skin, lipids have been shown to help other reptiles, like snakes, avoid water loss.¹⁸³ The lipids act like a protective barrier in the skin to prevent desiccation, which is imperative to the survival of reptiles. In this instance, lipids associated with reptile skin may be a by-product of a separate system-level requirement. It is important to note however that desiccation preventative lipids are located in the mesos layer of the epidermis, rather than the surface, and skin surfaces like the gecko tail do not leave behind detectable lipid residue.²³ Finally, consider that many species of gecko live in the tropics, which can have significant environmental implications for the setal material, and ultimately the lipid layer that coats the surface of the adhesive setae. Specifically, Young's modulus of bird feathers (made of β -keratin) significantly decreases as humidity increases,²³¹ even at moderate levels (i.e. approx. 4 GPa at 0% RH to approx. 2.5 GPa at 50% RH); however, gecko setae resist this

reduction up to 80% RH.^{41,131,151,232} In this case, perhaps having a hydrophobic lipid layer keeps water from softening the structural keratin fibrils within the setae, allowing the setae to maintain integrity in tropical environments. Lastly, it has become clear that adhesion to wet surfaces benefits from the superhydrophobic toe pad; however, the role of lipids in this function is difficult to determine since adhesion on wet surfaces is also highly substrate dependent.^{116,142} It does appear that in whole-animal adhesion tests, an air-filled plastron resulting from the superhydrophobic toe pads is required for successful attachment on wet surfaces, a surface condition that could be common in the tropics.^{122,142} We believe that resolving the role of lipids, if one exists, in the gecko adhesive and anti-adhesive systems will significantly contribute to the design of gecko-inspired synthetics which are able to capture more of the remarkable properties of the natural system.

To resolve the question about the role of lipids in the adhesive and anti-adhesive systems of the gecko, we specifically focused our attention on the non-covalently bonded lipid layer (discussed in the previous chapter) that likely coats the surface of gecko setae. The material composition and structure of the gecko setae is not fully clarified, however here we will use the model proposed in the earlier chapter²³ to direct this study. We developed a structural model for gecko setae that consists of β -keratin filaments surrounded by covalently bound lipids and "coated", or covered by a non-covalently bound lipid layer on the outside of the gecko setae.²³ In this study, we directly target the non-covalently bound surface lipid layer, as it is likely to be relevant to both the adhesive and anti-adhesive systems. Variation in adhesive performance in several key scenarios that are relevant to gecko adhesion in their natural environment will be explored, as well as the role of this lipid layer on anti-adhesion.

The gecko adhesive system must function in a variety of contexts. Here, we will focus on three specific environmental challenges that are relevant to both the adhesive and anti-adhesive systems of the gecko. First, to investigate the role of the surface lipid layer on the adhesive system of the gecko, we will test adhesion of gecko setae on hydrophilic glass and on glass coated with a hydrophobic octadecyltrichlorosilane self-assembled monolayer (OTS-SAM). Adhesion to these two substrates will be tested with surface lipids intact and when removed using a chemical treatment. If adhesion between untreated and treated samples differs, this would be the first example of a functional role for lipids in gecko adhesion. Additionally, Persson proposed that a compliant, soft, liquid-like material layer on the surface of setae may be used to conform to small, nanometer-scale surface asperities, improving adhesion on these challenging substrates.²³³ We could not neglect the relevance of this assertion to the discovery of the presumably soft lipid coating that wears from gecko feet when they walk.¹¹⁸ To investigate the role of surface lipids on adhesion to fine surface roughness, we tested adhesion of treated and untreated gecko setae to fine grit sandpaper in air. If the hypothesis by Persson is supported, the anti-adhesive nature of the gecko toe may be a by-product of adhesion to rough surfaces in air, rather than have a direct function specific to anti-adhesion. roles anti-adhesion may contribute to the overall gecko system. Then, we will explore the question of optimization, or the balance between adhesion and anti-adhesion, using a targeted experimental approach to investigate the role of surface lipids in adhesion in air, underwater and on rough substrates.

To investigate the role of surface lipids on the anti-adhesive system of the gecko, we will measure water contact angle on treated and untreated setae. If the anti-adhesive system of the setae is dependent on surface lipids, the treated setae will wet, transitioning

from the Cassie-Baxter non-wetting state to the Wenzel wetting state. Lastly, to investigate the interaction of the adhesive and non-adhesive gecko systems, adhesion to the hydrophobic OTS-SAM coated glass will be tested in water with and without surface lipids. We have found that adhesion underwater requires the maintenance of both the anti-adhesive and the adhesive system, as well as contact with a hydrophobic or intermediately wetting surface. Thus, by comparing this result to the results of the experiments aimed at the adhesive and anti-adhesive systems independently, we will be able to understand system-level requirements for each system. These four tests are far from exhaustive, but represent a first look into the role of surface lipids on the hierarchically structured gecko toe pad with a focus on teasing apart the influence of the adhesive and anti-adhesive systems.

6.2 Experimental Section

Sample preparation and characterization: Adhesive setae were collected in the form of a toe pad skin shed, which is epidermis that geckos shed at approximately monthly intervals. Shed skin from six moulting Tokay geckos (*G. gecko*) was stored at -20°C .^{23,116} Adhesion of single toe sheds was tested in air on three substrates: glass, OTS-SAM-coated glass and sandpaper. The OTS-SAM-coated glass surface has been described previously¹¹⁶ and has a water contact angle of $95\pm 2^{\circ}$. The water contact angle on the glass surface was fully wetting at the beginning of all experiments. The sandpaper surface (2500A, 3M Wet/Dry sandpaper, Lee Valley Tools, Canada) has a root mean square roughness of approximately 500nm ($50\times 50\mu\text{m}$ sample area), as determined using atomic force microscopy (Veeco Dimension Icon AFM), and a water contact angle of $56\pm 4^{\circ}$. This fine microstructure was used to specifically target scale of the spatulae, where it is likely

incomplete contact will occur due to the similarity in dimensions of the sandpaper asperities and the spatulae.²³⁴ We also measured adhesion of toe pad sheds in water using the OTS- SAM-coated glass substrate. Each of the substrates (glass, OTS-SAM-coated glass and sandpaper) and environments (air or water) were tested with sheds that had either been left untreated or were chemically treated to remove surface lipids from the setae. There were eight total pairings of surface, environment and treatment (lipids intact or removed), where six toe pad sheds were used per pairing, totalling 48 toe pad sheds across all adhesion experiments. Each of the six geckos contributed one toe pad shed per pairing, which allowed us to control for individual differences across all treatments. We used a chloroform–methanol treatment, outlined first by Swartzendruber et al.²⁰⁶ and adapted in our previous study (Chapter V) to remove surface lipids from the toe pad sheds.²³ Briefly, the toe pad sheds were immersed in three solutions of chloroform–methanol with concentration ratios of 2 : 1, 1 : 1, 1 : 2 for 2h each and then for 1h each. We confirmed removal of surface lipids using TLC and solution-state NMR, as detailed elsewhere.²³ To investigate the effect of chemical treatment, we tested adhesion of toe pad sheds that had been treated with acetone on glass (an additional six sheds per treatment). Acetone was used because it does not significantly remove the lipids of interest,^{235,236} but reflects chemical treatment and handling that the experimental groups received. The treated toe pad sheds were air dried for 7 days post-treatment and vacuum dried for 45 min after the drying period. Treated toe pad sheds appeared both mechanically and visually intact.²³ Adhesive area of the sheds was measured after experiments using a dissecting microscope with a mounted camera and IMAGEJ software (National Institutes of Health, Bethesda, MD, USA).

Adhesion Testing : Adhesion measurements were collected using a motorized force testing apparatus^{16,116} in an environmentally controlled chamber that was maintained at $23.8 \pm 0.1^\circ\text{C}$ and $32.6 \pm 0.2\%$ RH. Samples were mounted onto a glass slide using double-sided copper tape and positioned in a testing arena described elsewhere.¹¹⁶ A weighted glass slide, a weighted OTS-SAM glass coated slide and a weighted glass slide with sandpaper attached to the back (all ~46g) were used to test for the effect of surface lipids on adhesion to hydrophilic, hydrophobic and rough surfaces respectively. Slides were cleaned with ethanol and water before each sample test (except the sandpaper slide). The glass slide was also cleaned in base bath and oven dried at 120°C prior to experiments. The test substrate (weighted slides) were attached to a motorized force sensor using a nylon string. A motorized force sensor then slid the test substrate across the setal samples at a controlled rate, recording force as a function of time. The same procedures were followed to test samples on the OTS-SAM coated glass substrate in water, except that after the sample was mounted in the test arena, the arena was filled with enough water to cover the sample. The acetone experiment followed the same procedure as all other treatments performed in air. Maximum shear adhesion was determined as the highest force reading during the approximately 4cm slide of the substrate across the shed sample. Samples were tested randomly within treatment groups and test order of treatment groups was also randomized.

Anti-adhesion Testing: To investigate the effect of surface lipids on the anti-adhesive system of the gecko, we compared water contact angle of untreated and treated samples using methods from Badge et al.¹¹⁶ We used three toe pad sheds per treatment, and measured water contact angle at three different locations per sample. None of the samples used in adhesion trials were used for water contact angle measurements.

Statistical Analysis: To investigate the role of surface lipids on the gecko adhesive system, we used an analysis of covariance (ANCOVA) to test for differences in maximum shear adhesion of toe pad sheds, where treatment (lipid removal), substrate (glass, OTS-SAM coated glass and sandpaper) were the main effects and toe pad area was a covariate. To investigate the role of surface lipids on the gecko anti-adhesive system, we used Student's t-test to compare average water contact angle of treated and untreated samples. Next, to investigate the interaction of the adhesive and anti-adhesive gecko systems jointly, we used an ANCOVA which tested for a difference in maximum shear adhesion on the hydrophobic OTS-SAM coated glass substrate where treatment (lipid removal), environment (air or water) were the main effects and area was the covariate. Finally, to test shear adhesion of toe pad sheds that were treated with acetone or left untreated we used an ANCOVA where treatment (acetone treatment or untreated) was the main effect and area was the covariate. Maximum shear adhesion was log transformed in all adhesion tests to conform to the assumptions of the models used. To test for differences within groups we used a Tukey HSD test to control for multiple comparisons. Means are reported as mean \pm 1 s.e.m.

6.3 Results

Role of lipids in adhesion: Our first goal was to investigate the role of surface lipids on the gecko adhesive system by measuring shear adhesion of gecko toe pad sheds on hydrophilic glass, hydrophobic OTS-SAM coated glass and fine sandpaper in air. We found that lipid treatment, substrate and their interaction all had a significant effect on shear adhesion of gecko toe pad sheds ($F_{6,29} = 50.43$, $p < 0.0001$; Appendix A). Specifically, we found that samples that had their surface lipids removed had significantly higher adhesion

to glass than untreated samples, and that there was no difference in adhesion across treatment in the other two substrates (Figure 6.1).

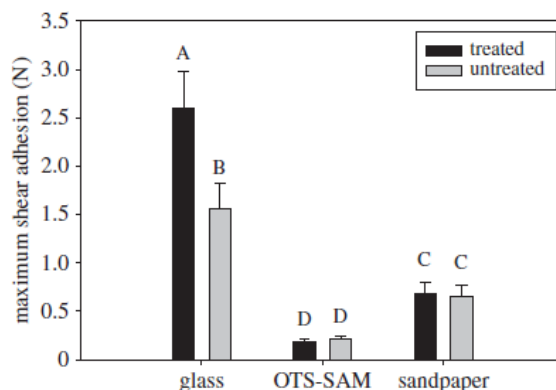


Figure 6.1 Adhesion of gecko toe pad sheds in air on hydrophilic glass, hydrophobic OTS-SAM coated glass and fine sandpaper (root mean square roughness $\sim 500\text{nm}$ for a $50 \times 50 \mu\text{m}$ sample area) after treatment to remove the setal surface lipids. Letters above the bars indicate statistical significance, where bars with different letters are significantly different from one another. Error bars are mean ± 1 s.e.m.

Role of surface lipids in anti-adhesion: Our second goal was to investigate the role of surface lipids on the gecko anti-adhesive system by measuring water contact angle. Unlike oxygen plasma treatment of gecko setae, which changed the elemental chemical signatures at the setal surface and caused structural deformity,¹¹⁶ the water contact angle measurements of setae with surface lipids removed was no different than pristine setae ($142.2 \pm 1.83^\circ$; $t = -1.81$, $df = 15.56$, $p = 0.0897$). This suggests that the surface lipids removed using this treatment do not significantly contribute to the anti-adhesive behavior (i.e., superhydrophobicity) of the gecko toe.

Effect of surface lipids on relationship between adhesion and anti-adhesion: Our third and final goal was to investigate the role of surface lipids in the adhesive and anti-adhesive systems jointly. Here we saw no difference in adhesion between treated and untreated samples. Specifically, we found that differences in shear adhesion on OTS-SAM coated glass were driven by environment (air or water) only, and that treatment had no effect ($F_{4,19} = 7.93$, $p = 0.0006$; see appendix for details). In this study adhesion in water was higher than in air (with treatments pooled across environment; Figure 6.2). Improved adhesion in water compared to air has been reported previously in other substrates such as polytetrafluoroethylene (PTFE), fluorinated ethylene propylene (FEP), ethylene tetrafluoroethylene (ETFE) and polydimethylsiloxane (PDMS), and this trend was nearly significant in the similar study by Badge et al.^{116,142–144} The reason for these differences remains unclear.

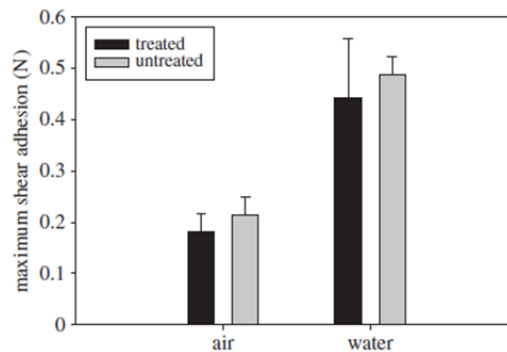


Figure 6.2. Adhesion of gecko toe pad sheds in air and water on hydrophobic OTS-SAM coated glass after treatment to remove the setal surface lipids. There was no significant difference between treatment in air or in water, but adhesion was overall higher in water than air. Error bars are mean \pm 1 s.e.m.

6.3 Discussion

Our first study suggests that surface lipids impair adhesion on hydrophilic surfaces but not hydrophobic or rough surfaces. This could be due to increased polar interactions between the treated setae (i.e., hydrophobic surface lipids removed) and glass. Overall, we also found that adhesion to glass was higher than the other two substrates. We have observed this difference in adhesion between glass and OTS-SAM coated glass previously in toe pad sheds, and thermodynamic models support this trend, but these models do not explain the magnitude of this difference.¹¹⁶ Interestingly the difference in adhesion to glass and OTS-SAM coated glass is not observed at the whole-animal level.¹⁴² Finally, our results also lead us to reject the hypothesis by Persson that the surface lipid layer conforms to rough asperities on the surface to improve adhesion.²³³ However, this was only tested at one scale and at ambient temperature and humidity. The results were consistent with the expected reduced adhesion to the fine-scale sandpaper, as shown by Huber et al.,²³⁴ but it is unclear why adhesion to the OTS-SAM coated glass is even lower than the sandpaper surface. We found no difference in adhesion between the acetone treated and untreated shed samples ($F_{2,9} = 0.14$, $p = 0.8680$; Figure 6.3), however observationally the acetone treated sheds appear to produce similar adhesion values on glass as the lipid treated sheds (these could not be compared statistically). Previous work has shown successful removal of lipids in the integuments of geckos and other vertebrates using the methods described,^{23,206,210} and limited removal of these lipids using acetone,^{235,236} thus we believe that the lipid removing treatment did not significantly alter the setae, however the similarity between the two on glass warrants further investigation.

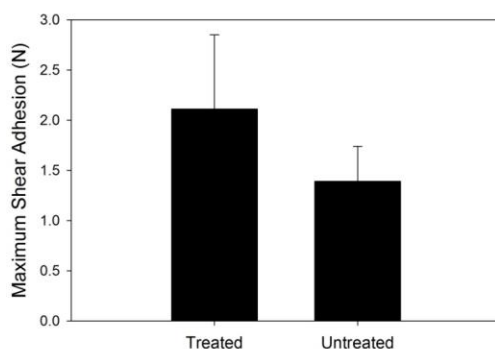


Figure 6.3. Maximum shear adhesion of toe pad sheds tested on a glass substrate either treated in acetone or untreated. There was no significant difference in adhesion between the treated (acetone) and untreated toe pad sheds ($p > 0.05$). Error bars are mean \pm 1 s.e.m.

The results of these experiments suggest that the gecko adhesive system is negatively impacted by surface lipids, at least when adhering to hydrophilic surfaces, and that adhesion to a rough surface at the scale tested here is not aided by surface lipids either. Because surface lipids do not effect the anti-adhesive property, nor do they effect the adhesive performance on hydrophobic OTS-SAM coated glass, there is no performance trade-off related to surface lipids when the two systems are considered jointly in water.

6.4 Conclusion

This work represents the first investigation of the role of surface lipids on the adhesive and anti-adhesive systems since the finding of lipid footprints left behind geckos when they walk,¹¹⁸ and contrary to the common expectation that lipids contribute to some positive performance enhancement, they do not, and rather they hinder adhesion in one specific context. Future work should focus on other system requirements such as self-cleaning and detachment. Another important step in exploring the interaction of the adhesive and anti-adhesive systems of the gecko and how surface lipids contribute to,

hinder, or provide no functional benefit, is to consider the ecology of the gecko. Natural history studies investigating the substrates geckos use in their native environment are lacking,²³⁷ thus it is difficult to predict how the reduction of adhesion on hydrophilic substrates due to surface lipids impacts geckos. If geckos encounter few hydrophilic surfaces in their environment, the role of surface lipids in adhesion and anti-adhesion is inconsequential, however, if geckos encounter hydrophilic surfaces regularly, we may then question if the reduction in adhesion due to surface lipids is relevant to the functional needs of the gecko. For instance, perhaps adhesion to hydrophilic surfaces is strong enough to support a gecko, or in contrast, perhaps adhesive toe pads without surface lipids are too sticky to quickly and reliably detach from these surfaces. The answers to these questions will provide the next steps in understanding the evolution of the adhesive and anti-adhesive systems of the gecko, and accelerate functional improvements of synthetic designs that mimic them.

CHAPTER VII

MACRO AND MOLECULAR RESPONSE OF GECKO SETAE TO HUMIDITY: IMPLICATIONS FOR ADHESION

7.1 Introduction

Geckos are spread worldwide throughout various geographical zones. Their dwelling habitat encompasses regions such as deserts, temperate/tropical rainforests and cold mountains, each having a contrasting humidity and temperature profile.^{238–241} Geckos move, climb and run in these natural habitats covered with different surfaces by means of an excellent attachment strategy based on their specialized foot pads.^{19,110,114,190,191} The unique, van der Waals-based adhesive strategy,¹¹⁵ employs millions of tiny hairs called as ‘setae’, that split further at the tip into smaller nanostructures called ‘spatulae’.^{19,110,114,190,191} Considering the complex structural and material design of setae (i.e., integrated hair-like structures made of β -keratin^{120,130,132,192–194} and lipids^{23,118,119}), the special properties associated with it (fast, reversible, directional, superhydrophobic and self-cleaning)^{24,110,117,124,125,196}, and the diversity of geckos in the natural world^{238–240,242}, it becomes important to understand how the fundamental adhesive components respond and function in different natural conditions. This will undoubtedly provide valuable insights into the fabrication of gecko-inspired attachment strategies that can work in variable environmental conditions.²⁴³

One relevant environmental factor is humidity, that has been of keen interest to gecko adhesion researchers since the past decade. Specifically, humidity enhances gecko adhesion at all scales (i.e., spatula, setae, whole animal).^{16,41,145–149} Multiple hypotheses including capillary bridge formation, change in setal surface energy and setal softening have been proposed but yet no clear consensus has still been established on the mechanism of how these microscopic hairs stick in presence of humidity. The first attempts were back in 2005 when Huber et al.¹⁴⁵ and Sun et al.¹⁴⁹ investigated the nanoscopic adhesion using AFM by testing single spatula and deduced role of capillary bridge formation in mediating adhesion. In 2008 Niewiarowski et al.¹⁶ extended the study to whole animal adhesion in a range of humidity and temperature environments and saw adhesion increasing with increase in humidity. In 2009, Pesika et al.¹⁴⁶ explored the surface wetting properties of the gecko toe pad and suggested a change in the conformation of surface proteins and hydrophilic-lyophilic balance (HLB) of hairs by observing a decrease in the surface hydrophobicity when a drop of water was placed on setal arrays for twenty minutes. The hypothesis of surface hydration and capillary force was ruled out in a series of studies^{41,147,148,151} which stated the dominance of van der Waals forces in controlling humidity driven adhesion. Puthoff et al.⁴¹ studied the adhesion of setal arrays on hydrophilic and hydrophobic surfaces and found similar pull-off forces in presence of humidity. Additionally, they reported increase in softness of setal β -keratin with an increase in humidity, thus laying a new hypothesis related to change in material properties of β -keratin present in hairs contributing to humidity driven adhesion. This hypothesis was further supported by a series of subsequent three studies. Chen and Gao numerically modelled the effect of material stiffness on vertical pull-off of spatular pad, found increase

in adhesion with reduction in setal mechanical properties and suggested humidity being an important factor contributing to van der Waals interaction by modulating the stiffness of setae.¹⁴⁸ Prowse et al. focused on testing the mechanical properties including tensile deformation, fracture and dynamic mechanic response of setae in presence of humidity. The study reported the complex elastic modulus of setae at 100% RH to be one-third of when the setae were dry suggesting softening of setal keratin.¹⁵¹ Finally, in a recent report by Tao et al. based on studying the correlated effect of active (preload, sliding velocity and sliding direction) and passive factors including humidity on isolated setal arrays adhesion showed a 60% enhancement in pull-off forces, when tested in a set of preloads and sliding velocities.¹⁴⁷ Thus, at present the hypothesis is based on van der Waals forces enhanced by softening of setae.

So far we have seen that there are missing links in our understanding of the influence of humidity on gecko adhesion. In that perspective, studying the effect of humidity on the material components of setae is critical. Gecko setae is a complex ensemble of relatively hydrophilic and polar amino acids constituting β -keratin.^{120,129,192,193} The two proteins that are known to be present on the setae surface are glycine cysteine rich beta proteins, HgGC10 (major component) and HgGC3 (minor component). HgGC10 comprising of 13% glycine, 14.5% cysteine and other polar amino acids is hydrophilic and a neutral protein, while HgGC3 (~9% cysteine) is negatively charged. The difference in the composition of the proteins in and around setae is hypothesized to create a microenvironment that enhances the absorption of water and ultimately softens the setae and increase adhesion.¹³⁰ If the hypothesis related to setal softening holds true, then softening should reflect in terms of water uptake by hairs and interaction of amino acid

moieties with water at a molecular level. Detailed knowledge on aspects related to setal hygroscopicity and molecular view of keratin softening in presence of water is absent from the current literature and needs to be evaluated. The other component ‘lipids’ discovered recently in setae,^{23,118,119} are hypothesized to be present as covalently bound and non-covalently bound to the setal proteins. While evaluation of their potential roles in setae has started to generate interest, assessing their participation in humidity response of setae is critical since lipids are known to dictate water uptake in keratin systems such as stratum corneum.

Based on the above-mentioned unknowns, we devised the current investigation to probe the softening hypothesis by evaluating humidity response of gecko toe sheds (obtained from tropical gecko, *Gekko gekko*) that majorly comprise of setae. On a macro level, we first studied the water uptake of pristine, delipidized and oxygen plasma treated toe sheds across a range of relative humidity conditions (30% RH, 60% RH and 90% RH) to understand hygroscopicity of setae, both in presence and absence of lipids. Next, for a molecular level understanding, we carried Solid-State NMR (ssNMR) based Cross Polarization Magic Angle Spinning (CP/MAS) studies on pristine toe sheds exposed to room and high humidity environments. Finally, to check if adhesion enhances upon increase in humidity, we tested shear adhesion of setal arrays on glass substrate in different humidity conditions. The results presented help to add credibility to the outstanding question related to gecko adhesion in presence of humidity and provide a source to stir up ideas in creating gecko synthetics matching natural composition and performance.

7.2 Experimental Section

Collection and preparation of gecko sheds: Natural toe and skin sheds (molts) were collected from Tokay geckos, *Gekko gecko* during their monthly shedding cycle. Details about the precautions taken during shed collection and preparation have been elaborated in our earlier studies (including Chapter V and VI).¹¹⁶ The sheds were used as pristine (native state) and in some experiments in delipidized and plasma treated form. Delipidization²⁰⁶ was carried in the same way as described in Chapter V and VI while protocol for plasma treatment has been explained in an earlier report.¹¹⁶ The sheds (pristine, delipidized and plasma treated) were stored in the freezer at -20°C until further experiments.

Water uptake measurements: To understand the water absorbing capacity of setae present in toe sheds in presence (pristine) and absence of lipids (delipidized: removal of non-covalent lipids and oxygen plasma treated: removal of total (non-covalent and covalent lipids), water uptake measurements were carried across a range of humidity environments: 30% RH, 60% RH and 90% RH. A single toe shed (pristine or delipidized or plasma treated) (mass ~ 1-2 mg) was placed in the Cahn microbalance to measure the mass change. The microbalance was linked to a custom-built humidity set up that was attached to a nitrogen cylinder and included parts such as inlets and controllers for dry and humid air as well as a hygrometer (VWR) to monitor the humidity values (as described in Chapter IV). Before loading in the microbalance, the shed was first exposed to vacuum for about 10 hours to get the dry mass. This dry mass of the shed was then used for the water uptake calculations. After each humidity (30% RH-90% RH) was reached in the microbalance set up, mass was noted for a total of thirty minutes. The water uptake at each humidity was

calculated by subtracting the dry mass (vacuum treated) from the mass at the end of thirty minutes recorded and dividing and the obtained value divided by the dry mass.

Solid-State NMR Measurements: To understand the molecular effects of humidity on the setae present in the toe sheds, NMR experiments were carried out. (a) *Sample preparation:* Pristine toe sheds weighing around 30-35 mg were used for experiments. The humidity ranges studied were 40%-50% RH and 100% RH. For equilibrating at 40%-50% RH, the sheds were exposed to room humidity overnight and for 100% RH, the sheds were placed in a humidity chamber filled with water for 12 hours. After each of the separate exposures, the equilibrated sheds were subsequently packed in a 4mm NMR rotor (Bruker) and loaded in the machine for experiments. Teflon tape pieces were often used to pack the sample tightly in the rotor. (b) *NMR measurements:* All experiments were conducted in Bruker AVANCE 300 MHz NMR spectrometer loaded with a 4mm double resonance VT CPMAS probe. The detailed description of the experimental parameters has been outlined in our earlier NMR-shed study (Chapter V). The experiments were carried at 25⁰C with MAS rate ~ 6000 ± 5 Hz.

Shear adhesion studies: To investigate the effect of softening of setae on adhesion, shear adhesion measurements were carried out. (a) *Sample Preparation:* The pristine sheds collected from geckos were prepared to isolate individual setal arrays also known as lamellae and mounted on 1"x 1" glass pieces using crazy glue. Care was taken to ensure that the glue does not cover the setal hairs. The size of lamellar strip could vary with the position on the toe pad and the individual, thus images were captured before the shear measurements to allow normalization of shear forces with setal area. The same lamellar strip was tested for shear adhesion at all different relative humidity conditions, so that the

effect of humidity was least affected by sample-to-sample variation. Samples were inspected after adhesion tests at each relative humidity to minimize the effect of sample damage on the force measurements. (b) *Method of measurement*: We performed shear adhesion measurements using a homebuilt biaxial friction cell as described in a previous publication.²⁴⁴ The force sensors (made of spring steel) were calibrated by hanging known weights in the range of 1-450 mN. The glass piece with the lamellar strip and the clean glass substrate were mounted on the friction cell. An enclosure around the friction cell helped in maintaining a controlled environment for the shear adhesion tests. We performed shear adhesion tests at four different RH levels (10-15%, 35-40%, 60-65% and 80-85%). The relative humidity inside the enclosure was precisely tuned by adjusting the ratio of dry and wet N₂ (bubbling through water). The relative humidity was monitored using a hygrometer positioned inside the enclosure. The schematic for the setup has been depicted in Figure 7.1. Samples were equilibrated for 15 min at the desired humidity before applying a 5-mN normal force (preload) to bring the setal array in contact with a glass substrate. The sample was then sheared with a velocity of 250 pulses/s using the Newport Optics picomotor in a direction that results in engagement of hairs with the substrate. The shear force was recorded as a function of time at each RH. The maximum force recorded during the run was used for making comparison across different RH and was normalized with the setal pad area to get force per unit area. Comparison has been made between shear force per unit area across different relative humidity conditions and along between pristine sheds. We used an analysis of variance (ANOVA) to test the effect of humidity (10-15%, 35-40%, 60-65% and 80-85%) and lipid state (pristine and delipidized) on the shear force/area values independently. A Tukey HSD test was used to compare significant interactions

while controlling for multiple comparisons. The effect of humidity ($p < 0.0001$) and lipid state ($p < 0.0001$) was highly significant.

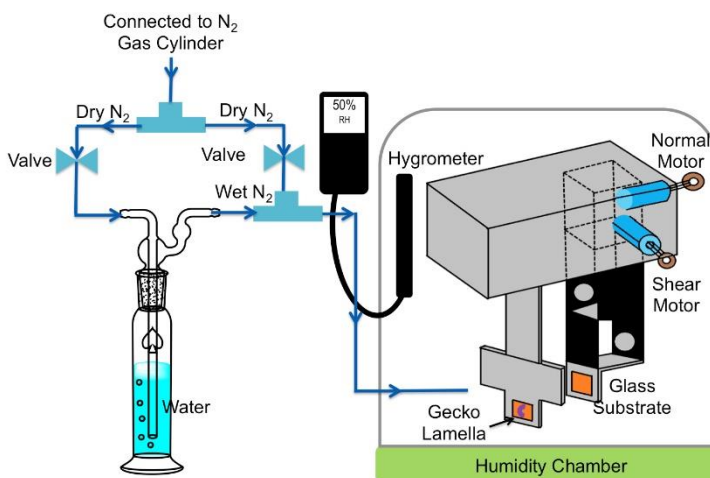


Figure 7.1 Schematic showing humidity set up with the biaxial friction cell for shear adhesion measurements.

7.3 Results

Macro level softening: Figure 7.2a shows the water uptake of a pristine toe shed (setae) across different relative humidity conditions. This is a first direct quantification of the water absorbing capacity of gecko setae. Here, we observe that when humidity is increased, there is an increase in the water uptake by setae. A significant increase (~ 3 times) in uptake was visible when the relative humidity was increased from 30% RH to 90% RH. The total water uptake at 90% RH of gecko setae is similar to natural keratin materials, bird feather (β -keratin) and sheep wool (α -keratin) (Figure 1b). On comparing the hygroscopicity of setae with and without lipids, we found no significant difference at 90% RH (Figure 1c).

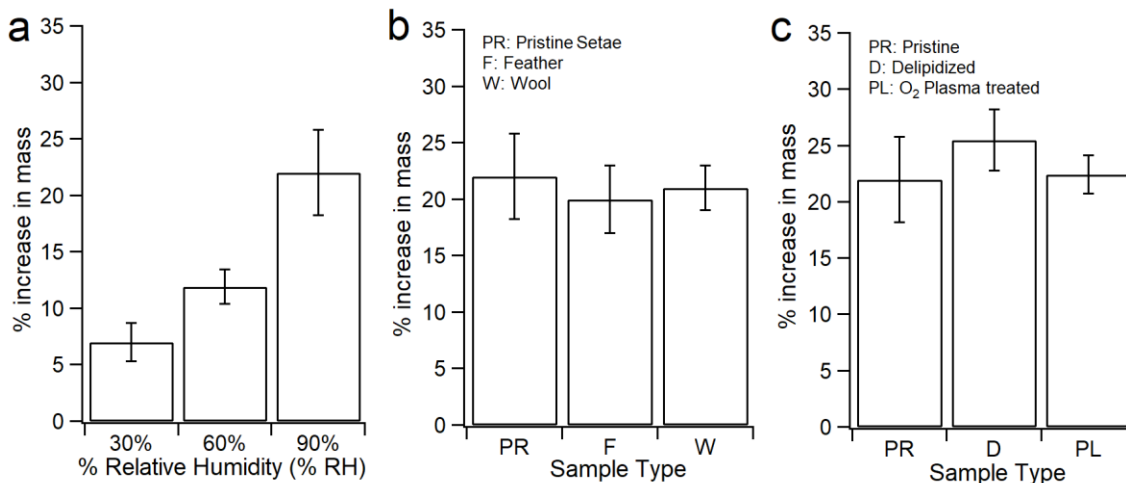


Figure 7.2 (a) shows the water uptake (as a function of % RH) of pristine setae. (b) is the comparison of hygroscopicity at 90% RH between different keratin systems: setae, feather and wool. (c) is the comparison of water uptake of pristine setae with two types of treated setae, delipidized setae (removal of unbound lipids) and oxygen plasma treated setae (total removal of lipids, unbound and bound) at 90% RH. The reported values are \pm standard deviation.

Molecular level softening: To investigate molecular level softening, we compared the response of toe sheds at room humidity (\sim 50% RH) to that at high humidity (\sim 100% RH) using Solid-State NMR based CP/MAS technique (Figure 7.3). To assure that water was not lost during the high spinning NMR experiments, ^1H NMR spectra were recorded before and after the CP/MAS experiments, where water was observed to be intact within the samples. The β -keratin and lipid signatures of setae have been identified in our previous NMR study. On exposure to high humidity, the overall intensity drops as compared to its response at room humidity. In case of β -keratin signatures, there is a decrease in intensity

of aromatic and aliphatic regions indicating increase in the mobility of the protein backbone. The protein moieties that are largely affected include carbonyl, Phe C_{δ,ε,ζ}/Tyr C_γ, C_α regions of glycine and other amino acids, Cys C_β/Pro C_γ/Leu C_γ and Val C_γ/ Thr C_γ. This decrease in intensity for keratinous signatures at high humidity for the toe shed is a first-time report of setae absorbing water, getting mobile and softening at a molecular level. In case of lipids, signatures related to methylene (CH₂)_n and methyl (ωCH₃) moieties are also affected by the hydration process. This change in intensity of the lipid region has been linked to presence of fluid lipids in the system that get affected by presence of water.²⁰³ Past studies with NMR, IR and ESR spectroscopy on stratum corneum have revealed the changes in the lipid hydrocarbon chain mobility upon hydration.

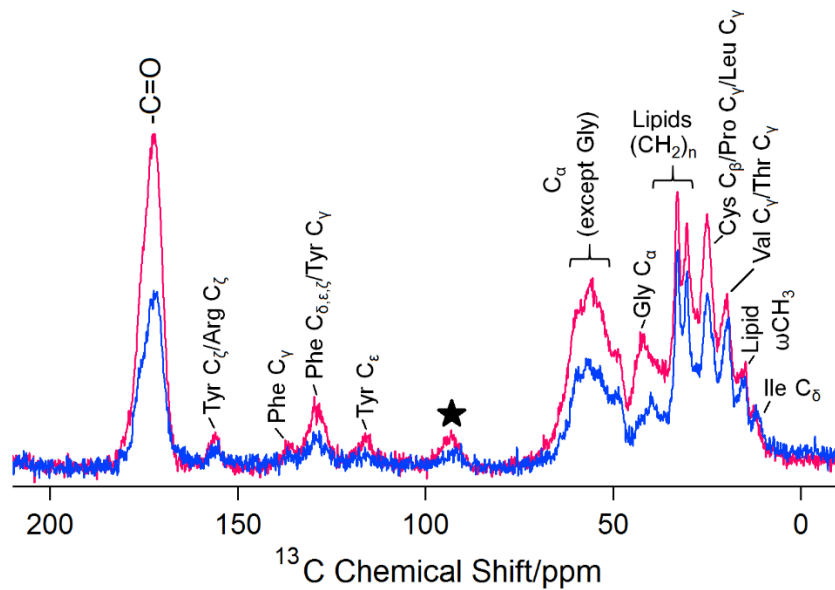


Figure 7.3 CP/MAS spectra of pristine toe sheds exposed at 50% RH (pink) and 100% RH (blue). There is an overall decrease in the intensity of various regions related to β -keratin (majorly) and lipids in presence of 100% RH indicating an increase in the softness of setae at molecular level. Starred peak refers to the spinning sideband. The spectra were recorded at MAS frequency at ~ 6 kHz.

Shear adhesion measurements: To relate the setae softening with adhesion and complement our water uptake and NMR findings, we carried adhesion studies on isolated setal arrays in presence of different relative humidity environments. The effect of humidity on the adhesion of pristine lamellar setal arrays on glass substrate was tested in the shear configuration, results of which are shown in Figure 7.4. When setae are exposed to dry environment (10% RH), the adhesion is minimum. Being extremely dry, the hairs are unable to have proper contact with glass surface. The increase in adhesion is noticeable with the increase in adhesion with humidity. This trend directly correlates with the setae absorbing water and getting softer to increase the surface area of contact resulting in enhanced adhesion.

Similar experiments were performed with delipidized sheds (devoid of unbound lipids) (Figure 7.4) to isolate the effect of surface chemistry from the setal softening effect. The observed forces for delipidized sheds were similar or higher at all relative humidities because the removal of unbound lipids could result in a more polar surface. Future experiments will address the characterization of surface chemistry of pristine and delipidized sheds using surface-sensitive spectroscopic techniques. However, the shear adhesion force values were insensitive to the RH in contrast to pristine sheds. Currently, we don't completely understand why the shear adhesion of delipidized sheds is insensitive to humidity.

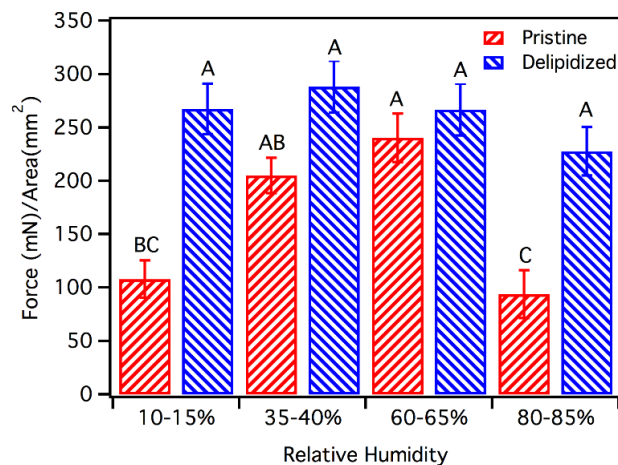


Figure 7.4 Shear force values normalized by the area of lamellae, measured for pristine and delipidized samples as a function of relative humidity. Levels connected by different letters are statistically different.

7.4 Discussion

The primary goal of this investigation is to demonstrate humidity driven softening of setae, an effect that is hypothesized to enhance gecko adhesion in presence of increasing levels of environmental humidity. Our results are first of its kind to depict both macro and molecular level softening of setae. On a macro level, there is a significant increase in the water uptake by setae as relative humidity is increased from 30% to 90% (Figure 7.2a). This complies well with the fact that keratin shows water vapor sorption^{245,246} as seen in natural systems including avian feathers²³¹, ostrich claw²⁴⁷, horse hoof^{248,249}, wool²⁵⁰, human hair, nails²⁵¹ and stratum corneum²⁵²⁻²⁵⁴ that exhibit similar trend of enhanced hydration (Figure 7.2b) with increase in relative humidity. Hydration studies based on wool, claws, hoof and horn have shown a loss in mechanical properties (decrease in properties such as stiffness, modulus) with water sorption leading to an effect on their performance.²⁴⁷⁻²⁵⁰ Our results further strengthen the setae softening hypothesis as seen in

the previous gecko studies. Studies by Puthoff et al.⁴¹ and Prowse et al.¹⁵¹ showed by means of Dynamic Mechanical Analysis (DMA), an increase in viscoelastic dampening and a ~ 1/3 decrease as compared to dry sample, in complex elastic modulus at high humidity (~80% RH) leading to the softening of setae.

The water absorption tendency of keratin is due to presence of hydrophilic amino acids. Proteins hydrate by associating water molecules to the polar sites such as free amino, carboxyl and hydroxyl moieties.²⁴⁶ Our setae based molecular studies show the plasticization (shown by decrease in intensity of CP/MAS spectrum, Figure 7.3) of different amino acid based regions (majorly carboxyl and C_α signatures) at high humidity conditions. These observations are further supported by the numerous studies^{21,67,167,203,255–259} involving the softening of proteins of various kinds at molecular scale, in presence of high humidity. The closely related system is stratum corneum, which has been studied extensively for its hydration properties.^{203,256} Other systems include different kinds of spider silks: dragline^{167,255,257,258} and capture silk.^{21,67} Dragline silk (consisting of α-helix glycine and β-sheet alanine domains) upon exposure to water undergoes supercontraction, which molecularly has been shown to plasticize glycine domains, implying a decrease in modulus of silk. Capture silk, a combination of glycoproteins and hygroscopic salts softens in presence of humidity leading to consequences on its adhesion mechanism. Thus, water penetrates the protein domains and disrupts the structure corresponding to a lower CP/MAS NMR intensity and overall softening or plasticizing of the system as seen in our setae experiments. Our findings also support the hypothesis of hydration of HgGC proteins¹³⁰ as we observed glycine (C_α) and cysteine (C_β) signatures (major constituents of setal proteins

described previously) to be affected greatly (Figure 7.3) by the exposure of setae to humidity.

In case of lipids, we compared the hygroscopicity of pristine sheds with that of delipidized (absence of non-covalent lipids) and plasma treated (absence of total lipids, non-covalent and covalent) sheds. Their total water uptake behavior (at equilibrium condition) at 90% RH was not significantly different from each other (Figure 7.2c) (rate of diffusion might be different). These results imply that the hygroscopicity of setae is controlled by the keratin component as compared to lipids. If lipids (either non-covalent or covalent or both) were contributing as a barrier to water loss, their removal should have resulted in an increase in uptake.

Correlating softening of setae to adhesion in presence of humidity is important since an increase in the flexibility of setae is expected to improve the contact area of hairs with the substrate. This increase in contact area is critical in terms of rough surfaces which are usually encountered by geckos in their natural environment. Our shear adhesion results for pristine setal arrays show a dependence of adhesive forces generated by setae with different RH environments. When setae are dry (at 10% RH), their sticking ability is significantly less as compared to when they have absorbed water, ie at higher RH, ~30% RH and ~ 60% RH. This directly correlates with our water uptake results and supports the softening-adhesion argument. Enhancement in adhesion based on softening of proteins has been seen in other biological fibrillar adhesives as well. In one example, ‘resilin’, which makes up the setal tips of beetles like *Coccinella septempunctata*, was recently seen to be affected by hydration with Young’s modulus showing a drastic change from 7.2 GPa to 1.2 MPa, leading to enhancing effect on adhesion.^{30,33} Other example is hairy foot pads of

spider *Philodromus dispar* where enhancement of adhesion at intermediate humidity was possibly due to reduction in elastic modulus of cuticular proteins.³² Even non-fibrillar adhesives such as capture silk produced by web building spiders where the ‘glycoproteins’ in presence of low molecular mass components soften with increasing RH, leading to enhanced adhesion.^{21,67} However, we see a decline in adhesion at RH above 60% (ie 80% RH- 85% RH). This contradicts the earlier observations for gecko setal array adhesion at high humidity seen in the work by Puthoff et al.⁴¹ and Pesika et al.¹⁴⁶ One possibility of lower forces at high humidity can be due to the ‘aquaplaning effect’ seen previously with insect foot pad adhesion as well as with recent synthetic fibrillar adhesive experiments where condensation of water on substrate leads to slipping of hairs in contact.^{33,243} Another factor may be due to lack of incorporation of temperature component^{16,260,261} in our adhesion experiments. Work by Niewiarowski et al. by considered the combined effect of temperature and humidity on whole animal adhesive capabilities. Results were found to be highly temperature dependent, in presence of high humidity with an increase in adhesion at a combination of lower temperature (12⁰C) and higher humidity (80% RH).¹⁶ Nevertheless, despite the drop in adhesion at high humidity, the results match our expectations with correlation of setae softening and enhanced adhesion until 60% RH.

The ever-expanding gecko synthetics community have churned out numerous inspired impressive adhesives that stick better than natural gecko adhesive and serve novel high-performance applications.²⁶²⁻²⁶⁵ However, there is still lack of a strong connect with the performance of geckos in their natural environments. Research focusses largely on shape or the architecture of adhesive pillars/hairs for enhancing contact while chemical composition of synthetics is largely neglected. The present findings stressing upon the role

of keratin softening in enhancing adhesion can provide necessary insights in developing synthetics that strike a balance between chemistry and contact mechanics to fabricate adhesives matching natural functioning of setae. In a recent report, Xue et al. took the advantage of material properties of block copolymers to create insect setae inspired porous fibrillar adhesive pads that imparted wet adhesion and hydration induced softening for enhanced adhesion in presence of humidity.³⁴ Such efforts when made in creating gecko synthetics that are either made fully or in part with humidity sensitive materials incorporated in diverse contact architectures can potentially help in adhesion on rough surfaces or even in self-cleaning where flexibility (hyperextension) is a prime concern.

7.5 Conclusion

Geckos, about >1000 species encounter water in their natural environment such as tropical rainforests where water in the form of rains or due to high humidity makes the surfaces they move on, frequently wet. In the light of understanding gecko adhesion in environmentally relevant conditions, the mechanism of setal adhesion in presence of water has been of interest to researchers lately. The current investigation primarily tests setae softening, that is hypothesized to enhance humidity driven adhesion of gecko hairs. We show softening at both macro (water uptake) and molecular (NMR) levels. Setae show an increase in hygroscopicity with uptake at 90% RH being ~3X that at 30% RH. This uptake by setae is directly reflected at a molecular level where the water penetrates keratin based amino acid domains leading to plasticization of hairs at high humidity. These softening evidences are complemented by our shear adhesion results for setal arrays on glass substrate, where we show an increase in adhesion with increase in RH and optimization at around 60% RH.

CHAPTER VIII

SUMMARY AND RECOMMENDATIONS FOR FUTURE STUDIES

The main aim of the research was to study the role of humidity in influencing the adhesive performance of two biological adhesive systems: (1) capture silk present on spider webs and (2) hairy setae on gecko feet, by the virtue of its interaction with the material composition (LMMCs and glycoproteins in capture silk; keratin and lipids in gecko setae) of these naturally adhesive systems. The first part of the dissertation (Chapter III) focused on exploring the capture silk adhesives present in the cobwebs of ‘Black Widow’ (*Latrodectus hesperus*), called as gumfoot silk for its composition, adhesion and molecular response in presence of humidity. As compared to ‘viscid silk’, which is produced by orbweb-weaving spiders and comprises of viscoelastic glycoproteins and diverse hygroscopic low molecular mass compounds, relatively less is known about ‘gumfoot silk’ produced by cobweb-weaving spiders in terms of its composition (only water-soluble peptides reported in literature) and humidity dependent adhesive mechanism. Here, for the first time, we showed gumfoot silk majorly comprised of novel hygroscopic LMMCs and glycoproteins while the previously reported peptides were present in small concentrations. Both pull-off adhesion measurements and Solid-State NMR results showed synergistic role of LMMCs and glycoproteins in adhesion across a range of humidity conditions.

Motivated by the findings from our first study (Chapter III) and host of other published reports^{22,67} from our group related to importance of low molecular mass (LMM) compounds in

capture silk adhesion, we devised the second study presented in the dissertation (Chapter IV) to understand the role of diverse LMMCs in capture silk. While there are many hypotheses that outline their functional role in capture silks, we tested their potential contribution in driving adhesion in presence of humidity. Spiders optimize adhesion of their capture silks as per their habitat or foraging humidity. We tested the hypothesis related to the contribution of the hygroscopic strength of LMMCs mixtures present in the glues of four diverse spider species, in controlling their maximum adhesion performance. We found that LMMCs mixtures, on their own couldn't explain the adhesion trends of capture silks. The results from the study strengthen the other adhesion related hypothesis of the interaction of LMMCs diverse chemistry with glycoproteins to produce the optimized adhesion response in humidity.

The third, fourth and fifth part of the dissertation (Chapter V, VI and VII respectively) were based on studies dealing with understanding the material composition and humidity response of the adhesive hairs present on gecko feet. For this, we developed a new and a unique strategy of utilizing the sheds or molts from the gecko epidermis (*Gekko gecko* used in all the studies) including that belonging to gecko feet regions. The pathway in studying humidity response and its correlation with adhesion involved: (1) Characterization of setae for the presence of β -keratin and lipids using tools including first time molecular level analysis with Solid State NMR (Chapter V); (2) Analyzing role of lipids in adhesion and anti-adhesion properties of setae (Chapter VI) and (3) Studying macro and molecular level response of keratin and lipid components in presence of humidity (Chapter VII).

β -keratin present in the setae has been characterized using a variety of techniques while the discovery of lipids in setae have been recent. However, there have been gaps in our understanding in relation to the quantity and types of lipids, molecular picture of the setal constituents along with the arrangement of β -keratin and lipids in the setae. In the

third study (Chapter V), we tackled these aspects by performing TLC and NMR (Solution and Solid) studies. Firstly, we isolated non-covalently attached lipids present in the setae by delipidizing toe sheds using chloroform-methanol treatment and identified them to be of different types (TLC and Solution State NMR). These lipids were found to be 10% of the mass of a toe shed and were similar in chemistry as those present in non-adhesive epidermis of gecko. Secondly, we performed novel molecular level characterization (Solid State NMR) of setae to identify keratin and lipids; confirm delipidization and establish differences in lipid dynamics between setae and non-adhesive epidermis. We found there was a clear difference in mobility of lipids in setae (fluid like) as compared to that in epidermis (packed). This observation paved the way to develop a model for keratin and lipid arrangement in setae where we proposed lipids to be present as a thin surface layer as well as be a part of matrix pools in a disordered manner in keratin hairs.

To understand the role of these loosely bound fluid lipids, we tested the hypothesis of their contribution to adhesive and anti-adhesive nature of the setae (Chapter VI). By testing shear adhesion of delipidized sheds and its comparison with adhesion of pristine sheds over range of substrates including hydrophilic, hydrophobic and rough surfaces (sandpaper), it was seen that these unbound lipids do not have a contribution to adhesion mechanism of setae. Moreover, they had negative impact on hydrophilic surfaces, with adhesion being stronger in absence of lipids. Anti-adhesion or superhydrophobicity remained intact on removal of lipids as seen with our static contact angle measurements.

The last study in the dissertation (Chapter VII) was based on investigating the humidity response of β -keratin and lipid components of setae for studying the effects on adhesion. Studies were done on both macro and molecular level to test the hypothesis of ‘ β -keratin softening’ in presence of humidity, that is thought to enhance gecko adhesion in presence of

water vapors in environment. Water uptake measurements of setae across range of humidity environments (30% RH to 90% RH) depicted the hygroscopic nature of setae. Comparison of hygroscopicity for pristine, delipidized and plasma treated sheds confirmed β -keratin to be major component leading to water absorption of setae. Molecular investigations using NMR on pristine sheds in high humidity confirmed the softening of β -keratin component as compared to lipids. These softening observations were reflected in shear adhesion measurements of toe sheds where we saw an increase in adhesion of setae to glass with increase in humidity.

Following are the recommendations for future studies:

1. Inorganic LMMCs form 10-20% of the water solubles of capture silk. Chemically, these types of LMMCs have been known to contain H_2PO_4^- , K^+ , NO_3^- , Na^+ , Cl^- and Ca^{2+} signatures. However, these have been detected in a limited number of species and their presence and diversity across family of spiders is unknown. Future experiments directed in collecting LMMCs from glues of various spiders and using analytical tools to characterize inorganic LMMCs in them should be made. Importantly, their role in complexing with glycoproteins in mediating humidity driven adhesion as seen in other biological adhesives such as caddisflies should be investigated.

2. Apart from hygroscopic organic and inorganic LMMCs, it is shown that capture silk contains lipid like molecules, with their function being unknown till now. Complete characterization of lipids present in glue droplets is lacking and efforts to isolate them using solvent based treatments like chloroform-methanol, pentane or dichloromethane should be made and extracts be identified with techniques such as those based on mass spectrometry. One potential role of lipids could be their aggregation on the surface of glue droplets and interaction with the hydrophobic cuticle of insects leading to aid in adhesion. Using

interface sensitive spectroscopy, Sum Frequency Generation Spectroscopy (SFG) to probe air-glue interface for pristine and delipidized capture silks should be done to answer the hypothesis.

3. The chemistry of glycoproteins present in capture silk threads is relatively unknown. One of the hurdles have been their complete isolation from flagelliform thread. Our recent attempts in this direction, by performing alkaline hydrolysis on glue threads to separate glycoproteins have been fruitful and needs further investigation for their complete characterization. Methods such as Infrared spectroscopy, NMR, Mass spectrometry, SDS-PAGE among others can be performed on the extracted proteins to understand its chemical composition. Another opportunity is to compare the glycoproteins of orb and cobweb glues in terms of their chemistry, since visually they seem to have different morphologies. Understanding glycoproteins can shed light on their potential interactions with diverse chemical functionalities of LMMCs, which may be responsible for humidity mediated adhesion.

4. The use of SFG spectroscopy in understanding the mechanism of humidity driven capture silk adhesion is a promising opportunity. Some initial investigations based on orb glues in our group have shown the presence of -NH moieties at the glue-substrate interface and sequestration of water from the interface due to the action of LMMCs, at high humidity environments. Extending this research to the cob web glues such as those of *Latrodectus hesperus* (Black Widow) should be made, since their adhesion characteristics is different from orb glues (cob web glues show consistent adhesion till high humidity range and their glycoproteins visually look different in morphology).

5. Humidity responsive synthetic adhesives can be designed based on the structures of organic LMMCs by incorporating their common structural unit (amine based functionalities) in the backbone polymer. In another way, hygroscopic polymers can be mixed with LMMCs in different proportions (mimicking natural LMMCs recipes present in glue) to create adhesives that respond to humidity.
6. The strategy of successfully delipidizing toe molts to remove non-covalently attached lipids (Chapter V) can be used to detect the presence of lipid molecules at the contact interface. By using SFG spectroscopy, the interface between either pristine or delipidized setae with substrate can be probed and compared for the presence of lipids. Additionally, humidity can be introduced to check its influence on the protein and lipid signatures at the interface, to deduce implications on the adhesion mechanism.
7. The combination of humidity and temperature has shown to affect gecko adhesion on a whole animal level. Shear adhesion experiments can be designed for the pristine and delipidized toe shed molts on various substrates to study different combinations explored in the study by Niewiarowski et al. to study the complex relationship between these two environmental factors.

REFERENCES

1. Petrie, E. *Handbook of Adhesives and Sealants*. (McGraw Hill, 2007).
2. White, C. *et al.* Mechanisms of criticality in environmental adhesion loss. *Soft Matter* **11**, 3994–4001 (2015).
3. Tan, K. T. *et al.* On the origins of sudden adhesion loss at a critical relative humidity: Examination of bulk and interfacial contributions. *Langmuir* **24**, 9189–9193 (2008).
4. Abdel Wahab, M. M. Fatigue in Adhesively Bonded Joints: A Review. *ISRN Mater. Sci.* **2012**, 1–25 (2012).
5. Brewis, D. M., Comyn, J., Raval, A. K. & Kinloch, A. J. The effect of humidity on the durability of aluminium-epoxide joints. *Int. J. Adhes. Adhes.* **10**, 247–253 (1990).
6. Flammang, P. & Santos, R. Biological adhesives: from biology to biomimetics. *Interface Focus* **5**, 1–3 (2015).
7. Smith, A.M. *Biological Adhesives*. (Springer Berlin Heidelberg, 2016).
8. Hennebert, E., Maldonado, B., Ladurner, P., Flammang, P. & Flammang, P. Experimental strategies for the identification and characterization of adhesive proteins in animals : a review. *Interface Focus* **5**, 20140064 (2015).
9. von Byern, J. & Grunwald, I. *Biological Adhesive Systems : From Nature to Medical Applications*. (Springer Wien New York, 2010).
10. Sever, M. J., Weisser, J. T., Monahan, J., Srinivasan, S. & Wilker, J. J. Metal-mediated cross-linking in the generation of a marine-mussel adhesive. *Angew. Chemie* **116**, 454–456 (2004).
11. Gohad, N. V *et al.* Synergistic roles for lipids and proteins in the permanent adhesive of barnacle larvae. *Nat. Commun.* **5**, 4414 (2014).
12. Santos, R. *et al.* First insights into the biochemistry of tube foot adhesive from the sea urchin *Paracentrotus lividus* (Echinoidea, Echinodermata). *Mar. Biotechnol.* **11**, 686–698 (2009).
13. Stewart, R. J. & Wang, C. S. Adaptation of caddisfly larval silks to aquatic habitats by phosphorylation of H-fibroin serines. *Biomacromolecules* **11**, 969–974 (2010).

14. Wang, C. S. & Stewart, R. J. Multipart copolyelectrolyte adhesive of the sandcastle worm, *Phragmatopoma californica* (Fewkes): Catechol oxidase catalyzed curing through peptidyl-DOPA. *Biomacromolecules* **14**, 1607–1617 (2013).
15. Burkett, J. R., Hight, L. M., Kenny, P. & Wilker, J. J. Oysters produce an organic-Inorganic adhesive for intertidal reef construction. *J. Am. Chem. Soc.* **132**, 12531–12533 (2010).
16. Niewiarowski, P. H., Lopez, S., Ge, L., Hagan, E. & Dhinojwala, A. Sticky gecko feet: the role of temperature and humidity. *PLoS One* **3**, e2192 (2008).
17. Sahni, V., Dhinojwala, A., Opell, B. D. & Blackledge, T. A. in *Biotechnology of Silk* (eds. Asakura, T. & Miller, T.) **5**, 203–215 (Springer Netherlands, 2014).
18. Lin, H., Lizarraga, L., Bottomley, L. A. & Carson Meredith, J. Effect of water absorption on pollen adhesion. *J. Colloid Interface Sci.* **442**, 133–9 (2015).
19. Autumn, K., Niewiarowski, P. H. & Puthoff, J. B. Gecko adhesion as a model system for integrative biology, interdisciplinary science, and bioinspired engineering. *Annu. Rev. Ecol. Evol. Syst* **45**, 445–70 (2014).
20. Jain, D. *et al.* Composition and function of spider glues maintained during the evolution of cobwebs. *Biomacromolecules* **16**, 3373–80 (2015).
21. Jain, D., Blackledge, T. A., Miyoshi, T., & Dhinojwala, A. in *Biological Adhesives* (ed. Smith, A.M.) 303–319 (Springer International Publishing, 2016).
22. Amarpuri, G. *et al.* Spiders tune glue viscosity to maximize adhesion. *ACS Nano* **9**, 11472–11478 (2015).
23. Jain, D., Stark, A. Y., Niewiarowski, P. H., Miyoshi, T. & Dhinojwala, A. NMR spectroscopy reveals the presence and association of lipids and keratin in adhesive gecko setae. *Sci. Rep.* **5**, 9594 (2015).
24. Stark, A. Y., Subarajan, S., Jain, D., Niewiarowski, P. H. & Dhinojwala, A. Superhydrophobicity of the gecko toe pad: biological optimization versus laboratory maximization. *Philos. Trans. R. Soc. A* **374**, 20160184 (2016).
25. Sahni, V., Blackledge, T. A. & Dhinojwala, A. Changes in the adhesive properties of spider aggregate glue during the evolution of cobwebs. *Sci. Rep.* **1**, 1–8 (2011).
26. Fratzl, P. & Barth, F. G. Biomaterial systems for mechanosensing and actuation. *Nature* **462**, 442–448 (2009).
27. Chen, X., Mahadevan, L., Driks, A. & Sahin, O. Bacillus spores as building blocks for stimuli-responsive materials and nanogenerators. *Nat. Nanotechnol.* **9**, 137–141 (2014).
28. Elbaum, R., Zaltzman, L., Burgert, I. & Fratzl, P. The role of wheat awns in the seed dispersal unit. *Science* **316**, 884–6 (2007).
29. Eliason, C. M. & Shawkey, M. D. Rapid, reversible response of iridescent feather color to ambient humidity. *Opt. Express* **18**, 21284–92 (2010).

30. Peisker, H., Michels, J. & Gorb, S. N. Evidence for a material gradient in the adhesive tarsal setae of the ladybird beetle *Coccinella septempunctata*. *Nat. Commun.* **4**, 1661 (2013).
31. Dawson, C., Vincent, J. F. V. & Rocca, A.-M. How pine cones open. *Nature* **390**, 668 (1997).
32. Wolff, J. O. & Gorb, S. N. The influence of humidity on the attachment ability of the spider *Philodromus dispar* (Araneae, Philodromidae). *Proc. Biol. Sci.* **279**, 139–43 (2012).
33. Heepe, L., Wolff, J. O. & Gorb, S. N. Influence of ambient humidity on the attachment ability of ladybird beetles (*Coccinella septempunctata*). *Beilstein J. Nanotechnol.* **7**, 1322–1329 (2016).
34. Xue, L., Kovalev, A., Eichler-Volf, A., Steinhart, M. & Gorb, S. N. Humidity-enhanced wet adhesion on insect-inspired fibrillar adhesive pads. *Nat. Commun.* **6**, 6621 (2015).
35. Tian, E. *et al.* Colorful humidity sensitive photonic crystal hydrogel. *J. Mater. Chem.* **18**, 1116 (2008).
36. He, M., Duan, B., Xu, D. & Zhang, L. Moisture and solvent responsive cellulose/SiO₂ nanocomposite materials. *Cellulose* **22**, 553–563 (2015).
37. Liu, K. *et al.* Bio-inspired Humidity Responsive Switch for Directional Water Droplet Delivery. *J. Mater. Chem. A* (2015).
38. Dai, M. *et al.* Humidity-responsive bilayer actuators based on a liquid-crystalline polymer network. *ACS Appl. Mater. Interfaces* **5**, 4945–50 (2013).
39. Shen, L., Fu, J., Fu, K., Picart, C. & Ji, J. Humidity responsive asymmetric free-standing multilayered film. *Langmuir* **26**, 16634–7 (2010).
40. Westphal, A. J., Price, P. B., Leighton, T. J. & Wheeler, K. E. Kinetics of size changes of individual *Bacillus thuringiensis* spores in response to changes in relative humidity. *Proc. Natl. Acad. Sci. U. S. A.* **100**, 3461–6 (2003).
41. Puthoff, J. B., Prowse, M. S., Wilkinson, M. & Autumn, K. Changes in materials properties explain the effects of humidity on gecko adhesion. *J. Exp. Biol.* **213**, 3699–704 (2010).
42. Lin, H., Gomez, I. & Meredith, J. C. Pollenkitt wetting mechanism enables species-specific tunable pollen adhesion. *Langmuir* **29**, 3012–3023 (2013).
43. Nakamura, E., Yoshioka, S. & Kinoshita, S. Structural color of rock dove's neck feather. *J. Phys. Soc. Japan* **77**, 124801 (2008).
44. Shawkey, M. D. *et al.* Structural color change following hydration and dehydration of iridescent mourning dove (*Zenaidura macroura*) feathers. *Zoology* **114**, 59–68 (2011).
45. Liu, F., Dong, B. Q., Liu, X. H., Zheng, Y. M. & Zi, J. Structural color change in

- longhorn beetles *Tmesisternus isabellae*. *Opt. Express* **17**, 16183–16191 (2009).
46. Blackledge, T. A. *et al.* How super is supercontraction? Persistent versus cyclic responses to humidity in spider dragline silk. *J. Exp. Biol.* **212**, 1981–9 (2009).
 47. Van Beek, J. D., Kümmerlen, J., Vollrath, F. & Meier, B. H. Supercontracted spider dragline silk: A solid-state NMR study of the local structure. *Int. J. Biol. Macromol.* **24**, 173–178 (1999).
 48. Suarez, J. C. in *Handbook of adhesion technology* (eds. da Silva, L. F. M., Öchsner, A. & Adams, R. D.) 1385–1408 (Springer, 2011).
 49. Rising, A. & Johansson, J. Toward spinning artificial spider silk. *Nat. Chem. Biol.* **11**, 309–15 (2015).
 50. Sahni, V., Blackledge, T. A. & Dhinojwala, A. A review on spider silk adhesion. *J. Adhes.* **87**, 595–614 (2011).
 51. Blackledge, T. A. *et al.* Reconstructing web evolution and spider diversification in the molecular era. *Proc. Natl. Acad. Sci. U. S. A.* **106**, 5229–34 (2009).
 52. Foelix, R. *Biology of Spiders*. (Oxford University Press, USA, 2011).
 53. Vollrath, F. & Selden, P. The role of behavior in the evolution of spiders, silks, and webs. *Annu. Rev. Ecol. Evol. Syst.* **38**, 819–846 (2007).
 54. Opell, B. D., Tran, A. M. & Karinshak, S. E. Adhesive compatibility of cribellar and viscous prey capture threads and its implication for the evolution of orb-weaving spiders. *J. Exp. Zool. A. Ecol. Genet. Physiol.* **315**, 376–84 (2011).
 55. Townley, M. A. & Tillinghast, E. K. in *Spider Ecophysiology* (ed. Nentwig, W.) 283–302 (Springer Berlin Heidelberg, 2013).
 56. Sinohara, H. & Tillinghast, E. K. Carbohydrates associated with the orb web protein of *Argiope aurantia*. *Biochem. Int.* **9**, 315–317 (1984).
 57. Opell, B. D. & Hendricks, M. L. The role of granules within viscous capture threads of orb-weaving spiders. *J. Exp. Biol.* **213**, 339–46 (2010).
 58. Vollrath, F. Glycoprotein glue beneath a spider web's aqueous coat. *Naturwissenschaften* **78**, 557–559 (1991).
 59. Chores, O., Bayarmagnai, B. & Lewis, R. V. Spider web glue: two proteins expressed from opposite strands of the same DNA sequence. *Biomacromolecules* **10**, 2852–6 (2009).
 60. Collin, M. A., Clarke, T. H., Ayoub, N. A. & Hayashi, C. Y. Evidence from multiple species that spider silk glue component ASG2 is a Spidroin. *Sci. Rep.* **6**, 21589 (2016).
 61. Townley, M. A., Bernstein, D. T., Gallagher, K. S. & Tillinghast, E. K. Comparative study of orb web hygroscopicity and adhesive spiral composition in three araneid spiders. *J. Exp. Zool.* **259**, 154–165 (1991).

62. Townley, M. A., Pu, Q., Zercher, C. K., Neefus, C. D. & Tillinghast, E. K. Small organic solutes in sticky droplets from orb webs of the spider *Zygiella atrica* (Araneae; Araneidae): β -alaninamide is a novel and abundant component. *Chem. Biodivers.* **9**, 2159–2174 (2012).
63. Townley, M. A., Tillinghast, E. K. & Neefus, C. D. Changes in composition of spider orb web sticky droplets with starvation and web removal, and synthesis of sticky droplet compounds. *J. Exp. Biol.* **209**, 1463–86 (2006).
64. Tillinghast, E., Huxtable, R., Watson III, W. & Townley, M. Evidence of the presence of GABamide on the web of orb weaving spiders. *Comp. Biochem. Physiol. Part B Comp. Biochem.* **88B**, 457–460 (1987).
65. Anderson, C. M. & Tillinghast, E. K. GABA and taurine derivatives on the adhesive spiral of the orb web of *Argiope* spiders, and their possible behavioural significance. *Physiol. Entomol.* **5**, 101–106 (1980).
66. Vollrath, F. *et al.* Compounds in the droplets of the orb spider's viscid spiral. *Nature* **345**, 526–528 (1990).
67. Sahni, V. *et al.* Direct solvation of glycoproteins by salts in spider silk glues enhances adhesion and helps to explain the evolution of modern spider orb webs. *Biomacromolecules* **15**, 1225–1232 (2014).
68. Vollrath, F.; Edmonds, D. Modulation of the mechanical properties of spider silk by coating with water. *Nature* **340**, 305–307 (1989).
69. Amarpuri, G., Chaurasia, V., Jain, D., Blackledge, T. A. & Dhinojwala, A. Ubiquitous distribution of salts and proteins in spider glue enhances spider silk adhesion. *Sci. Rep.* **5**, 9030 (2015).
70. Sahni, V., Blackledge, T. A. & Dhinojwala, A. Viscoelastic solids explain spider web stickiness. *Nat. Commun.* **1**, 19 (2010).
71. Opell, B. D., Karinshak, S. E. & Sigler, M. A. Humidity affects the extensibility of an orb-weaving spider's viscous thread droplets. *J. Exp. Biol.* **214**, 2988–93 (2011).
72. Opell, B. D., Karinshak, S. E. & Sigler, M. A. Environmental response and adaptation of glycoprotein glue within the droplets of viscous prey capture threads from araneoid spider orb-webs. *J. Exp. Biol.* **216**, 3023–34 (2013).
73. Opell, B. D., Buccella, K. E., Godwin, M. K., Rivas, M. X. & Hendricks, M. L. Humidity-mediated changes in an orb spider's glycoprotein adhesive impact prey retention time. *J. Exp. Biol.* **220**, 1313–1321 (2017).
74. Griswold, C. E., Coddington, J. A., Hormiga, G. & Scharff, N. Phylogeny of the orb-web building spiders (Araneae, Orbiculariae: Deinopoidea, Araneoidea). *Zool. J. Linn. Soc.* **123**, 1–99 (1998).
75. Blackledge, T. A., Coddington, J. & Gillespie, R. Are three-dimensional spider webs defensive adaptations? *Ecol. Lett.* **6**, 13–18 (2003).

76. Blackledge, T. A., Summers, A. P. & Hayashi, C. Y. Gumfooted lines in black widow cobwebs and the mechanical properties of spider capture silk. *Zoology (Jena)*. **108**, 41–6 (2005).
77. Blackledge, T. A. & Zevenbergen, J. M. Condition-dependent spider web architecture in the western black widow, *Latrodectus hesperus*. *Anim. Behav.* **73**, 855–864 (2007).
78. Chamberlin, R. V & Ivie, W. The black widow spider and its varieties in the united states. *Bulletin of the University of Utah* **25**, 3–29 (1935).
79. d'Amour, F., Becker, F. & Riper, W. Van. The black widow spider. *Q. Rev. Biol.* **11**, 123–160 (1936).
80. Garb, J. E., González, A. & Gillespie, R. G. The black widow spider genus *Latrodectus* (Araneae: Theridiidae): Phylogeny, biogeography, and invasion history. *Mol. Phylogenet. Evol.* **31**, 1127–1142 (2004).
81. Eberhard, W. G., Agnarsson, I. & Levi, H. W. Web forms and the phylogeny of theridiid spiders (Araneae: Theridiidae): Chaos from order. *Syst. Biodivers.* **6**, 415–475 (2008).
82. Benjamin, S. P. & Zschokke, S. Webs of theridiid spiders : construction , structure and evolution. *Biol. J. Linn. Soc.* **78**, 293–305 (2003).
83. Argintean, S., Chen, J., Kim, M. & Moore, A. M. F. Resilient silk captures prey in black widow cobwebs. *Appl. Phys. A* **82**, 235–241 (2006).
84. Blackledge, T. A., Swindeman, J. E. & Hayashi, C. Y. Quasistatic and continuous dynamic characterization of the mechanical properties of silk from the cobweb of the black widow spider *Latrodectus hesperus*. *J. Exp. Biol.* **208**, 1937–1949 (2005).
85. Sahni, V., Harris, J., Blackledge, T. A. & Dhinojwala, A. Cobweb-weaving spiders produce different attachment discs for locomotion and prey capture. *Nat. Commun.* **3**, 1106 (2012).
86. Frontali, N., Ceccarelli, B. & Gorio, A. Purification from black widow spider venom of a protein factor causing the depletion of synaptic vesicles at neuromuscular junctions. *J. Cell Biol.* **68**, 462–479 (1976).
87. Meldolesi, J., Scheer, H., Madeddu, L. & Wanke, E. Mechanism of action of α -latrotoxin: the presynaptic stimulatory toxin of the black widow spider venom. *Trends Pharmacol. Sci.* **7**, 151–155 (1986).
88. Ushkaryov, Y. A., Volynski, K. E. & Ashton, A. C. The multiple actions of black widow spider toxins and their selective use in neurosecretion studies. *Toxicon* **43**, 527–42 (2004).
89. Finkelstein, A., Rubin, L. L. & Tzeng, M. C. Black widow spider venom: effect of purified toxin on lipid bilayer membranes. *Science* **193**, 1009–11 (1976).
90. Casem, M., Turner, D. & Houchin, K. Protein and amino acid composition of silks

- from the cob weaver, *Latrodectus hesperus*(black widow). *Int. J. Biol. Macromol.* **24**, 103–108 (1999).
91. Moore, A. & Tran, K. Material properties of cobweb silk from the black widow spider *Latrodectus hesperus*. *Int. J. Biol. Macromol.* **24**, 277–282 (1999).
 92. Lawrence, B. A., Vierra, C. A. & Moore, A. M. F. Molecular and mechanical properties of major ampullate silk of the black widow spider, *Latrodectus hesperus*. *Biomacromolecules* **5**, 689–695 (2004).
 93. Hu, X. *et al.* Egg case protein-1. A new class of silk proteins with fibroin-like properties from the spider *Latrodectus hesperus*. *J. Biol. Chem.* **280**, 21220–30 (2005).
 94. Hu, X. *et al.* Araneoid egg case silk: A fibroin with novel ensemble repeat units from the black widow spider, *Latrodectus hesperus*. *Biochemistry* **44**, 10020–10027 (2005).
 95. Hu, X., Yuan, J., Wang, X. & Vasanthavada, K. Analysis of aqueous glue coating proteins on the silk fibers of the cob weaver, *Latrodectus hesperus*. *Biochemistry* **46**, 3294–3303 (2007).
 96. Vasanthavada, K. *et al.* Aciniform spidroin, a constituent of egg case sacs and wrapping silk fibers from the black widow spider *Latrodectus hesperus*. *J. Biol. Chem.* **282**, 35088–97 (2007).
 97. Vasanthavada, K. *et al.* Spider glue proteins have distinct architectures compared with traditional spidroin family members. *J. Biol. Chem.* **287**, 35986–35999 (2012).
 98. Blasingame, E. *et al.* Pyriform spidroin 1, a novel member of the silk gene family that anchors dragline silk fibers in attachment discs of the black widow spider, *Latrodectus hesperus*. *J. Biol. Chem.* **284**, 29097–108 (2009).
 99. Jenkins, J. E. *et al.* Characterizing the secondary protein structure of black widow dragline silk using solid-state NMR and X-ray diffraction. *Biomacromolecules* **14**, 3472–83 (2013).
 100. Xu, D., Yarger, J. L. & Holland, G. P. Exploring the backbone dynamics of native spider silk proteins in black widow silk glands with solution-state NMR spectroscopy. *Polymer (Guildf)*. **55**, 3879–3885 (2014).
 101. Swanson, B. O., Blackledge, T. A., Beltrán, J. & Hayashi, C. Y. Variation in the material properties of spider dragline silk across species. *Appl. Phys. A* **82**, 213–218 (2006).
 102. Peters, H. in *Ecophysiology of Spiders* (ed. Nentwig, W.) (Springer Berlin Heidelberg, 1987).
 103. Kelly, S.L. The chemical composition of the defensive secretion of the spider *Latrodectus mactans* (Fabricius). MS Thesis, University of New Hampshire (1989).
 104. Kovoov, J. Données histochimiques sur les glandes séricigènes de la veuve noire

- Latrodectus mactans* Fabr. (Araneae: Theridiidae). *Ann. des Sci. Nat.* **19**, 63–87 (1977).
105. Kovoov, J. in *Ecophysiology of Spiders* (ed. Nentwig, W.) (Springer Berlin Heidelberg 1987).
 106. Schulz, S. Composition of the silk lipids of the spider *Nephila clavipes*. *Lipids* **36**, 637–47 (2001).
 107. Salles, H. C. *et al.* The venomous secrets of the web droplets from the viscid spiral of the orb-weaver spider *Nephila clavipes* (araneau, tetragnatidae). *Chem. Biodivers.* **3**, 727–741 (2006).
 108. Schulz, S. The chemistry of spider toxins and spider silk. *Angew. Chemie-International Ed. English* **36**, 314–326 (1997).
 109. Schulz, S. in *Bioorganic chemistry: highlights and new aspects* (eds. Diederichsen, U, Lindhorst, T., Westermann, B & Wessjohann, L.) (Wiley-VCH, Weinheim, 1999).
 110. Autumn, K. in *Biological Adhesives* (eds. Smith, A. M. & Callow, J. A.) 225–256 (Springer Berlin Heidelberg, 2006).
 111. Gamble, T., Greenbaum, E., Jackman, T. R., Russell, A. P. & Bauer, A. M. Repeated origin and loss of adhesive toepads in Geckos. *PLoS One* **7**, (2012).
 112. Autumn, K. & Peattie, A. M. Mechanisms of adhesion in geckos. *Integr. Comp. Biol.* **42**, 1081–90 (2002).
 113. Niewiarowski, P. H., Stark, A. Y. & Dhinojwala, A. Sticking to the story: outstanding challenges in gecko-inspired adhesives. *J. Exp. Biol.* **219**, 912–919 (2016).
 114. Autumn, K. *et al.* Adhesive force of a single gecko foot-hair. *Nature* **405**, 681–5 (2000).
 115. Autumn, K. *et al.* Evidence for van der Waals adhesion in gecko setae. *Proc. Natl. Acad. Sci. U. S. A.* **99**, 12252–6 (2002).
 116. Badge, I., Stark, A. Y., Paoloni, E. L., Niewiarowski, P. H. & Dhinojwala, A. The role of surface chemistry in adhesion and wetting of gecko toe pads. *Sci. Rep.* **4**, 6643 (2014).
 117. Autumn, K. & Hansen, W. Ultrahydrophobicity indicates a non-adhesive default state in gecko setae. *J. Comp. Physiol. A Neuroethol. Sensory, Neural, Behav. Physiol.* **192**, 1205–1212 (2006).
 118. Hsu, P. Y. *et al.* Direct evidence of phospholipids in gecko footprints and spatula-substrate contact interface detected using surface-sensitive spectroscopy. *J. R. Soc. Interface* **9**, 657–664 (2011).
 119. Alibardi, L. *et al.* Histochemical and ultrastructural analyses of adhesive setae of lizards indicate that they contain lipids in addition to keratins. *J. Morphol.* **272**, 758–

68 (2011).

120. Alibardi, L. Cell biology of adhesive setae in gecko lizards. *Zoology (Jena)*. **112**, 403–24 (2009).
121. Stark, A. Y., Sullivan, T. W. & Niewiarowski, P. H. The effect of surface water and wetting on gecko adhesion. *J. Exp. Biol.* **215**, 3080–6 (2012).
122. Stark, A. Y., McClung, B., Niewiarowski, P. H. & Dhinojwala, A. Reduction of water surface tension significantly impacts gecko adhesion underwater. *Integr. Comp. Biol.* **54**, 1026–1033 (2014).
123. Stark, A. Y., Wucinich, N. A., Paoloni, E. L., Niewiarowski, P. H. & Dhinojwala, A. Self-drying: A gecko's innate ability to remove water from wet toe pads. *PLoS One* **9**, (2014).
124. Hansen, W. R. & Autumn, K. Evidence for self-cleaning in gecko setae. *Proc. Natl. Acad. Sci. U. S. A.* **102**, 385–9 (2005).
125. Hu, S., Lopez, S., Niewiarowski, P. H. & Xia, Z. Dynamic self-cleaning in gecko setae via digital hyperextension. *J. R. Soc. Interface* **9**, 2781–90 (2012).
126. Wang, B., Yang, W., McKittrick, J. & Meyers, M. A. Keratin: Structure, mechanical properties, occurrence in biological organisms, and efforts at bioinspiration. *Prog. Mater. Sci.* **76**, 229–318 (2016).
127. McKittrick, J. *et al.* The structure, functions, and mechanical properties of keratin. *JOM* **64**, 449–468 (2012).
128. Toni, M., Valle, L. D. & Alibardi, L. Hard (Beta-)keratins in the epidermis of reptiles: composition, sequence, and molecular organization. *J. Proteome Res.* **6**, 3377–92 (2007).
129. Alibardi, L. Immunolocalization of specific beta-proteins in pad lamellae of the digits in the lizard *Anolis carolinensis* suggests that cysteine-rich beta-proteins provides flexibility. *J. Morphol.* **275**, 504–513 (2014).
130. Alibardi, L. Immunolocalization of keratin-associated beta-proteins in developing epidermis of lizard suggests that adhesive setae contain glycine--cysteine-rich proteins. *J. Morphol.* **274**, 97–107 (2013).
131. Huber, G., Orso, S., Spolenak, R., Wegst, U. G., Enders, S., Gorb, S. N., & Arzt, E. Mechanical properties of a single gecko seta. *Int. J. Mater. Res.* **99**, 1113–1118 (2008).
132. Rizzo, N. W. *et al.* Characterization of the structure and composition of gecko adhesive setae. *J. R. Soc. Interface* **3**, 441–51 (2006).
133. Fahy, E. *et al.* A comprehensive classification system for lipids. *J. Lipid Res.* **46**, 839–861 (2005).
134. Metzler, D. E. *Biochemistry: The chemical reactions of living cells.* (Academic Press, 2003).

135. Hadley, N. Lipid water barriers in biological systems. *Prog. Lipid Res.* **28**, 1–33 (1989).
136. Alibardi, L. & Toni, M. Cytochemical and molecular characteristics of the process of cornification during feather morphogenesis. *Prog. Histochem. Cytochem.* **43**, 1–69 (2008).
137. Menon, G., Brown, B. & Elias, P. Avian epidermal differentiation: role of lipids in permeability barrier formation. *Tissue Cell* **18**, 71–82 (1986).
138. Sponner, A. *et al.* Composition and hierarchical organisation of a spider silk. *PLoS One* **2**, e998 (2007).
139. Dobson, H. E. M. Survey of pollen and pollenkitt lipids - chemical cues to flower visitors? *Am. J. Bot.* **75**, 170–182 (1988).
140. Vötsch, W. *et al.* Chemical composition of the attachment pad secretion of the locust *Locusta migratoria*. *Insect Biochem. Mol. Biol.* **32**, 1605–13 (2002).
141. Hsu, P. Y. Vibrational sum frequency generation studies of aqueous and biological relevant interfaces. PhD Thesis, University of Akron (2011).
142. Stark, A. Y. *et al.* Surface wettability plays a significant role in gecko adhesion underwater. *Proc. Natl. Acad. Sci. U. S. A.* **110**, 6340–5 (2013).
143. Stark, A. Y. *et al.* Gecko adhesion on wet and dry patterned substrates. *PLoS One* **10**, 1–12 (2015).
144. Stark, A. Y. *et al.* Adhesive interactions of geckos with wet and dry fluoropolymer substrates. *J. R. Soc. Interface* **12**, 20150464- (2015).
145. Huber, G. *et al.* Evidence for capillarity contributions to gecko adhesion from single spatula nanomechanical measurements. *PNAS* **102**, 16293–16296 (2005).
146. Pesika, N. S. *et al.* Gecko adhesion pad: a smart surface? *J. Phys. Condens. Matter* **21**, 464132 (2009).
147. Tao, D. *et al.* Adhesion and friction of an isolated gecko setal array: The effects of substrates and relative Humidity. *Biosurface and Biotribology* **1**, 1–8 (2015).
148. Chen, B. & Gao, H. An alternative explanation of the effect of humidity in gecko adhesion: stiffness reduction enhances adhesion on a rough surface. *Int. J. Appl. Mech.* **2**, 1–9 (2010).
149. Sun, W., Neuzil, P., Kustandi, T. S., Oh, S. & Samper, V. D. The nature of the gecko lizard adhesive force. *Biophys. J.* **89**, L14-7 (2005).
150. Kim, T. W. & Bhushan, B. The adhesion model considering capillarity for gecko attachment system. *J. R. Soc. Interface* **5**, 319–327 (2008).
151. Prowse, M. S., Wilkinson, M., Puthoff, J. B., Mayer, G. & Autumn, K. Effects of humidity on the mechanical properties of gecko setae. *Acta Biomater.* **7**, 733–8 (2011).

152. Yu, M., Hwang, J. & Deming, T. J. Role of 1-3,4-Dihydroxyphenylalanine in mussel adhesive proteins. *J. Am. Chem. Soc.* **121**, 5825–5826 (1999).
153. Sever, M. J., Weisser, J. T., Monahan, J., Srinivasan, S. & Wilker, J. J. Metal-mediated cross-linking in the generation of a marine-mussel adhesive. *Angew. Chem. Int. Ed. Engl.* **43**, 448–50 (2004).
154. Addison, J. & Ashton, N. β -Sheet nanocrystalline domains formed from phosphorylated serine-rich motifs in caddisfly larval silk: a solid state NMR and XRD study. *Biomacromolecules* **14**, 1140–1148 (2013).
155. Alberts, E. M. *et al.* Structural and compositional characterization of the adhesive produced by reef building oysters. *ACS Appl. Mater. Interfaces* **7**, 8533–8 (2015).
156. Neuendorf, R. E., Saiz, E., Tomsia, A. & Ritchie, R. O. Adhesion between biodegradable polymers and hydroxyapatite: Relevance to synthetic bone-like materials and tissue engineering scaffolds. *Acta Biomater.* **4**, 1288–1296 (2008).
157. Korta, J., Mlyniec, A. & Uhl, T. Experimental and numerical study on the effect of humidity-temperature cycling on structural multi-material adhesive joints. *Compos. Part B Eng.* **79**, 621–630 (2015).
158. Schindler, M., Koller, M. & Müller-Buschbaum, P. Pressure-sensitive adhesives under the influence of relative humidity: Inner structure and failure mechanisms. *ACS Appl. Mater. Interfaces* **7**, 12319–12327 (2015).
159. Comyn, J. in *Adhesives in Marine Engineering* (ed. Weitzenbock, J.R.) 187 (Woodhead Publishing Limited, Cambridge, UK, 2012).
160. Opell, B. D. & Hendricks, M. L. Adhesive recruitment by the viscous capture threads of araneoid orb-weaving spiders. *J. Exp. Biol.* **210**, 553–60 (2007).
161. Tillinghast, E. K. Selective removal of glycoproteins from the adhesive spiral of the spiders orb web. *Naturwissenschaften* **68**, 3–4 (1981).
162. Tillinghast, E. K., Townley, M. A., Wight, T. N., Uhlenbruck, G. & Janssen, E. in *MRS Online Proc. Libr.* **292**, 9–23 (1992).
163. Tillinghast, E. K. & Christenson, T. Observations on the chemical composition of the web of *Nephila clavipes* (Araneae, Araneidae). *J. Arachnol.* **12**, 69–74 (1984).
164. Wilson, N., Karlsson, N. & Packer, N. in *Separation Methods in Proteomics* (eds. Smejkal, G.B., Lazarev, A.) 350 (CRC Press: Boca Raton, FL, 2005).
165. Augsten, K., Mühlig, P. & Herrmann, C. Glycoproteins and skin-core structure in *Nephila clavipes* spider silk observed by light and electron microscopy. *Scanning* **22**, 12–15 (2000).
166. Wishart, D. S., Bigam, C. G., Holm, A., Hodges, R. S. & Sykes, B. D. ^1H , ^{13}C and ^{15}N random coil NMR chemical shifts of the common amino acids. I. Investigations of nearest-neighbor effects. *J. Biomol. NMR* **5**, 67–81 (1995).
167. Creager, M. S. *et al.* Solid-state NMR comparison of various spiders' dragline silk

- fiber. *Biomacromolecules* **11**, 2039–43 (2010).
168. Cognard, J. Influence of water on the cleavage of adhesive joints. *Int. J. Adhes. Adhes.* **8**, 93–99 (1988).
 169. Kinloch, A. J., Little, M. S. G. & Watts, J. F. The role of the interface in the environmental failure of adhesive joints. *Acta Mater.* **48**, 4543–4553 (2000).
 170. Waite, J. H. Nature's underwater adhesive specialist. *Int. J. Adhes. Adhes.* **7**, 9–14 (1987).
 171. Stellwagen, S. D., Opell, B. D. & Short, K. G. Temperature mediates the effect of humidity on the viscoelasticity of glycoprotein glue within the droplets of an orb-weaving spider's prey capture threads. *J. Exp. Biol.* **217**, 1563–9 (2014).
 172. Tillinghast, E. K. The chemical fractionation of the orb web of *Argiope* spiders. *Insect Biochem.* **14**, 115- (1984).
 173. Opell, B. D. & Schwend, H. S. The effect of insect surface features on the adhesion of viscous capture threads spun by orb-weaving spiders. *J. Exp. Biol.* **210**, 2352–60 (2007).
 174. Liao, C., Blamires, S. J., Hendricks, M. L. & Opell, B. D. A re-evaluation of the formula to estimate the volume of orb web glue droplets. *J. Arachnol.* **43**, 97–100 (2015).
 175. Gent, A. N. Adhesion and strength of viscoelastic solids. Is there a relationship between adhesion and bulk properties? *Langmuir* **12**, 4492–4496 (1996).
 176. Yancey, P. H. Organic osmolytes as compatible, metabolic and counteracting cytoprotectants in high osmolarity and other stresses. *J. Exp. Biol.* **208**, 2819–30 (2005).
 177. Arakawa, T. & Timasheff, S. N. Preferential interactions of proteins with salts in concentrated solutions. *Biochemistry* **21**, 6545–6552 (1982).
 178. Horkay, F., Tasaki, I. & Basser, P. Osmotic swelling of polyacrylate hydrogels in physiological salt solutions. *Biomacromolecules* **1**, 84–90 (2000).
 179. Du, J. & Zhang, X. Role of polymer–salt–solvent interactions in the electrospinning of polyacrylonitrile/iron acetylacetonate. *J. Appl. Polym. Sci.* **109**, 2935–2941 (2008).
 180. Zhang, Z. *et al.* Effect of salt on phosphorylcholine-based zwitterionic polymer brushes. *Langmuir* **32**, 5048–57 (2016).
 181. Phadke, M. A., Musale, D. A., Kulkarni, S. S. & Karode, S. K. Poly(acrylonitrile) ultrafiltration membranes. I. Polymer-salt-solvent interactions. *J. Polym. Sci. Part B Polym. Phys.* **43**, 2061–2073 (2005).
 182. Tan, K. *et al.* Role of salt on adhesion of an epoxy/aluminum (oxide) interface in aqueous environments. *Polym. Eng. Sci.* **56**, 18–26 (2015).

183. Roberts, J. B. & Lillywhite, H. B. Lipid barrier to water exchange in reptile epidermis. *Science* **207**, 1077–1079 (1980).
184. Menon, G. K., Cleary, G. W. & Lane, M. E. The structure and function of the stratum corneum. *Int. J. Pharm.* **435**, 3–9 (2012).
185. Sweeney, T. & Downing, D. The role of lipids in the epidermal barrier to water diffusion. *J. Invest. Dermatol.* **55**, 135–140 (1970).
186. Bullock, J. M. R., Drechsler, P. & Federle, W. Comparison of smooth and hairy attachment pads in insects: friction, adhesion and mechanisms for direction-dependence. *J. Exp. Biol.* **211**, 3333–43 (2008).
187. Gorb, S. N. The design of the fly adhesive pad: distal tenent setae are adapted to the delivery of an adhesive secretion. *Proc. R. Soc. B Biol. Sci.* **265**, 747–752 (1998).
188. Flammang, P., Michel, A., Cauwenberge, A., Alexandre, H. & Jangoux, M. A study of the temporary adhesion of the podia in the sea star *asterias rubens* (Echinodermata, asteroidea) through their footprints. *J. Exp. Biol.* **201**, 383–95 (1998).
189. Heim, M., Elsner, M. B. & Scheibel, T. Lipid-specific β -sheet formation in a mussel byssus protein domain. *Biomacromolecules* **14**, 3238–45 (2013).
190. Ruibal, R. & Ernst, V. The structure of the digital setae of lizards. *J. Morphol.* **117**, 271–293 (1965).
191. Russell, A. P. A contribution to the functional analysis of the foot of the Tokay, *Gekko gecko* (Reptilia: Gekkonidae). *J. Zool. London* **176**, 437–476 (1975).
192. Alibardi, L. Immunolocalization of specific keratin associated beta-proteins (beta-keratins) in the adhesive setae of *Gekko gecko*. *Tissue Cell* **45**, 231–40 (2013).
193. Alibardi, L. Immunolocalization of keratin-associated beta-proteins (beta-keratins) in pad lamellae of geckos suggest that glycine-cysteine-rich proteins contribute to their flexibility and adhesiveness. *J. Exp. Zool. A. Ecol. Genet. Physiol.* **319**, 166–78 (2013).
194. Toni, M., Valle, L. D. & Alibardi, L. The epidermis of scales in gecko lizards contains multiple forms of β -keratins including basic glycine-proline-serine rich proteins *J. Proteome Res.* **6**, 1792–1805 (2007).
195. Idris, A. *et al.* Dissolution of feather keratin in ionic liquids. *Green Chem.* **15**, 525–534 (2013).
196. Liu, K., Du, J., Wu, J. & Jiang, L. Superhydrophobic gecko feet with high adhesive forces towards water and their bio-inspired materials. *Nanoscale* **4**, 768–772 (2012).
197. Duer, M. J., McDougal, N. & Murray, R. C. A solid-state NMR study of the structure and molecular mobility of α -keratin. *Phys. Chem. Chem. Phys.* **5**, 2894 (2003).
198. Nishikawa, N., Horiguchi, Y., Asakura, T. & Ando, I. Carbon13 solid state n.m.r of ^{13}C -enriched human hair keratin. *Polymer (Guildf)*. **40**, 2139–2144 (1999).

199. Yoshimizu, H., Mimura, H. & Ando, I. ^{13}C CP/MAS NMR study of the conformation of stretched or heated low-sulfur keratin protein films. *Macromolecules* **24**, 862–866 (1991).
200. Yoshimizu, H., Mimura, H. & Ando, I. A high-resolution solid-state ^{13}C NMR study on conformation and molecular motion of low-sulfur keratin protein films obtained from wool. *J. Mol. Struct.* **246**, 367–379 (1991).
201. Yoshimizu, H. & Ando, I. Conformational characterization of wool keratin and S-(carboxymethyl) kerateine in the solid state by ^{13}C CP/MAS NMR spectroscopy. *Macromolecules* **23**, 2908–2912 (1990).
202. Lazo, N. D., Meine, J. G. & Downing, D. T. Lipids are covalently attached to rigid corneocyte protein envelopes existing predominantly as β -sheets: A Solid-State Nuclear Magnetic Resonance Study. *J. Invest. Dermatol.* **105**, 296–300 (1995).
203. Björklund, S., Nowacka, A., Bouwstra, J.A., Sparr, E. & Topgaard, D. Characterization of stratum corneum molecular dynamics by natural-abundance ^{13}C solid-state NMR. *PLoS One* **8**, e61889 (2013).
204. Jokura, Y., Ishikawa, S., Tokuda, H. & Imokawa, G. Molecular analysis of elastic properties of the stratum corneum by solid-state ^{13}C -nuclear magnetic resonance spectroscopy. *J. Invest. Dermatol.* **104**, 806–812 (1995).
205. Saitô, H., Ando, I. & Naito, A. *Solid state NMR spectroscopy for biopolymers: principles and applications* (Springer, 2006).
206. Swartzendruber, D. C., Wertz, P. W., Madison, K. C. & Downing, D. T. Evidence that the corneocyte has a chemically bound lipid envelope. *J. Invest. Dermatol.* **88**, 709–713 (1987).
207. Schiller, J. & Arnold, K. Application of high resolution ^{31}P NMR spectroscopy to the characterization of the phospholipid composition of tissues and body fluids - a methodological review. *Med. Sci. Monit.* **8**, MT205-22 (2002).
208. Skipski, V. P., Peterson, R. F. & Barclay, M. Quantitative analysis of phospholipids by thin-layer chromatography. *Biochem. J.* **90**, 374–8 (1964).
209. White, T., Bursten, S., Federighi, D., Lewis, R. a & Nudelman, E. High-resolution separation and quantification of neutral lipid and phospholipid species in mammalian cells and sera by multi-one-dimensional thin-layer chromatography. *Anal. Biochem.* **258**, 109–17 (1998).
210. Weldon, P. J. & Bagnall, D. A survey of polar and nonpolar skin lipids from lizards by thin-layer chromatography. *Comp. Biochem. Physiol. Part B Comp. Biochem.* **87**, 345–349 (1987).
211. Spanner, S. in *Form and function of phospholipids* (eds. Ansell, G., Hawthorne, J. & Dawson, R.M.C.) 43–65 (Elsevier Scientific Publishing Co.,1973).
212. Hatzakis, E., Koidis, A., Boskou, D. & Dais, P. Determination of phospholipids in olive oil by ^{31}P NMR spectroscopy. *J. Agric. Food Chem.* **56**, 6232–40 (2008).

213. Hallahan, D. L. *et al.* Analysis of gene expression in gecko digital adhesive pads indicates significant production of cysteine- and glycine-rich beta-keratins. *J. Exp. Zool. B. Mol. Dev. Evol.* **312**, 58–73 (2009).
214. Deniz, K. U. *et al.* Nuclear magnetic resonance and thermal studies of drug doped dipalmitoyl phosphatidyl choline-H₂O systems. *J. Biosci.* **15**, 117–123 (1990).
215. Wishart, D. S. & Nip, A.M. Protein chemical shift analysis: a practical guide. *Biochem. Cell Biol.* **76**, 153–63 (1998).
216. Ripamonti, A., Alibardi, L., Falini, G., Fermani, S. & Gazzano, M. Keratin-lipid structural organization in the corneous layer of snake. *Biopolymers* **91**, 1172–81 (2009).
217. Alibardi, L. Adaptation to the Land: The skin of reptiles in comparison to that of amphibians and endotherm amniotes. *J. Exp. Zool. (Mol. Dev. Evol.)* **298**, 12–41 (2003).
218. van Smeden, J., Janssens, M., Gooris, G. S. & Bouwstra, J. A. The important role of stratum corneum lipids for the cutaneous barrier function. *Biochim. Biophys. Acta* **1841**, 295–313 (2014).
219. Bouwstra, J. A., Honeywell-nguyen, P. L. & Gooris, G. S. Structure of the skin barrier and its modulation by vesicular formulations. *Prog. Lipid Res.* **42**, 1-36 (2003).
220. Spiess, H.W. Length Scales in Heterogeneous Polymers From. *Macromol. Symp.* **117**, 257–265 (1997).
221. Norlén, L. Stratum corneum keratin structure, function and formation—a comprehensive review. *Int. J. Cosmet. Sci.* **28**, 397–425 (2006).
222. Bushan, B. *Biomimetics: Bioinspired Hierarchical-Structured Surfaces for Green Science and Technology* (Springer Science & Business Media, Berlin, Germany, 2012).
223. Kinoshita, S. & Yoshioka, S. Structural colors in nature: The role of regularity and irregularity in the structure. *ChemPhysChem* **6**, 1442–1459 (2005).
224. Cheng, Y. T., Rodak, D. E., Wong, C. A. & Hayden, C. A. Effects of micro- and nano-structures on the self-cleaning behaviour of lotus leaves. *Nanotechnology* **17**, 1359–1362 (2006).
225. Meyers, M. A., Chen, P.-Y., Lin, A. Y.-M. & Seki, Y. Biological materials: Structure and mechanical properties. *Prog. Mater. Sci.* **53**, 1–206 (2007).
226. Ray, R. P., Nakata, T., Henningson, P. & Bomphrey, R. J. Enhanced flight performance by genetic manipulation of wing shape in *Drosophila*. *Nat. Commun.* **7**, 10851 (2016).
227. Autumn, K. How Gecko Toes Stick The powerful, fantastic adhesive used by geckos is made of nanoscale hairs that engage tiny forces, inspiring envy among human

- imitators. *Am. Sci.* **94**, 124–132 (2006).
228. Jacob, F. Evolution and tinkering. *Science* **196**, 1161–1166 (1977).
229. Tian, Y. *et al.* Adhesion and friction in gecko toe attachment and detachment. *Proc. Natl. Acad. Sci. U. S. A.* **103**, 19320–19325 (2006).
230. Zhao, B. *et al.* Role of tilted adhesion fibrils (setae) in the adhesion and locomotion of gecko-like systems. *J. Phys. Chem. B* **113**, 3615–3621 (2009).
231. Taylor, A., Bonser, R. & Farrent, J. The influence of hydration on the tensile and compressive properties of avian keratinous tissues. *J. Mater. Sci.* **9**, 939–942 (2004).
232. Peattie, A. M., Majidi, C., Corder, A. & Full, R. J. Ancestrally high elastic modulus of gecko setal beta-keratin. *J. R. Soc. Interface* **4**, 1071–6 (2007).
233. Persson, B. N. J. On the mechanism of adhesion in biological systems. *J. Chem. Phys.* **118**, 7614–7621 (2003).
234. Huber, G., Gorb, S. N., Hosoda, N., Spolenak, R. & Arzt, E. Influence of surface roughness on gecko adhesion. *Acta Biomater.* **3**, 607–610 (2007).
235. Abrams, K. *et al.* Effect of organic solvents on in vitro human skin water barrier function. *J. Invest. Dermatol.* **101**, 609–613 (1993).
236. Rissmann, R., Oudshoorn, M. H. M., Hennink, W. E., Ponc, M. & Bouwstra, J. A. Skin barrier disruption by acetone: Observations in a hairless mouse skin model. *Arch. Dermatol. Res.* **301**, 609–613 (2009).
237. Russell, A. P. Integrative functional morphology of the gekkotan adhesive system (Reptilia: Gekkota). *Integr. Comp. Biol.* **42**, 1154–1163 (2002).
238. Huey, R. B. Parapatry and niche complementarity of Peruvian Desert geckos (*Phyllodactylus*): the ambiguous role of competition. *Oecologia* **38**, 249–259 (1979).
239. Kubisch, E. *et al.* Do higher temperatures increase growth in the nocturnal gecko *homonota darwini* (Gekkota: Phyllodactylidae)? A skeletochronological assessment analyzed at temporal and geographic scales. *J. Herpetol.* **46**, 587–595 (2012).
240. Case, T. J. *et al.* Invasions and competitive displacement among house geckos in the tropical pacific. *Ecology* **75**, 464–477 (1994).
241. Niewiarowski, P. H., Stark, A., McClung, B., Chambers, B. & Timothy, S. Faster but not stickier : Invasive house geckos can out-sprint resident mournful geckos in Moorea , French Polynesia. *J. Herpetol.* **46**, 194–197 (2012).
242. Pianka, E. R., & Pianka, H. D. Comparative ecology of twelve species of nocturnal lizards (Gekkonidae) in the Western Australian desert. *Copeia*, 125-142 (1976).
243. Stark, A. Y., Klittich, M. R., Sitti, M., Niewiarowski, P. H. & Dhinojwala, A. The effect of temperature and humidity on adhesion of a gecko-inspired adhesive: implications for the natural system. *Sci. Rep.* **6**, 30936 (2016).

244. Nanjundiah, K., Hsu, P. Y. & Dhinojwala, A. Understanding rubber friction in the presence of water using sum-frequency generation spectroscopy. *J. Chem. Phys.* **130**, (2009).
245. Watt, I. C. Sorption of water vapor by keratin. *J. Macromol. Sci. Part C Polym. Rev.* **18**, 169–245 (1980).
246. Leeder, J. D. & Watt, I. C. The role of amino groups in water absorption by keratin. *J. Phys. Chem.* **69**, 3280–4 (1965).
247. Bonser, R. Hydration sensitivity of ostrich claw keratin. *J. Mater. Sci. Lett.* **21**, 1563–1564 (2002).
248. Kitchener, A. & Vincent, J. F. V. Composite theory and the effect of water on the stiffness of horn keratin. *J. Mater. Sci.* **22**, 1385–1389 (1987).
249. Bertram, J. E. & Gosline, J. M. Functional design of horse hoof keratin: the modulation of mechanical properties through hydration effects. *J. Exp. Biol.* **130**, 121–36 (1987).
250. Speakman, J. B. The rigidity of wool and its change with adsorption of water vapour. *Trans. Faraday Soc.* **25**, 92 (1929).
251. Barba, C. *et al.* Water absorption/desorption of human hair and nails. *Thermochim. Acta* **503–504**, 33–39 (2010).
252. Blank, I. H., Moloney, J., Emslie, A. G., Simon, I. & Apt, C. The diffusion of water across the stratum corneum as a function of its water content. *J. Invest. Dermatol* **82**, 188–94 (1984).
253. Barba, C., Martí, M., Carilla, J., Manich, A. . & Coderch, L. The effect of internal lipids on the water sorption kinetics of keratinized tissues. *J. Therm. Anal. Calorim.* 2013–2020 (2015).
254. Kasting & Barai. Equilibrium water sorption in human stratum corneum. *J. Pharm. Sci.* **92**, 1624–1631 (2003).
255. Holland, G. P., Jenkins, J. E., Creager, M. S., Lewis, R. V & Yarger, J. L. Solid-state NMR investigation of major and minor ampullate spider silk in the native and hydrated states. *Biomacromolecules* **9**, 651–7 (2008).
256. Wiedmann, T. Application of solid-state nuclear magnetic resonance (NMR) to the study of skin hydration. *Pharm. Res.* **5**, 611–4 (1988).
257. Holland, G. P., Lewis, R. V & Yarger, J. L. WISE NMR characterization of nanoscale heterogeneity and mobility in supercontracted *Nephila clavipes* spider dragline silk. *J. Am. Chem. Soc.* **126**, 5867–72 (2004).
258. Wang, S., Kang, J., Jain, D. & Miyoshi, T. Application of NMR in polymer characterization. *Nucl. Magn. Reson.* **45**, 53-95 (2016).
259. Round, A. *et al.* The influence of water on the nanomechanical behavior of the plant biopolyester cutin as studied by AFM and solid-state NMR. *Biophys. J.* **79**, 2761–

2767 (2000).

260. Bergmann, P. J. & Irschick, D. J. Effects of temperature on maximum clinging ability in a diurnal gecko: Evidence for a passive clinging mechanism? *J. Exp. Zool. Part A Comp. Exp. Biol.* **303**, 785–791 (2005).
261. Losos, J. B. Thermal sensitivity of sprinting and clinging in tokays. *Asian Herpetol. Res.* **3**, 54–59 (1990).
262. Ge, L., Sethi, S., Ci, L., Ajayan, P. M. & Dhinojwala, A. Carbon nanotube-based synthetic gecko tapes. *Proc. Natl. Acad. Sci. U. S. A.* **104**, 10792–5 (2007).
263. Wasay, A. & Sameoto, D. Gecko gaskets for self-sealing and high-strength reversible bonding of microfluidics. *Lab Chip* **15**, 2749–2753 (2015).
264. Mahdavi, A. *et al.* A biodegradable and biocompatible gecko-inspired tissue adhesive. *Proc. Natl. Acad. Sci. U. S. A.* **105**, 2307–2312 (2008).
265. Kwak, M. K. *et al.* Towards the next level of bioinspired dry adhesives: New designs and applications. *Adv. Funct. Mater.* **21**, 3606–3616 (2011).

APPENDICES

APPENDIX A

STATISTICAL ANALYSIS

p-values	AT	LC	BW	TL
AT	--	.266	0.000	0.000
LC		--	0.174	0.000
BW			--	0.000
TL				

Table A.1 p-values for t-test of water uptake of suspended glue droplet at 90% RH. Notice that p-value < 0.05 suggests statistically significant difference between the means.

% RH	<i>Argiope vs Tetragnatha</i>
30%	0.065
60%	0.164
90%	0.282

Table A.2 p-values from t-test of mean comparison of water uptake of synthetic LMMCs mixtures for two species, *Argiope* and *Tetragnatha* at 30%, 60% and 90% RH.

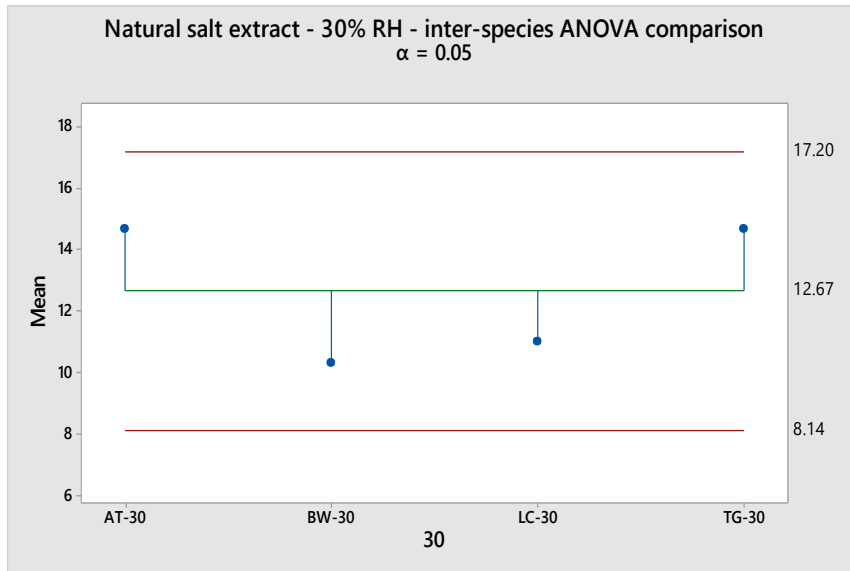


Figure A.1 ANOVA test for water uptake values for natural LMMCs (salt) extracts at 30% RH.

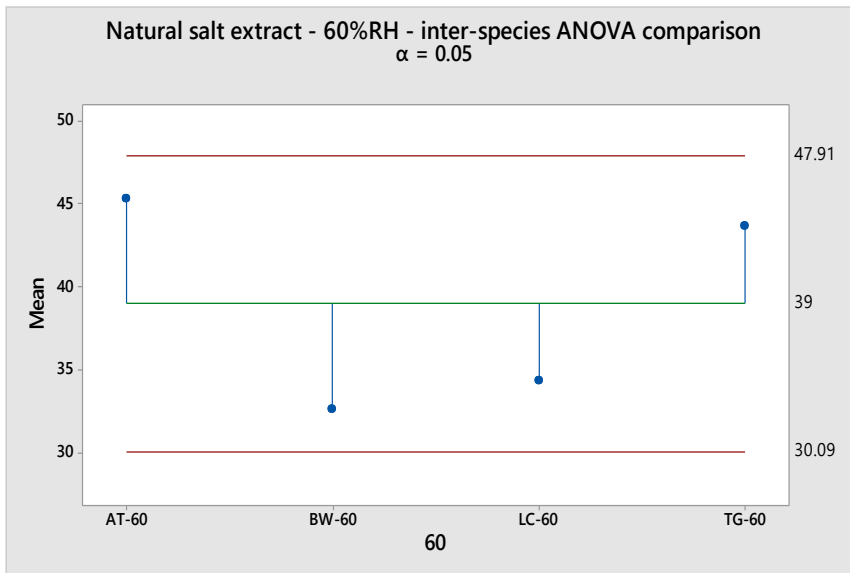


Figure A.2 ANOVA test for water uptake values for natural LMMCs (salt) extracts at 60% RH.

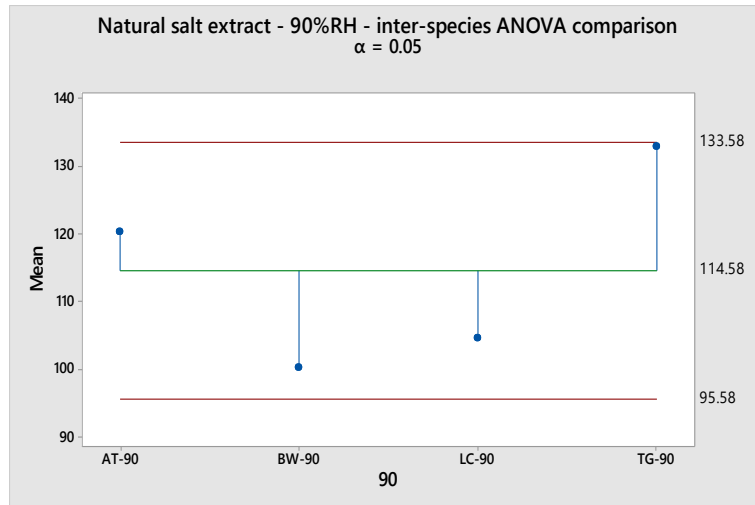


Figure A.3 ANOVA test for water uptake values for natural LMMCs (salt) extracts at 90% RH.

Source	Df	SS	F Ratio	P Value
Treatment	1	0.0944	4.2711	0.0478*
Substrate	2	6.2833	142.1630	<0.0001*
Treatment X Substrate	2	0.1493	3.3770	0.0480*
Area (covariate)	1	0.3718	16.8223	0.0003*

Table A.3 The effect of treatment (lipid removal) on maximum shear adhesion of gecko toe pad sheds to three substrates (glass, OTS-SAM coated glass and sandpaper) in air.

Source	Df	SS	F Ratio	P Value
Treatment	1	0.0076	0.2382	0.6311
Environment	1	0.7461	23.4110	0.0001*
Treatment X Environment	1	0.0022	0.0678	0.7974
Area (covariate)	1	0.1513	4.7464	0.0422*

Table A.4 The effect of treatment (lipid removal) on maximum shear adhesion of gecko toe pad sheds to OTS-SAM coated glass in both air and water.

APPENDIX B
CALCULATIONS

1. Calculations for testing the proposed models for keratin lipid associations (related to Chapter V)

In order to calculate the amount of lipid present in each of the proposed models, we want to first estimate the following parameters:

- (a) Mass of hairs in toe pad shed (Text B1.1)
- (b) Number of hairs in toe pad shed (Text B1.2)
- (c) Mass of extracted lipid from toe pad shed (Text B1.3)
- (d) Amount of lipids in skin shed (based on the known brick and mortar model) and toe pad shed (based on the brick and mortar model, mass of hairs in toe pad shed and experimentally extracted lipid from toe shed) (Text B1.4)

B1.1 Estimating mass of hairs in a toe pad shed

Measured mass of the toe shed = $2.9 \cdot 10^{-3} \pm 2.0 \cdot 10^{-4}$ g

Mass of setal hairs in the toe shed = $N \cdot \rho \cdot l \cdot b \cdot h$

where,

N is the number of rows of setae in toe shed

ρ is the density of keratin

l is the length of a row of hairs

b is the width of a row of hairs

h is the height of a row of hairs

$N \sim 15 \pm 2$, $l \sim 0.25 \pm 0.06$ cm, $h \sim 0.014 \pm 0.001$ cm, $b \sim 0.030 \pm 0.003$ cm

The dimensions (l, w) and N are measured from a toe shed image captured using an optical microscope. ImageJ was used to measure all other parameters.

Considering the density of keratin (~ 1.28 g/cm³ with a known range of $\rho \sim 1.28$ -1.33 g/cc), we can take the average values for all parameters and vary only one: "l" to get the mass of the setal hairs in the toe pad shed.

Mass of setal hairs = 1.9×10^{-3} g \pm 0.4×10^{-3} g

Hence, the % of the whole toe pad shed that is comprised of setae alone is as follows:

$(\text{Mass of setal hairs} / \text{Mass of toe shed}) \times 100 = 65 \pm 12$ %

The estimate suggests that setae contributes to the majority of the mass of a toe shed ~ 65%, while the non-adhesive skin is around ~35%.

B1.2 Estimating number of hairs in a toe pad shed

Dimensions of gecko setae = r_{setae} : 2.5 μ m and h_{setae} : 100 μ m

$$\text{Mass of single setae} = \rho_{\text{keratin}} * 3.14 * r_{\text{setae}}^2 * h_{\text{setae}} \quad (\rho_{\text{keratin}} : 1.28 \text{ g/cm}^3)$$

$$\text{Mass of single setae} = 2.55 * 10^{-9} \text{ g} \pm 0.1 * 10^{-9} \text{ g}$$

As per earlier calculations (Text B1.1),

Number of setal hairs in experimental toe shed = Mass of hairs in toe shed / Mass of single setae

$$\sim 7 * 10^5 \pm 2 * 10^5$$

Known number of hairs per foot pad of gecko $\sim 10^3$ - 10^6

Hence, the estimated value lies in the range published in the literature.

B1.3 Estimating mass of extracted lipid contributed by setae from a toe pad shed

Amount of lipid removed from toe shed $\sim 10\%$ of the toe shed mass

$$\text{Extracted amount} = 2.9 * 10^{-4} \pm 2 * 10^{-5} \text{ g}$$

Lipid extracted from setae $\sim 65\%$ of the total extracted amount from the toe shed (since $\sim 65\%$ is the amount of setae in toe shed and the rest is the non-adhesive skin)

$$\text{Lipid contribution from the setae in a toe shed is} = 65\% * 2.9 * 10^{-4} \text{ g}$$

$$= 1.8 * 10^{-4} \text{ g}$$

B1.4 Estimating lipid present in the toe pad shed and skin shed

For Skin Shed

In the mesos and α -layer we consider "bricks" as keratin cylinders with a radius of $3 \mu\text{m}$ (diameter ~ 6 - $8 \mu\text{m}$) and height $2 \mu\text{m}$. Hence, the volume of the keratin cylinder is:

$$\text{Volume of each keratin cylinder} = \pi * 3^2 * 2 = 18\pi \mu\text{m}^3$$

In the "brick and mortar" model we consider the "mortar" layer to be a 100 nm thick lipid layer between the keratin bricks.

In order to calculate the volume of a keratin brick and lipid layer, the new radius and height would be:

$$\text{Radius} = \text{keratin brick} + \text{lipid layer} = 3 + 50/1000 = 3.05 \mu\text{m}$$

$$\text{Height} = \text{keratin brick} + \text{lipid layer} = 2 + 100/1000 = 2.1 \mu\text{m}$$

where the effective thickness of lipid layer is taken to be 50 nm since it is shared between two keratin cylinders.

$$\text{Hence, the volume of skin shed is} = \pi * 3.05^2 * 2.1 = 19.5\pi \mu\text{m}^3$$

Therefore, the % of the total mass of the skin shed that is comprised of lipid alone (present in the mesos and α -layer) is as follows:

$$\% \text{ Lipid in Skin Shed} = (19.5\pi - 18\pi / 19.5\pi) * 100 \sim 8\%$$

For Toe pad shed

We know as per earlier calculations (Text B1.1), setal hairs comprise approximately ~65% of the mass of the toe shed and rest is the non-adhesive skin (including the mesos, α -layer, lacunar and shedding layers).

Also earlier estimates found that ~ 10% of the mass of the toe pad is removed by lipid extraction.

Thus, considering the amount of extracted lipid from toe shed, % contribution of lipid from the setal hairs (M) alone can be calculated as:

$M \cdot \% \text{ of hairs in toe shed} + \% \text{ lipid from mesos and } \alpha\text{-layer} \cdot \% \text{ of non-adhesive skin in toe shed} = 10\%$

Substituting the parameters,

$$M \cdot 65\% + 8\% \cdot 35\% = 10\%$$

Solving the equation for M, the % of lipid from the setal hairs alone is: $M \sim 11\%$

% of lipid in setal hairs is $\sim 11\%$

B1.5 Estimating lipid present in the setal hairs as per earlier models of lipid-keratin arrangement

(a) *Homogeneous Model (Lipids coating the setal rods)*

Considering 2 nm thick layer of lipid coating each of the setae rods,

$$\text{Mass of lipid coating each setae} = \rho_{\text{lipid}} \cdot V_{\text{lipid}}$$

$$= 0.9 \text{ g/cm}^3 \cdot [3.14 \cdot (2.502 \cdot 10^{-4})^2 \cdot 100.2 \cdot 10^{-4} - 3.14 \cdot (2.5 \cdot 10^{-4})^2 \cdot 100 \cdot 10^{-4}] \text{ cm}^3$$

$$= 5.85 \cdot 10^{-12} \text{ g}$$

Now, total number of setal hairs in toe shed is $\sim 7 \cdot 10^5$,

Hence, amount of lipid present as per homogeneous model $\sim 4 \cdot 10^{-6} \text{ g}$

(b) *Heterogeneous Model (Lipids forming spatulae)*

Dimensions of a spatula: L: 0.8 μm and d: 0.1 μm

$$\text{Mass of a single spatula} = \rho_{\text{keratin}} \cdot 3.14 \cdot r_{\text{spatula}}^2 \cdot l_{\text{spatula}} = 8 \cdot 10^{-15} \text{ g}$$

Number of spatula per setae $\sim 100\text{-}1000$

Hence, total spatula in toe shed $\sim 10^8$ (Taking 1000 spatula per setae)

Mass of spatulae in toe shed or amount of lipid present considering lipid forming spatulae

$$\equiv 10^8 * 8 * 10^{-15} \text{ g} \sim 8 * 10^{-7} \text{ g}$$

The results show that amount of lipid predicted to be present considering either of the models is less than the experimental results ($\sim 1.8 * 10^{-4}$ g) suggesting that lipids are not arranged with keratin like either of these proposed models in an exclusive manner. However, they may be present in combination of the models described. The 11% lipid present in the setae should be a combination of the two models described above, in addition to the presence of lipid in the 'matrix' material present within setae fibrils

According to the model described, it is known that 69% (by volume) keratinized regions are present with 31% 'matrix'. Taking into consideration this distribution and the 11% lipid in setal hairs, we can calculate lipid present in matrix (P), as follows:

$$\% \text{ of matrix in setae} * \% \text{ lipid in matrix region} + \% \text{ of keratinized (non-matrix) in setae} * \% \text{ lipid in keratinized (non-matrix) region} = \% \text{ lipid found in setae}$$

$$31\% * P\% + 69\% * 0\% = 11\%$$

Hence, unbound lipid present in matrix (P) $\sim 37\%$

In summary, the unbound lipid distribution in the setae (11%) is proposed to be a combination of models described above.

APPENDIX C

LIST OF PUBLICATIONS

The following list (in chronological order) comprises of published and in preparation technical papers associated with dissertation as well as with other projects accomplished during the doctoral studies:

1. Sahni, V., Miyoshi, T., Chen, K., **Jain, D.**, Blamires, S. J., Blackledge, T. A. & Dhinojwala, A. Direct solvation of glycoproteins by salts in spider silk glues enhances adhesion and helps to explain the evolution of modern spider orb webs. *Biomacromolecules* **15**, 1225–1232 (2014).
2. **Jain, D.**, Sahni, V.* & Dhinojwala, A. Synthetic adhesive attachment discs inspired by spider's pyriform silk architecture. *J. Polym. Sci. Part B Polym. Phys.* **52**, 553–560 (2014).
3. Amarpuri, G., Chaurasia, V., **Jain, D.**, Blackledge, T. A. & Dhinojwala, A. Ubiquitous distribution of salts and proteins in spider glue enhances spider silk adhesion. *Sci. Rep.* **5**, 9030 (2015)
4. **Jain, D.**, Stark, A. Y., Niewiarowski, P. H., Miyoshi, T. & Dhinojwala, A. NMR spectroscopy reveals the presence and association of lipids and keratin in adhesive gecko setae. *Sci. Rep.* **5**, 9594 (2015).
5. **Jain, D.**, Zhang, C., Cool, L.R., Blackledge, T.A., Wedemiotis, C., Miyoshi, T. & Dhinojwala, A. Composition and Function of Spider Glues Maintained During the Evolution of Cobwebs. *Biomacromolecules*, **16**, 3373-3380 (2015).
6. Stark, A. Y., Subarajan, S., **Jain, D.**, Niewiarowski, P. H. & Dhinojwala, A. Superhydrophobicity of the gecko toe pad: biological optimization versus laboratory maximization. *Philos. Trans. R. Soc. A Math. Phys. Eng. Sci.* **374**, 20160184 (2016).

7. **Jain, D.**, Blackledge, T. A., Miyoshi, T., & Dhinojwala, A. Unraveling the Design Principles of Black Widow's Gumfoot Glue. in *Biological Adhesives*, 303–319. Springer International Publishing (2016).
8. Wang, S., Kang, J., **Jain, D.** & Miyoshi, T. Application of NMR in polymer characterization. *Nucl. Magn. Reson.* **45**, 53-95 (2016).
9. Ying X., Liu Q., Narayanan, A., **Jain, D.**, Dhinojwala, A. & Joy, A. Mussel-Inspired Polyesters with Aliphatic Pendant Groups Demonstrate the Importance of Hydrophobicity in Underwater Adhesion *Adv. Mater. Interfaces* (2017).
10. Opell, B.D., **Jain, D.**, Dhinojwala, A. & Blackledge, T.A. Tuning orb spider glycoprotein glue performance to habitat humidity *J. Exp. Biol.*, under review (2017).
11. **Jain, D.**, Amarpuri, G.*, Fitch, J., Blackledge, T. A. & Dhinojwala, A. Role of hygroscopic low molecular mass compounds in the adhesion of spider's capture silk, in preparation (2017).
12. **Jain, D.**, Singla, S., Zoltowski, C., Voleti, S., Stark, A. Y., Niewiarowski, P. H., Miyoshi, T. & Dhinojwala, A. Macro and molecular response of gecko setae to humidity: implications for adhesion, in preparation (2017).

* equal contributors to the project